AFRL-AFOSR-UK-TR-2010-0013

Control of Flow Structure and Ignition of Hydrocarbon Fuel in Cavity and behind Wallstep of Supersonic Duct by Filamentary DC Discharge

Sergey B Leonov

Institute of High Temperatures RAS
IVTAN, Izhorskaya str., 13/19
Moscow, Russia 125412

EOARD ISTC 04-7001

January 2011

Final Report for 01 December 2004 to 30 November 2010

Distribution Statement A: Approved for public release distribution is unlimited.

Air Force Research Laboratory
Air Force Office of Scientific Research
European Office of Aerospace Research and Development
Unit 4515 Box 14, APO AE 09421

REPORT DOCUMENTATION PAGE

Form Approved OMB No. 0704-0188

Public reporting burden for this collection of information is estimated to average 1 hour per response, including the time for reviewing instructions, searching existing data sources, gathering and maintaining the data needed, and completing and reviewing the collection of information. Send comments regarding this burden estimate or any other aspect of this collection of information, including suggestions for reducing the burden, to Department of Defense, Washington Headquarters Services, Directorate for Information Operations and Reports (0704-0188), 1215 Jefferson Davis Highway, Suite 1204, Arlington, VA 22202-4302. Respondents should be aware that notwithstanding any other provision of law, no person shall be subject to any penalty for failing to comply with a collection of information if it does not display a currently valid OMB control number.
PLEASE DO NOT RETURN YOUR FORM TO THE ABOVE ADDRESS.

1. REPORT DATE *(DD-MM-YYYY)*	2. REPORT TYPE	3. DATES COVERED *(From – To)*
05-01-2011	Final Report	01 December 2004 – 30 November 2010

4. TITLE AND SUBTITLE

Control of Flow Structure and Ignition of Hydrocarbon Fuel in Cavity and behind Wallstep of Supersonic Duct by Filamentary DC Discharge

5a. CONTRACT NUMBER
ISTC Registration No: 3057p

5b. GRANT NUMBER
ISTC 04-7001

5c. PROGRAM ELEMENT NUMBER
61102F

6. AUTHOR(S)

Dr. Sergey B Leonov

5d. PROJECT NUMBER

5d. TASK NUMBER

5e. WORK UNIT NUMBER

7. PERFORMING ORGANIZATION NAME(S) AND ADDRESS(ES)

Institute of High Temperatures RAS
IVTAN, Izhorskaya str., 13/19
Moscow 125412
Russia

8. PERFORMING ORGANIZATION REPORT NUMBER

ISTC 04-7001

9. SPONSORING/MONITORING AGENCY NAME(S) AND ADDRESS(ES)

EOARD
Unit 4515 BOX 14
APO AE 09421

10. SPONSOR/MONITOR'S ACRONYM(S)

11. SPONSOR/MONITOR'S REPORT NUMBER(S)
AFRL-AFOSR-UK-TR-2010-0013

12. DISTRIBUTION/AVAILABILITY STATEMENT

Approved for public release; distribution is unlimited.

13. SUPPLEMENTARY NOTES

14. ABSTRACT

This report results from a contract tasking Institute of High Temperatures RAS as follows: The contractor will investigate the phenomena of plasma-induced ignition of high speed, low temperature air-fuel mixtures using a recirculation zone created by a rearward facing wall step and wall cavity. The plasma will be generated using a multi-electrode, quasi direct-current electrical discharge. Fuel injectors will be located in the recirculation zone. The effects of plasma induced ignition, mixing intensification, flame-stabilization, and combustion completeness will be evaluated. Investigations will be carried out using both gaseous and liquid hydrocarbon fuels. Diagnostics include high speed video, Schlieren photography, pressure distribution measurements, electrical measurements, optical spectroscopy and infrared absorption spectroscopy. The research is mainly experimental, but will include several analytical and computational efforts for better understanding and verification of the results.

15. SUBJECT TERMS
EOARD, Propulsion, Engines And Fuels, Combustion and Ignition

16. SECURITY CLASSIFICATION OF:			17. LIMITATION OF ABSTRACT	18, NUMBER OF PAGES	19a. NAME OF RESPONSIBLE PERSON
a. REPORT	b. ABSTRACT	c. THIS PAGE			Stephanie Masoni, Maj, USAF
UNCLAS	UNCLAS	UNCLAS	SAR	150	**19b. TELEPHONE NUMBER** *(Include area code)* +44 (0)1895 616420

ISTC Project No. 3057p

Control of Flow Structure and Ignition of Hydrocarbon Fuel in Cavity and behind Wallstep of Supersonic Duct by Filamentary DC Discharge

Final Project Technical Report

on the work performed from Dec 01, 2004 to Nov 30, 2010

Joint Institute for High Temperature Russian Academy of Science

Project Manager **Sergey B. Leonov**
DrSc

Deputy Director **Vladimir A. Zeigarnik**
DrSc

December 2010

This work was supported financially by EOARD and performed under the agreement to the International Science and Technology Center (ISTC), Moscow.

Title of the Project:	Control of Flow Structure and Ignition of Hydrocarbon Fuel in Cavity and behind Wallstep of Supersonic Duct by Filamentary DC Discharge
Commencement Date:	December 01, 2004
Duration:	From December 01, 2004 to November 30, 2010 for 72 months
Project Manager	Sergey Borisovich Leonov
phone number:	+7-(495) 484-1811
fax number:	+7-(495) 483-2285
e-mail address:	leonov@ihed.ras.ru
Leading Institute:	Joint Institute for High Temperature Russian Academy of Science Izhorskaya str., 13 bld 2, Moscow, 125412, Russia +7 (495) 483 22 75 Leonov@ihed.ras.ru www.oivtran.ru
Participating Institutes:	
Foreign Partner	European Office of Aerospace Research and Development (EOARD) 223-231 Old Marylebone Road, London, UK Phone: +44-171-514-4299; Fax: +44-171-514-4960 E-mail: Stephanie.Masoni@london.af.mil

Keywords:
Plasma-Assisted Combustion, Non-Premixed Composition, Electrical Discharge, High-speed Flow, Hydrocarbon Fuel, Plasma Non-uniformity, Separation Zone, Spectroscopy, Schlieren Measurement, 3-D Simulation.

Contents

i. List of key personnel.
ii. List of acronyms and definitions.

1. **Introduction.**
   1.1. Project‘s Objectives.
   1.2. Tasks‘ Description
2. **Review of activity.**
   2.1. Short review of the first year efforts.
   2.2. Short review of the second year efforts.
   2.3. Short review of the third year efforts.
   2.4. Short review of the fourth year efforts.
   2.5. Short review of the fifth year efforts
3. **Background.** Preliminary analysis of available data and previous experience.
   3.1. Plasma assistance for high-speed combustion.
   3.2. Discharges for Plasma-Assisted Combustion.
   3.3. Short review of DLAS-related publications.
4. **Task 1. Technical Results**
   4.1. Experimental facility description and updates.
   4.2. Measuring system.
      4.2.1. Gasdynamic measurements and observations.
      4.2.2. Spectroscopic observations.
      4.2.3. Realization of DLAS method for PWT-50H facility.
   4.3. Experimental study of the nonequilibrium discharge effect on effectiveness of plasma-based flameholding over plane wall.
      4.3.1. Near surface electrical discharge operational modes. Variation of E/n.
      4.3.2. Spectroscopic observations of ignition dynamics.
      4.3.3. Specific limitations for plasma-based flameholding in case of hydrocarbon fuel.
      4.3.4. Refined results on plasma-assisted combustion of hydrogen and ethylene in M=2 flow.
5. **Task 2. Technical Results**
   5.1. Measurements of reactant gas parameters distribution in area of plasma-gas interaction and combustion zone by laser-based non-intrusive diagnostics.
      5.1.1. DLAS – method description.
      5.1.2. DLAS - spectra processing.
      5.1.3. Result of measurements by laser absorption spectroscopy
      5.1.4. Some ideas about Y-inhomogeneity of gas parameters
   5.2. Analysis of two-stage scheme of plasma-enhances combustion.
      5.2.1. Numerical analysis of nonequilibrium plasma effect on fuel ignition.
      5.2.2. Two-stage scheme of plasma-based flameholding.
      5.2.3. Numerical analysis of fuel ignition by filamentary plasma. Mixing effect.
      5.2.4. How it might work in future?
6. **Conclusions**

Attachment 1.
List of published papers with abstracts
Attachment 2.
List of presentations at conferences and meetings with abstracts

i. List of Key Personnel.

Dr. Felix Akopov	Senior Scientist
Prof. Michail A. Bolshov,	Head of Laboratory
Mr. Vladimir A. Doronin	Master Student,
Mr. Alexander Firsov	PhD Student,
Dr. Yury I. Isaenkov	Head of Laboratory, Senior Researcher,
Dr. Igor V. Kochetov	Senior Scientist
Dr. Yury A. Kuritsyn	Leading Scientist,
Dr. Alexander P. Kuryachiy	Senior Researcher,
Dr. Sergey B. Leonov	Head of Laboratory, Project Manager,
Dr. Vladimir V. Liger	Senior Scientist,
Mr. Paul G. Makeev	Engineer,
Mr. Konstantin V. Savelkin	Senior Engineer,
Dr. Valery N. Sermanov,	Senior Scientist,
Dr. Victor R. Soloviev	Senior Researcher,
Dr. Michail V. Starodubtsev	Researcher,
Mr. Vladimir A. Storozhenko	Mechanical Engineer,
Dr. Valery N. Suchov	Leading Engineer,
Mr. Dmitry A. Yarantsev	Engineer-Physicist

Acknowledgements.

Dr. Valentin A Bityurin,
Dr. Campbell Carter,
Dr. Victor V. Kirichenko,
Maj. Stephanie Masoni,
Prof. Anatoly P. Napartovich,
Dr. Vladimir Sabelnikov,
Dr. Surya Surampudi,
Dr. Julian Tishkoff

ii. **List of Definitions and Acronyms.**

M -	Mach Number of the flow.
Kn-	Knudsen Number.
Re -	Reynolds Number.
Sc -	Strouhal Number.
C -	capacitance.
E-	electric field strength.
E/N-	reduced electric field strength.
I -	electric current.
k -	Boltzman‘s constant.
L-	inductivity.
N_e -	concentration of electrons.
N -	concentration of neutral gas particles.
N_n -	concentration of the different chemical species.
P_{st} -	static pressure in airflow.
P_o -	stagnation pressure in airflow.
R	resistivity.
$R_L=\omega L$	inductive resistivity.
S -	area of midsection.
T_g -	gas temperature.
T_v -	vibrational temperature of molecular gas.
T_e -	temperature of electrons in plasma.
V -	velocity of flow.
W -	power or power density.
ρ_0 -	gas density in flow.
ε_0 -	electrostatic constant.
δ -	boundary layer thickness.
λ -	wavelength.
τ -	relaxation time.
ω -	circular frequency of EM wave.
BL -	boundary layer.
AC -	alternative current.
DC -	direct current.
DLAS -	diode-laser absorption spectroscopy.
EMF -	electromagnetic field.
HF -	high frequency.
HV -	high voltage.
IR -	infra-red radiation.
MPA -	magneto plasma aerodynamics.
MF -	magnetic field.
OES -	optical emission spectroscopy.
PD -	pulse discharge.
PG -	plasma generator.
PWT -	pulse wind tunnel.
SW -	shock wave.
SD -	surface discharge.
TDE -	thermodynamic equilibrium.
TS -	test section.
UV -	ultra-violet radiation.
WT -	wind tunnel.

1. Introduction.

1.1. Project's Objectives.

The work in frames of the project #3057p was devoted to a study of the fundamental plasma technology application in a field of airflow parameters control by plasma, in particular, the researches for methods of fuel-air composition ignition at low-temperature and high-speed gas flow. The work performed under this intention will also result in obtaining a new experimental data on plasma-flow interaction. The work as a whole was performed during five-year period (24quarters, quarters #13 and #18-20 was not funded).

The project formal objective is *to study the phenomena of plasma-induced ignition of air-fuel mixture at direct fuel injection into separation zone downstream backwise wallstep and wall cavity by multi-electrode quasi-DC electrical discharge at high-speed flow*.

The work included several important steps, namely: (1) specification of the experimental configuration and explicit design of plasma generator at deep modification of the IVTAN experimental facility (from PWT-10 to PWT-50); (2) development of the appropriate diagnostics; (3) test runs and getting an experimental data concerning non-homogeneous plasma effect on ignition; (4) computational analysis at verification by experimental data; (5) analysis of results and recommendations for the further development; (6) demonstration of the plasma ignition effect under high-temperature conditions; (7) test runs and getting an experimental data concerning non-homogeneous plasma effect on ignition over plane wall; (8) measurements of reacting gas parameters by laser-based non-intrusive diagnostics; (9) analysis of two-step mechanism of plasma-assisted combustion; (10) recommendations on the improvement of plasma assisted combustion method and apparatus.

Steering of the chemical processes in high-speed flow is one of critically important domains of supersonic combustors improvement. Last years the interest grows in field of plasma-assisted combustion as one of the most promising method for speedup the ignition, enhancement of the chemistry, and intensification of the mixing. Number of publications rises quickly. At the same time the most works in this field are lab-scale with premixed air-fuel composition or theoretical. Such a position is understandable overall due to the full-scale experiments are expensive, complicated, and dangerous. The experimental facility PWT-50H is designed as an alternative variant to full-scale continuous experimental arrangement in accordance with the following requirements: flow parameters are close to typical for combustors; operation time in steady-stage mode is much more than characteristic gasdynamic time; test section dimensions much more than thickness of boundary layer; fuel portion is small enough to be non-hazardous but large enough to observe the physical and chemical effects;

number of runs in a range 10-100 per working day; special arrangement for plasma generation and diagnostics.

During the first year the work was aimed at available data analysis, the experimental facility modification, and preliminary runs for a flow structure adjustment. In a parallel line the diagnostics methods and equipment were prepared. Some computational efforts were done to attend the experimental data and measurements.

During the second year the efforts in frames of the project were arrowed on the low-temperature ignition test and preparation of the test with preheated air. The diagnostic methods were developed. Experimental works were supported by analytical and CFD efforts.

In the third year of the project a main attention was paid for the experiments at elevated temperature of the air and for analysis of the results based on experimental data and data of computational efforts.

The forth year efforts were arrowed to the hydrogen and gaseous hydrocarbon fuels ignition and flameholding by transversal surface DC discharge above the plane wall of supersonic duct. This experimental work was supported by the laser-based diagnostic and computational modeling.

The work in 5^{th} year was aimed at study of the hydrogen and gaseous hydrocarbon fuels ignition and flameholding by transversal surface DC discharge above the plane wall of supersonic duct under the variation of reduced electrical field. This experimental work was be supported by the spatial-resolved laser-based diagnostic to measure the specific rate of the fuel oxidation. Extra numerical simulations were performed to examine the effect of reduced field in plasma of electrical discharge on the ignition time. The results of calculations were analyzed in frames of idea of two-stage mechanism of the plasma-assisted combustion.

This Final Technical Report describes the most valuable results obtained in frames of the project ISTC#3057p due to experimental, computational, and analytical efforts. It covers the fifth year efforts in details, while the work from the 1st by the 4th year is described briefly. These previous data were presented in Final Technical Report on the Project ISTC#3057p dated March, 2009.

1.2. Tasks' Description

The work is divided conditionally on two main tasks in accordance with the idea to study the processes concomitant with plasma-induced ignition, and to develop appropriate diagnostics.

The entire period of the project is running by five-year sessions. It includes several important steps, namely:

- ◊ Specification of the experimental configuration and explicit design of plasma generator. Deep modification of the IVTAN experimental installations (from PWT-10 to PWT-50) for the plasma assisted combustion experiment.
- ◊ Development of the appropriate diagnostics.
- ◊ Running tests. Obtaining experimental data concerning the effect of inhomogeneous plasma on ignition.
- ◊ Computational analysis due to results of experiments.
- ◊ Considering input data and making out recommendations for further development.
- ◊ Demonstration of the plasma ignition effect under high-temperature.
- ◊ Running tests. Obtaining experimental data concerning the effect of inhomogeneous plasma on ignition over plane wall. Description of the effect of nonequilibrium excitation of molecular gas on chemical exothermal reactions in high-speed flow.
- ◊ Consideration of experimental conditions for plasma ignition – to flameholding transition. Factual (measured) data on the reactant gas parameters distribution in zones of (1) air-fuel-plasma interaction and (2) the combustion.
- ◊ Consideration of the electrical discharge role in supporting of the flow structure favourable for the flameholding in high-speed flow.
- ◊ Recommendations on the improvement of plasma assisted combustion method and apparatus.

Task 1

Task description and main milestones	Participating Institutions
Experimental study of plasma-induced ignition of non-premixed air-fuel composition under the conditions of wall step and wall cavity. 1.1. Preliminary analysis of available data and previous experience. 1.2. Experimental facility modification. Injection system design and manufacturing. 1.3. Adjustment of renewed plasma generator and power supply. Measurements of discharge and plasma parameters. 1.4. Study of plasma effect on flow structure near wall step and cavity. Study of plasma filaments dynamics in high-speed flow. 1.5. Experiments on plasma-induced ignition. 1.6. Analysis of results of lab-scale test on the base of experimental data and CFD simulations. 1.7. Test section design for hot test-bed experiment. 1.8. Nozzle and test section manufacturing and adjustment. 1.9. Preparation of high-temperature test, diagnostics adjustment. 1.10. Final experiments on gaseous fuel ignition under conditions of hot test-bed. 1.11. Final experiments on liquid fuel ignition under conditions of hot test-bed. 1.12. Preparation of Third-Year Report. 1.13. Preparation of flameholding test above a plane wall, diagnostics adjustment.	1-JIHT RAS

1.14. The experiments on gaseous fuel ignition and flameholding above a plane wall under conditions of T0=300K and T0=500-700K, M=2 test bed. 1.15. Analysis of data. Preparation of 4th Year Report. 1.16. Study of the nonequilibrium discharge effect on effectiveness of plasma-based flameholding over plane wall. Variation of E/n. 1.17. Analysis of data. Preparation of Fifth Year Report.	

Task 2

Task description and main milestones	Participating Institutions
Diagnostics development and computational support. 2.1. Preliminary review of available data and previous experience. Absorption spectrum calculations. 2.2. Design and manufacturing of parts and components for IR spectroscopy. 2.3. Diagnostic system modification. 2.4. CFD simulations of plasma effect on flow structure near wall step and cavity. 2.5. Diagnostic system modification and adjustment for hot test-bed. 2.6. Computational analysis of filamentary plasma effect on fuel ignition. 2.7. Measurements of plasma parameters and characterization of plasma ignition efficiency in hot test. 2.8. Review of results based on experimental data and CFD simulations. Final report preparation. 2.9. Measurements of reactant gas parameters in combustion zone by laser-based non-intrusive diagnostics. 2.10. Review of results of CFD simulations and comparison them with the experimental data. 2.11. Measurements of reactant gas parameters distribution in area of plasma-gas interaction and combustion zone by laser-based non-intrusive diagnostics. 2.12. Analysis of two-stage scheme of plasma-enhances combustion. Final report preparation.	1-JIHT RAS

The technical parameters of the test were defined by SOW. They are the following:

*	Initial Mach number in duct	M = 2 and 2.5;
*	Initial static pressure	P_{st} =0.15-0.3 Bar;
*	Stagnation temperature of the air	T_0=300-700K;
*	Typical duct dimensions	72*60mm;
*	Type of discharge	filamentary DC and AC discharges;
*	Duration of discharge	10-100ms;
*	Mean electrical input power	1 - 10 kW;
*	Range of reduced electrical field	$E/N=(1\text{-}10)\times10^{-16}Vcm^2$;
*	Fuel	hydrogen and ethylene.

The geometry of the test being considered is an aerodynamic duct with rectangular cross-section and discharge's arrangement on a horizontal wall as it shown in the Fig.1.2.1 below.

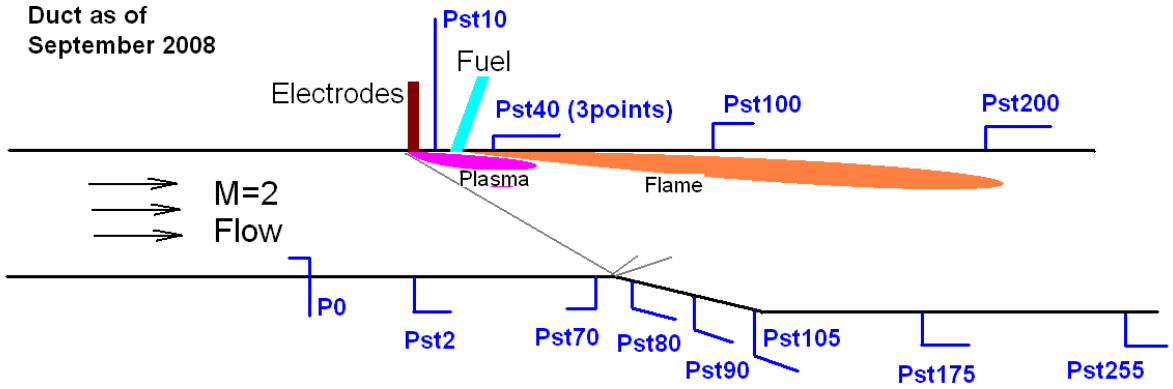

Fig.1.2.1. Basic geometry of the test.

Facilities/Basic Equipment:

- Short-time wind tunnel PWT-50H (JIHT RAS) - mid-scale high-temperature test-bed;
- Specialised control desks for PG operation and for registration of discharge and gas flow parameters;
- Laser-based diagnostic system.

Measurements and Diagnostics:

The following parameters were measured in the test:

* Gas temperature, T_g;
* Distribution of static and stagnation pressure, P_o, P_{st};
* Optical spectra of excited molecules;
* Spatial distribution of optical lines emission;
* Plasma power parameters;
* Dynamics of the ignition processes by video-records and shadow-video records;
* Spatial distribution of medium parameters by laser absorption spectroscopy.

The above parameters were measured by means of following diagnostic methods:

* Optical spectroscopy;
* Schlieren method;
* Set of pressure transducers;
* High-speed video camera;
* High-speed line-scan camera;
* Laser absorption spectroscopy;
* Thermo sensors, electric probes, etc.

2. Review of activity.

2.1. Short review of the first year efforts.

During the first year the work was aimed at available data analysis, the experimental facility modification, and preliminary runs for a flow structure adjustment. In a parallel line the diagnostics methods and equipment were prepared. Some computational efforts were done to attend the experimental data and measurements.

The first task –Experimental study of plasma-induced ignition of non-premixed air-fuel composition under the conditions of wall step and wall cavity" included four subtasks (see section 1.2). In frames of subtask1.1 two items were observed: fuel ignition behind a wallstep and in a cavity due to conventional technique; and the efforts of plasma assistance for the fuel ignition. This part also covered some steps for experimental setup design and determination of experimental conditions. The subtask 1.2 arrowed on the experimental facility design, determination of experimental conditions, and manufacturing/assembling of main parts and elements of the test-bed. Two different fuel injection systems were designed and tested: for gaseous (ethylene) and liquid (JP-line) hydrocarbons, accordingly. The third part covers the plasma generator and power supply design, determination of basic arrangement for typical experimental conditions, and manufacturing/assembling of main parts and elements of plasma generator. The electro-physical parameters of the discharge, structure and dynamics of the plasma filaments are studied. The main plasma parameters are measured spectroscopically. The fours quarter's efforts were fulfilled to study the plasma effect on flow structure and plasma dynamics itself.

The second task –Diagnostics development and computational support" included three subtasks 2.1-3. In frames of these subtasks the diagnostic's approach was developed, the most parts of diagnostics arrangement were designed and manufactured. IR spectrum was calculated to choose specific band for IR absorption spectroscopy, the apparatus for spectrum records and analysis was prepared. The results on the CFD simulations haven't to be reported in the first year. Nevertheless a preliminary computational analysis of flow structure near wall cavity in supersonic duct under the discharge impact was performed and included to the comprehensive report.

Review of plasma-assisted combustion method. Analysis of supersonic combustors performance shows that several principal problems related to the supersonic combustion and the flame stabilization, especially in the case of hydrocarbon fuels are to be solved for the practical implementation of such a technology. The plasma-based methods of the combustion management at high-speed conditions are considered now as one of the most promising technologies in this field [1-17].

An electrical discharge's properties strongly depend on the conditions of excitation, flow parameters and characteristics of supplying electromagnetic power. The analysis of applicable discharge types can be done from the viewpoint of plasma-assisted combustion concept, which consists of three important items: plasma-induced ignition, inflow mixing, and combustion chemistry enhancement (by acceleration of reactions and flow parameters management).

The mechanisms of the plasma of electrical discharges influence on chemical processes in high-speed flow may be considered and listed as follows:

- Fast local heating of the medium.
- Active radicals and particles deposition.
- Shock waves generation.
- Photo-dissociation and ionization.

Local heating of the medium leads to intensification of the chemical reactions in these areas. Besides of this the modification of flow structure may be done by means of controlled

energy deposition. At enough large level of the input power the artificial separation of the flow may be realized. It is a method to increase a local residence time to provide a zone of local combustion and the real mechanism of the mixing intensification. Active radicals‘ deposition occurs due to molecules‘ dissociation and excitation by electrons in electric field and by more complex processes. If the chain chemical reactions are realized, the deposition of active particles may lead to large (synergetic) benefit in reactions‘ rate as well as in required amplitude of power deposition. Very often the first two mechanisms are inseparable and the active radicals‘ generation is equal to hidden heating. Local shock waves generation promotes the mixing processes in heterogeneous medium and initiates chemical reactions due to heating in shock‘s front zone.

The electrical discharges, which are generated under the conditions of high-speed flow, possess several specific properties. These features might be important for the discharges‘ applications for flow parameters and structure control and combustion under unfavorable conditions. There may exist various types of plasma instabilities, for example, longitudinal-transversal instability of plasma filament, which has been found out recently [9]. It leads to intensive small scale mixing inflow. Extra method of combustion intensification is plasma jets blowing out to main flow.

It is clear that to manage the combustion process fully under any conditions a large level of additional energy deposition is required, of about 10% of the flow enthalpy. The combustor must operate properly under the conditions, which has been designed for. So the idea is not related to strong effect of energy release but to gentle control of chemical reactions rate and local multi-ignition. The second direction is to give the gear to force combustor to work under off-design conditions. It may be a temporal mode when the level of required electric energy is not vitally important. Such off-design conditions are: low temperature (probably, due to undesirably high speed of flow), relatively low pressure, lean composition, bad mixing, etc. Our experiments are going to simulate off-design regimes of the model combustor.

Unfortunately, specific information available now is not quite sufficient for proper choice of the discharge type. Our understanding now is that there is no universal decision in plasma assistance design and the method of application. Presence of even a small amount of free radicals (for example O, OH, H, ON) or vibrationally excited molecules may effectively improve ignition conditions but require not a small amount of electric power. Each specific situation has to be considered separately. Under these conditions the experimental tests and verification of some analytical predictions are urgently needed.

The paper [18] presents nonequilibrium RF plasma assisted combustion experiments in CO-air, ethylene-air, and methane-air flows using FTIR absorption spectroscopy and visible emission spectroscopy. Results of combustion completeness and emission spectroscopy measurements suggest that O and H atoms, as well as OH radicals are among key species participating in plasma chemical fuel oxidation reactions. Consistent with their previous measurements, the results show the highest fuel oxidation efficiency in lean air-fuel mixtures, as well as significant fuel conversion at the conditions when there is no flame in the test section. In the latter case, fuel species oxidation occurs in plasma chemical reactions, which are not related to combustion. However, since the net fuel oxidation process is exothermic, heat release during these reactions may result in achieving thermal ignition and flameholding in the plasma. Since CH emission peaks only after thermal ignition is achieved in hydrocarbon-air flows, CH radical is unlikely to be among key species in plasma chemical reactions. This indicates that to obtain further insight into the mechanism of plasma assisted ignition, future research effort should be focused on O and H atom, as well as OH radical concentration measurements, especially in lean air-fuel flows before thermal ignition occurs.

In the paper [19] the numerical simulations of hydrogen-air ignition by nonequilibrium gas discharge in supersonic flow was considered. The model of the discharge parameters

simulation in chemically-active mixture was developed at the first time. The results demonstrate that the electrical discharge of glow type is quite prospective candidate for ignition technique. The combustion acceleration effectiveness strongly depends on initial temperature and energy release. At the 700K of static temperature, atmospheric pressure, and power release about 200J/l the induction time occurs 3.4 times shorter than at the thermal initiation. That calculation was done for the conditions of real experiment, described in [20].

Numerous publications were offered by NEQ-Lab MIPT group [21, 22, for example], where a deep analysis of plasma-chemical kinetics under the plasma-assisted combustion was announced. As it was considered, a nonequilibrium plasma of nanosecond pulse discharge can affect a flame blow-off velocity significantly due to active radicals deposition. It occurs with energy input negligible in comparison with burner's chemical power.

The group of "Applied Plasma Technology" announced some devices for fuel ignition and flame stabilization [23]. Positive results of performed investigations indicated significant advantages of selected non-equilibrium plasma generator in comparison with the thermal plasma sources.

The successful efforts are being performed for plasma-assisted combustion in WPRL with colleagues. One of the last publications [24] is devoted to development of plasma igniter for use in high-speed and high-altitude air vehicle. Such an igniter produces a rich pool of radicals that would drive pre-ignition chemistry leading to ignition. The ignition concept demands a non-equilibrium plasma characterized by a high degree of feed-gas dissociation and little direct heating of the gas.

A serious experimental work is being carried out by joint team of MSU, CIAM and IGP [25]. The efforts are arrowed on a comparative test of different plasma sources by the criteria of ignition efficiency in high-speed flow.

Several groups of investigators demonstrate a successful ignition of premixed air-fuel composition and flame acceleration by non-equilibrium corona or barrier discharges, see for example [26-27]. As a rule in those works the conditions are rather far from practical schemes of high-speed combustion.

Last time many international meetings include the plasma-assisted combustion sessions to their schedule. The number of publications grows quickly. At the same time it is clear that some important events/features have not been studied in frames of those works and extra efforts are needed to be done in this field.

Experimental facility description. The experimental facility contains following main parts:

- Gasdynamic facility PWT-10/PWT-50;
- Plasma generator and power supply;
- Measuring and data acquisition system.
- Control and synchronization system.

The experimental facility PWT-50 is a deeply modified installation PWT-10 of IVTAN. The mail objective of this rebuilding was to increase the cross-section of flow from 20*50mm up to 72*60mm at Mach number M=2 and static pressure up to P_{st}=300Torr. An appropriate mass flow-rate is increased in 4.3 times that leads to rise the volume of storage tanks and cross-sections of all pipes and valves. General layout of the experimental facility PWT-50 and arrangements are presented in Fig.2.1.1. The following gasdynamic parameters of the test are provided by PWT-50 currently:

* Mach number in duct	M=0.3-0.75 and M=2;
* Initial static pressure	P_{st} =0.2-0.8 Bar;
* Stagnation temperature of the air	T_0=300K;
* Test section dimensions	72*60mm;
* Steady-stage operation time	0.3-0.5sec.

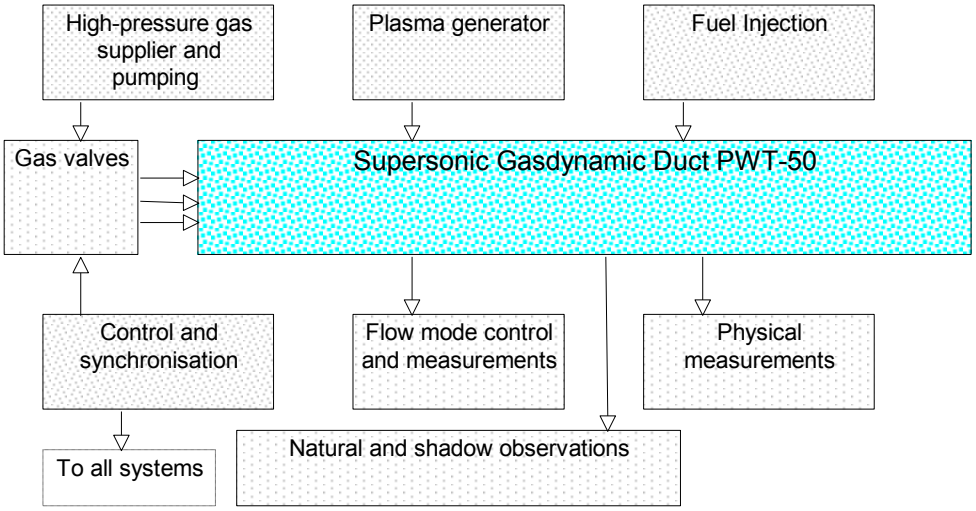

Fig.2.1.1. Layout of the PWT-50 arrangement.

Two methods were utilized mainly to study the discharge effect on flow structure behind wallstep and in cavity: pressure measurements and Schlieren visualization. 16-channels pressure recorder was used in the tests. The discharge dynamics in flow behind the wallstep and in cavity was explored using high-speed digital CMOS camera –Basler A504k". Two modes were tested: subsonic and supersonic in three configurations (wallstep, long cavity l/d=6.5, and short cavity l/d=3.3). The level of input power was varied by ballast resistances. The typical data is presented in Fig.2.1.2 below.

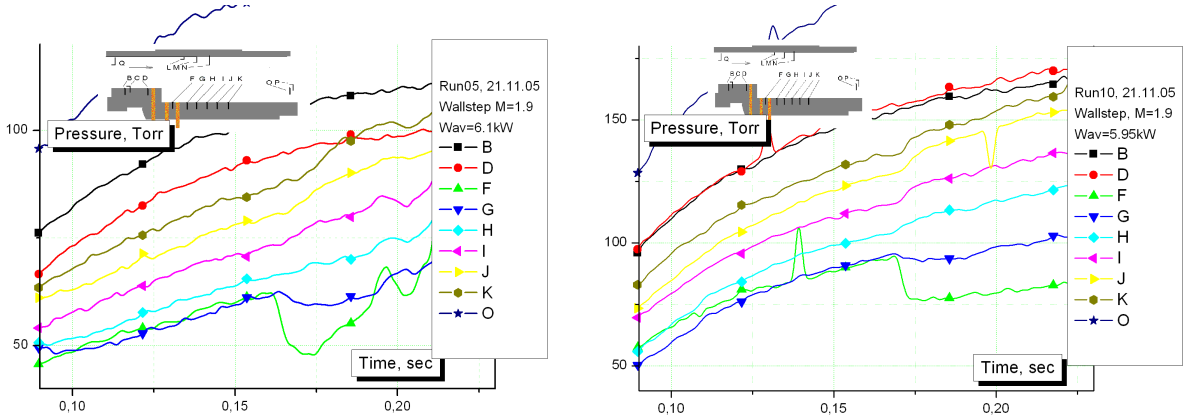

Fig.2.1.2. M=1.9, wallstep. Different pressure at the same power release W_{av}=*5.95-6.1kW*. The discharge effect was in a valuable increase of pressure just behind the wallstep.

Schlieren system was adjusted to work in pulse mode of flash-lamp with frame's frequency *f=100Hz*. The typical images are presented in Fig.2.1.3 by pair (discharge on/off). The investigations were done for the operation modes when the power deposition was in a range *Wav=5-7kW*, static pressure in subsonic *M≈0.7* mode *Pst=300-400Torr*, static pressure in supersonic *M≈1.9* mode *Pst=120-180Torr*. The exposure was *t=1mcs*.

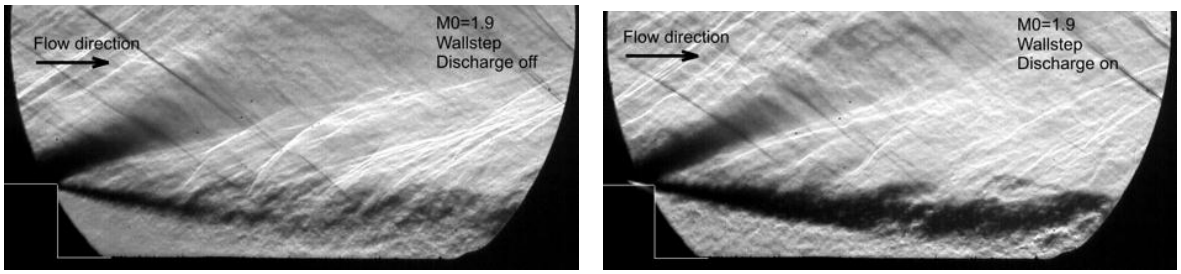

Fig.2.1.3. Schlieren photos of the discharge effect on flow structure. Supersonic mode, wallstep.

Summarizing the discharge effect on flow structure in cavity and behind wallstep it should be considered that, as a rule, an intensive turbulization is observed in interaction area at simultaneous some increase of the separation zone volume.

Diagnostics development. The following parameters of the gas and plasma were measured during the tests:

* Gas temperature, averaged and local values, T_g;
* Distribution of static and stagnation pressure, P_o, P_{st};
* Optical spectra of the excited molecules N_2, CN, OH, CH;
* Temporal evolution of optical lines OH, CH, etc.;
* Plasma energetic parameters;
* Dynamics of the ignition processes by video-records and Shadow photos;
* Relative concentration of important gas species.

Several diagnostic‘s methods are quite standard. A few methods applied are well known but their application requires extra efforts for adjustment for specific conditions of the test. As a rule each group of experimentalists improves such technique and procedure of data processing. In case of current project the most specific information is going to be obtained by passive optical spectroscopy and active absorption laser spectroscopy. Features of experimental approach, which complicate the issue, are: short time of run, strong inhomogeneity of object studied, numbers of simultaneous processes and species in interaction volume.

Computational support. Numerical modeling of flow in test facility was based on solution of three-dimensional time-dependent Reynolds Averaged Navier-Stocks equations (URANS-method) with the utilization of the wide used two-equation SST model of turbulence. Calculations were carried out from critical section of supersonic nozzle down to outlet section where zero gradients of flow parameters were fixed. No-slip and adiabatic conditions were determined on all walls and symmetry conditions were used in median section of the duct. Calculation domain contained 600000 mesh points.

At the first stage of calculations air flow without energy input in flow was considered for fixed duct height 60 mm, duct half-width 36 mm, cavity depth 12 mm and three variants of the cavity floor length: L=40, 80, and 160 mm. Steady-state solutions were obtained for L = 40 and 80 mm and time-periodical solution for L = 160 mm. In two first cases the cavity is closed and recirculation flow arises in all its volume. In third variant the cavity is open and the shear layer penetrates in cavity up to its floor. Small recirculation zones arise only near forward wall and ramp of the cavity.

Then the influence of five heat sources providing total heat input of 5 kW was considered for cavity floor length L = 80 mm. It has been established, that considered 3D heat supply leads to, particularly, significant amplification of mass transfer in the cavity. The calculated values of the mass transfer rate are equal F_0=0.0054 kg/s and F_Q=0.0074 kg/s respectively without and with heat input. Owing to heat input the pressure grows essentially not only in whole cavity, but also in a significant part of the channel. Maximum gas temperature T>15000 K is achieved on the cavity bottom close to heat sources. Significant increase of gas temperature in a cavity before vertical "cords" of heat sources is caused by recurrent flow.

References to section 2.1.

1. —Study of Plasma Assisted Ignition in Non-Premixed Air-Fuel High-Enthalpy Flows”, Ed. S. Leonov, Final Report on APL/JHU-IVTAN Contract No 854157, IVTAN, Moscow, April, 2003.
2. —Plasma Formation Influence on Ignition and Stabilization Processes and Combustion Efficiency in Hydrocarbon Fuelled Combustors.” Ed. S. Leonov, Final Report on APL/JHU-IVTAN/MTC Contract No 785461, IVTAN, Moscow, 2001.
3. S. Leonov, V. Bityurin, A. Bocharov, K. Savelkin, D. VanWie, D. Yarantsev, —Hydrocarbon Fuel Ignition in Separation Zone of High Speed Duct by Discharge Plasma”, Proceedings of the 4rd Workshop —PA and MHD in Aerospace Applications”, April, 2002, Moscow, IVTAN.

4. A. Klimov, V. Bityurin, A. Bocharov, A. Brovkin, A. Kuznetsov, S. Leonov, N. Sukovatkin, N. Vystavkin. "Plasma Assisted Combustion". Proceedings of the 3-rd Workshop "PA and MHD in Aerospace Applications", April, 2001, Moscow, IVTAN.
5. S. Leonov, V. Bityurin "Hypersonic/Supersonic Flow Control by Electro-Discharge Plasma Application." 11th AIAA/AAAF International Symposium Space Planes and Hypersonic Systems and Technologies, Orleans, 29 September – 4 October, 2002, AIAA-2002-5209.
6. S. Leonov, V. Bityurin, K. Savelkin, D. Yarantsev "The Features of Electro-Discharge Plasma Control of High-Speed Gas Flows." AIAA-2002-2180, 33-th Plasmadynamic and Laser Conference, 20-24 May, 2002, Maui, HI.
7. S. Leonov, V. Bityurin, K. Savelkin, D. Yarantsev "Effect of Electrical Discharge on Separation Processes and Shocks Position in Supersonic Airflow." 40th AIAA Aerospace Sciences Meeting & Exhibit, 13-17 January 2002 / Reno, NV, AIAA 2002-0355.
8. S. Leonov, V. Bityurin, A. Bocharov, E. Gubanov, Yu. Kolesnichenko, K. Savelkin, A. Yuriev, N. Savischenko "Discharge plasma influence on flow characteristics near wall step in a high-speed duct." The 3-rd Workshop on Magneto-Plasma Aerodynamics in Aerospace Applications, Proceedings, Moscow, IVTAN, 24-26 April, 2001.
9. S. Leonov, V. Bityurin, K. Savelkin, D. Yarantsev, Plasma-Induced Ignition and Plasma-Assisted Combustion of Fuel in High Speed Flow. Proceedings of the 5th Workshop "PA and MHD in Aerospace Applications", 7-10 April, 2003, Moscow, IVTAN.
10. Bocharov A., Bityurin V., Klement'eva I., Leonov S. Experimental and Theoretical Study of MHD Assisted Mixing and Ignition in Co- Flow Streams // Paper AIAA 2002- 2228, 40th AIAA Aerospace Sciences Meeting & Exhibit, 14-17 January 2002/ Reno, NV, P.8.
11. A.N. Bocharov, V.A. Bityurin, I.B. Klement'eva, S.B.Leonov A STUDY OF MHD ASSISTED MIXING AND COMBUSTION // Paper AIAA 2003- 0699, 42th AIAA Aerospace Sciences Meeting & Exhibit, January 2003/ Reno, NV, P.8.
12. L. Jacobsen, C. Carter, R. Baurie, T. Jackson "Plasma-Assisted Ignition in Scramjet", AIAA-2003-0871, 41st AIAA Aerospace Meeting and Exhibit, 6-9 January, Reno, NV, 2003.
13. S. Kuo, D. Bivolaru, C. Carter, L. Jacobsen, S. Williams "Operational Characteristics of a Plasma Torch in a Supersonic Cross Flow", AIAA-2003-0871, 41st AIAA Aerospace Meeting and Exhibit, 6-9 January, Reno, NV, 2003.
14. Morris R.A., Arnold S.T., Viggano A.A., Maurice L.Q., Carter C., Sutton E.A. "Investigation of the Effects of Ionization on Hydrocarbon-Air Combustion Chemistry". 2nd Weakly Ionized Gases Workshop, Norfolk, 1998.
15. Buriko Yu., Vinogradov, V., Goltsev, V., "Influence of active radical concentration on self-ignition delay of hydrocarbon fuel/air mixture". "Applied physics", 2000, P.10.
16. S.A.Bozhenkov, S.M.Starikovskaia, A.Yu.Starikovskii "Chemical Reactions and Ignition Control by Nanosecond High-Voltage Discharge", 11th AIAA/AAAF International Symposium Space Planes and Hypersonic Systems and Technologies, Orleans, 29 September – 4 October, 2002, AIAA-2002-5185.
17. Klimov A., Bityurin V., Brovkin V., Leonov S., Plasma Generators for Combustion, Workshop on Thermo-chemical Processes in Plasma Aerodynamics, Saint Petersburg, May 30- June 3, 2000, P.74.
18. Ainan Bao, Guofeng Lou, Munetake Nishihara, Igor V. Adamovich "On the Mechanism of Ignition of Premixed CO-Air and Hydrocarbon-Air Flows by Nonequilibrium RF Plasma", AIAA-2005-1197, 43rd AIAA Aerospace Meeting and Exhibit, 10-13 January, Reno, NV, 2005.
19. A. Napartovich, I. Kochetov, S. Leonov "Calculations of dynamics of hydrogen-air ignition by nonequilibrium discharge in high-speed flow", J. Thermophysics of High Temperature (rus), 2005, #2.
20. O. Voloschenko, S. Leonov, A. Nikolaev, N. Rogalsky, V. Sermanov, S. Zosimov, "Experimental study of hydrogen combustion in model supersonic duct", International Scientific Conference "High-Speed Flow: Fundamental Problems", Zhukovsky, 21-24 September 2004.
21. A. Starikovskii "Plasma Supported Combustion", invited lecture for 30th International Symposium on Combustion, Proceedings of the Combustion Institute, Chicago, 2004. Invited Lecture. P 326 .

22. S. Starikovskaia, I. Kosarev, A. Krasnochub, E. Mintoussov, A. Starikovskii —Control of Combustion and Ignition of Hydrocarbon-Containing Mixtures by Nanosecond Pulsed Discharges", AIAA-2005-1195, 43rd AIAA Aerospace Meeting and Exhibit, 10-13 January, Reno, NV, 2005.
23. I. Matveev, S. Matveeva, A. Gutsol, A. Fridman —Non-Equilibrium Plasma Igniters and Pilots for Aerospace Application", AIAA-2005-1191, 43rd AIAA Aerospace Meeting and Exhibit, 10-13 January, Reno, NV, 2005.
24. M. Brown, R. Forlines, B. Ganguly, C. Campbell, F. Egolfopoulos, —Pulsed DC Discharge Dynamics and Radical Driven Chemistry of Ignition", AIAA-2005-0602, 43rd AIAA Aerospace Meeting and Exhibit, 10-13 January, Reno, NV, 2005.
25. V. Vinogradov, I Timofeev —Initial Study of Different Plasma Discharges in a M=2 Air Flow", AIAA-2005-0988, 43rd AIAA Aerospace Meeting and Exhibit, 10-13 January, Reno, NV, 2005.
26. J. Liu, F. Wang, L. Lee, N. Theiss, P. Ronney, M. Gundersen, —Effect of Discharge Energy and Cavity Geometry on Flame Ignition by Transient Plasma", AIAA-2004-1011, 42nd AIAA Aerospace Meeting and Exhibit, 5-8 January, Reno, NV, 2004.
27. P. Magre, V. Sabel'nikov, D. Teixeira, A. Vincent-Randonnier (ONERA) —Effect of a Dielectric Barrier Discharge on the Stabilization of a Methane-Air Diffusion Flame", ISABE-2005-1147, 17th International Symposium on Air-Breathing Engines, Munich, Germany, 4-9 September 2005.

2.2. Short review of the second year efforts.

During the second year the efforts in frames of the project were arrowed on the low-temperature ignition test and preparation of the test with preheated air. The diagnostic methods were developed. Experimental works were supported by analytical and CFD efforts. The first task –Experimental study of plasma-induced ignition of non-premixed air-fuel composition under the conditions of wall step and wall cavity" included four subtasks 1.5-8 (see section 1.2). In frames of subtask1.5 the steps for the facility development, and experiments on fuel ignition in cavity and behind wallstep were performed .The subtask 1.6 arrowed on the analysis of experimental data on fuel ignition in cavity and behind wallstep. The third part (7^{th} quarter) covers draft-design of a new test section, analysis and test of refractory materials. The eighth quarter's efforts were fulfilled for the test section manufacturing and arrangement. The nozzle for the tests with preheated air was not changed due to the results of analysis of it's thermal performance.

The second task –Diagnostics development and computational support" included three subtasks 2.4-6. In frames of these subtasks the 3D Navier-Stocks computational analysis of flow structure near wallstep and cavity in supersonic duct under the discharge impact was performed. The scheme of supposed measuring system was presented. A short analysis of diagnostic methods was presented on the base of theirs availability and planned diagnostic system was announced as well. The first results of 3D Navier-Stokes computational analysis of hydrogen ignition in cavity and behind wallstep was presented in technical report

Experimental facility modification. General layout of the experimental facility PWT-50H and renewed arrangement are presented in Fig.2.2.1. It contains the following new components:

- Air heater with power supply, air supply, and fuel supply;
- IR monitor;
- Laser absorption spectroscopic system;
- Chemical analysis workstation.

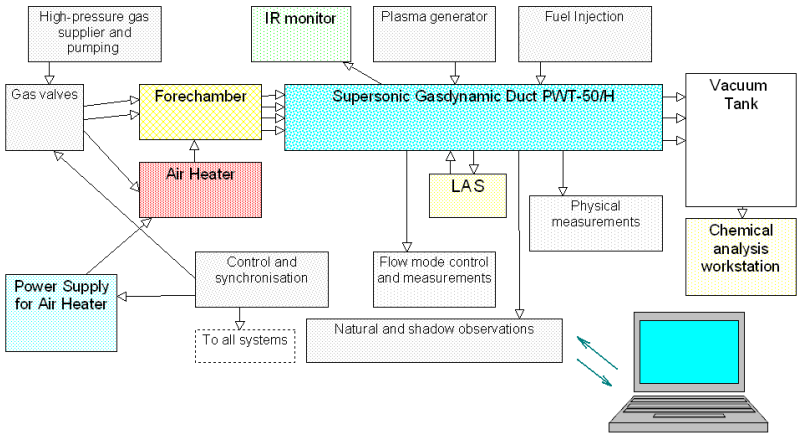

Fig.2.2.1. Layout of the PWT-50H arrangement.

The forthcoming tasks of the project require sufficient modification of experimental facility. A main change is in increase of gas temperature at operation. For this purpose a two-stages preheater is applied: electric + burner. The result of preliminary test of heater's operation was presented in the Second Year Technical Report.

Fuel ignition in cavity and behind wallstep. The numerous experiments were done at different conditions: subsonic and supersonic flow; wallstep, long cavity (l/d=6.5), and short cavity (l/d=3.3); different pressure; current from 5A to 20A; both polarities, etc. The data for wallstep and cavity in supersonic mode are shown in the Technical Report for typical electric current. Summarizing the discharge effect on pressure distribution in cavity and behind wallstep it should be considered that, as a rule, the pressure rises noticeably just near discharge zone and its distribution occurs more smooth in a cavity as a whole.

The results of the tests on hydrogen and ethylene ignition in separation zone of low-temperature supersonic flow were presented in the Technical Report. Several diagnostics were

applied: natural observations, schlieren photos, spectroscopy, pressure record, etc. The most reliable way to recognize –combustion" was a great pressure step in separation zone.

The hydrogen combustion in cavity takes place, if the power deposition in the discharge W>1kW. If the discharge was turned off, the combustion in cavity came to unstable mode. Increasing of hydrogen flow rate over stoichiometric ratio pushes the combustion above the cavity, if the power deposition is not less than W_{pl}=3kW. When the thermal power of combustion grew more than to W_{fuel}=20kW a thermal choking of the duct occurred. With hydrogen injection, the combustion takes place in the cavity as well as in the shear layer, in contrast to the combustion with ethylene. An estimation and comparison with numerical simulations indicate a level of pressure increase of ΔP=*10-20*Torr in the cavity in case the oxidizer is provided by circulating air.

It is well known that some widening of the gasdynamic duct downstream helps to prevent a thermal chocking. The Fig.2.2.2 demonstrates the hydrogen combustion in shear layer of free stream in a configuration with backwise wallstep for the hydrogen mass flow rate increased up to G_{H2}=*0.4g/sec*. The reactions were very intensive without blockage of supersonic operation mode. It is well seen how the flow disturbances produced by combustion occupied almost a whole duct.

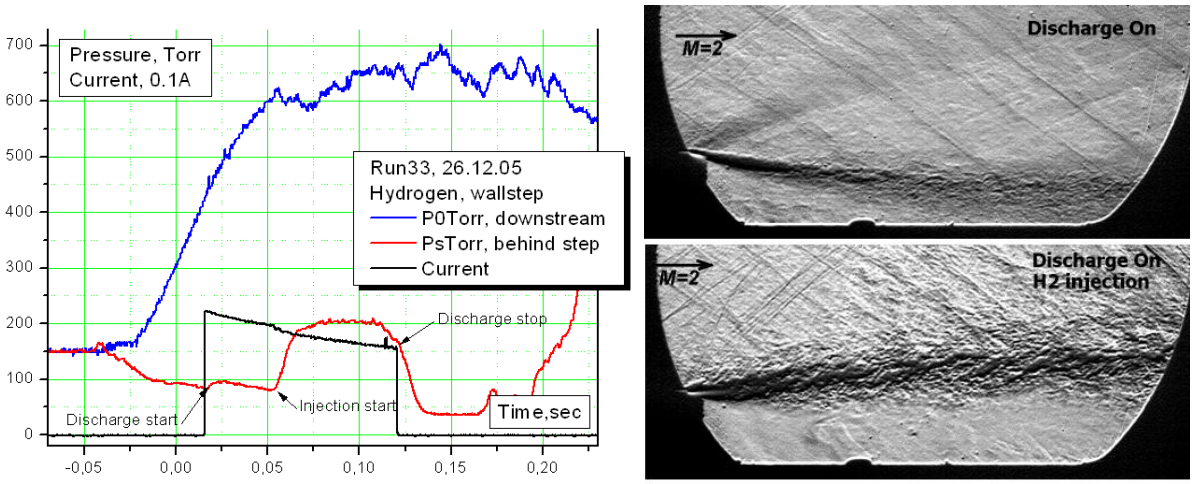

Fig.2.2.2. Discharge interaction with hydrogen behind wallstep. Pressure, schlieren photos.

Table 2.1. Plasma-assisted combustion power threshold. T0=300K, P0=1Bar.

	Threshold of ignition in separated zone	Threshold of ignition in shear layer
H2 (T0=300K)	W≈1kW	W≈3kW
C2H4 (T0=300K)	W≈4kW	W>9kW ???

That is, two modes of discharge-fuel-flow interaction were observed: fuel ignition and combustion just in a cavity, and fuel combustion in the freestream shear layer. In the case of hydrogen injection, both modes were detected. However, under our experimental conditions, ethylene combustion was detected in the cavity only. The resulting data of the plasma-assisted combustion is shown in the table below.

Diagnostics system modification and adjustment for hot test. The following parameters of the gas and plasma are supposed to be measured during the tests:

* Gas temperature, averaged and local values, T_g;
* Distribution of static and stagnation pressure, P_o, P_{st};
* Optical spectra of the excited molecules N_2, CN, OH, CH;
* Temporal evolution of optical lines OH, CH, etc.;
* Plasma energetic parameters;
* Dynamics of the ignition processes by video-records and Shadow photos;
* Relative concentration of important gas species.

Several decisions on diagnostics system modification were announced in the Technical Report. The main attention is paid for spectroscopic results and laser absorption technique the first test.

CFD analysis of filamentary plasma effect on fuel ignition.

Calculation of three-dimensional turbulent flow in the frame of reaction gas model was executed at modeling a heat supply caused by the direct current electric discharge. CFD modeling of flow in experimental set up was based on solution of 3D Reynolds Averaged Navier-Stocks equations (RANS-method) with the utilization of the wide used two-equation k-e model of turbulence. Two different channel geometries are in consideration: 1 – channel with cavity and 2 – channel with wall step as it shown in Fig.2.2.3.

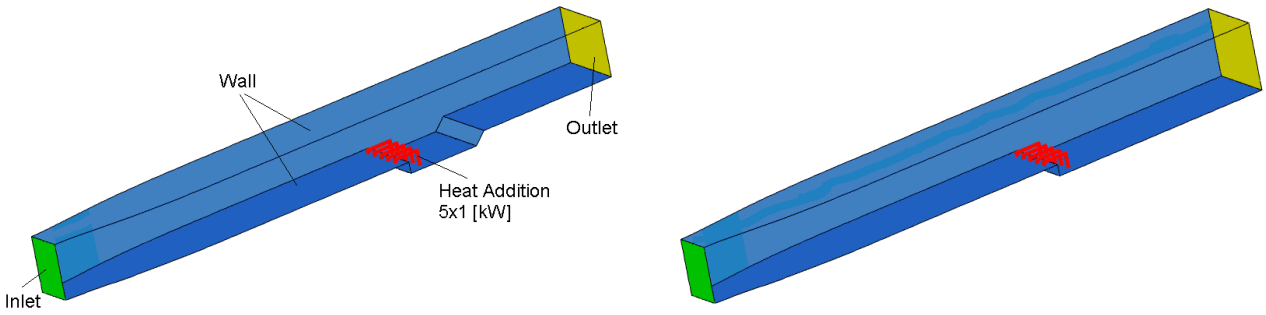

a. Channel with cavity b. Channel with wall step

Fig.2.2.3. Geometry of settlement area.

Thermal power of each source was equal to 1kW. Total heat input in the flow was equal to W=5kW. The 3D CFD of heat addition modeling takes into account the chemical reactions phenomenon, witches are critically important at high temperature.

The comparison of the results of simulation allows considering important features of combustion process: the combustion in cavity appears very intensive and the most part of the fuel completes the reactions. In the case of wallstep the most part of the fuel goes away from the zone of reactions. The increase of fuel mass flow rate leads to change the flow structure behind the wallstep and decreases the combustion completeness. The fuel jet goes to outlet instead of circulation. Such an effect was described previously. Fortunately the flow structure in real device is essentially 3D and the effect of the combustion saturation is not observed.

Analysis of results of lab-scale test of fuel ignition behind wallstep. The comparison of experimental data and results of simulations is being done for the gasdynamic configurations with cavity and backwise wallstep. Formally the conditions of experiment and CFD are very close each other. The table 2.2 presents integral result of calculations and estimation on the base of experimental data.

Table 2.2. Calculated and experimental data on the combustion completeness for wallstep-based flameholder.

	Output G_{H2}, g/s	Output G_{H2O}, g/s	Completeness
2D CFD, G_{H2}=0.1944g/s	0.162	0.307	0.16
2D CFD, G_{H2}=1.39g/s	1.32	0.742	0.05
Experiment, G_{H2}=0.4g/s	-	-	>0.6
Experiment, G_{H2}=0.9g/s	-	-	>0.55

Several notes have to be done. The fuel being injected into the zone of separation penetrates upstream wallstep with appropriate power deposition there. An interaction with shock near edge of the step leads to flow separation, and consequent amplification of fuel penetrating and the power deposition. The second valuable feature is that atomic oxygen density has a maximum forestream an area of intensive reactions and local minimum just behind the step, where a significant amount of fuel is observed. Actually two zones of combustion can be recognized: just near wallstep and downstream in the shear layer. Hopefully, the oncoming experiments give more details for comparison with more completed data of simulations.

Conclusions for the second year efforts. We considered various methods for high-speed combustion control: plasma-induced ignition, plasma-intensified mixing, and flameholding by plasma generation. The main physical mechanisms of the plasma effect are described as follows: they are not only heating of the gas and the enormously high value of radical deposition by nonequilibrium plasma, but also the flow structure regulation. The maximum effect at minimal power deposition can be realized under in-situ generation, and nonuniform discharge structure.

A previously proposed multi-electrode quasi-DC discharge through separation zone was developed for utilization in the cavity and wallstep configurations of a supersonic duct. The peculiarities of the filamentary discharge maintenance in a high-speed flow under separation were explored experimentally. 2D and 3D CFD simulation was performed to provide both a greater physical insight and a prediction of the critical parameters for the corresponding plasma-ignition experiment.

The results of model experiments on the ignition of the non-premixed air-fuel composition in high-speed, low-temperature flow behind a backward wallstep and in the cavity are presented. The energetic threshold for hydrogen ignition in the separated zone was about *W=1kW,* while the value required for plasma-assisted combustion in the shear layer was *W=3kW* for our experimental conditions. Of interest is the fact that the discharge switching off leads to immediate extinction of the hydrogen flame in the free stream, but unsteady combustion in the cavity continues if the H_2 mass flow rate is close to the stoichiometric value with respect to an air exchange rate in the separated zone of $G_{H2}\approx 0.15g/s$.

The analytical and experimental efforts in frame of project 3057p yield the following results the second year.

- The experimental facility PWT-50H was designed, assembled and tested. Modified experimental arrangement was prepared for the further test of high-temperature ignition in a separation zone of high-speed flow. Main operation modes were observed and described.
- The air heater with the power supply, and new test section were designed, manufactured and adjusted.

- The analysis of results of lab-scale test was performed on the base of experimental data and CFD simulations.
- Diagnostics‘ system for hot-air test was announced. The most diagnostic arrangement was prepared.
- 2D and 3D CFD simulations were performed for analysis of non-homogeneous energy release effect on gaseous fuel combustion in the vicinity of cavity and behind wallstep in supersonic duct.

References to section 2.2

1. –Control of Flow Structure and Ignition of Hydrocarbon Fuel in Cavity and behind Wallstep of Supersonic Duct by Filamentary DC Discharge”, *Ed. S. Leonov*, Project ISTC-EOARD-IVTAN #3057p, The second year report, December, 2006.
2. *S. Leonov, I. Kochetov, A. Napartovich, D. Yarantsev*. Plasma-Assisted Ignition and Flameholding in High-Speed Flow // Paper AIAA-2006-0563, 44th AIAA Aerospace Sciences Meeting & Exhibit, 9-12 January 2006, Reno, NV.
3. *I. Kochetov, A. Napartovich, S. Leonov* –Plasma ignition of combustion in a supersonic flow of fuel-air mixtures: Simulation problems”, J. High Energy Chemistry, **40**, 98–104, 2006.
4. *I.V. Kochetov, S.B. Leonov, A.P. Napartovich, E.A. Filimonova, D.A. Yarantsev “*Plasma-chemical reforming of the hydrocarbon fuel in the air flow”, International Workshop on *“*Thermochemical and plasma processes in aerodynamics" Saint-Petersburg, 19-21 June, 2006.
5. *S. B. Leonov, D. A. Yarantsev , A. P. Napartovich, I. V. Kochetov* –Plasma-Assisted Chemistry in High-Speed Flow”, Proceedings of the International Conference on Gas Discharges and their Applications, Xi‘an, China, 11-14 September 2006, paper L18.
6. *S. Leonov, C. Carter, M. Starodubtsev, D. Yarantsev* Mechanisms of Fuel Ignition by Electrical Discharge in High-Speed Flow // Paper AIAA-2006-7908, 14th AIAA/AHI Space Planes and Hypersonic Systems and Technologies Conference, Canberra, Australia, Nov. 6-9, 2006
7. *Sergey B. Leonov, and Dmitry A. Yarantsev* –Plasma-induced ignition and plasma-assisted combustion in high-speed flow” // **IOP**, Plasma Sources Science and Technology, **16** (2007), p.132-138, stacks.iop.org/PSST/16/132

2.3. Short review of the third year efforts.

In the third year of the project a main attention was paid for the experiments at elevated temperature of the air and for analysis of the results based on experimental data and data of computational efforts.

In the 9th quarter of the project a main activity was arrowed on the air heater adjustment, analysis of its operation after-effects, and evaluation of air temperature. A criterion of efficiency of plasma ignition is formulated. Also the progress in 3D Navier-Stokes computational analysis of fuel ignition in cavity and behind wallstep is presented in the report. Extra efforts were done to analyze the effect of the air pollution on the fuel ignition due to air heater operation. During the 10th quarter of the project a main activity was arrowed on the experiments on ethylene ignition behind wallstep at elevated temperature of air. Renewed data on the discharge behavior and plasma parameters were obtained. Also the effectiveness of fuel ignition behind wallstep was analyzed and presented in the report. In the 11th quarter a main activity was arrowed on the experiments on liquid hydrocarbon fuel ignition behind wallstep in cold flow and at elevated temperature of the air. New data on the correlation of the optical spectra with the regimes of airflow-fuel-discharge interaction were obtained and put in the Report. During the 12th quarter of the project the extra experiments were performed on the ethylene flameholding behind wallstep at different fuel mass flow-rate, different geometry of the fuel feeding, different discharge power, and different air temperature. A CFD method was applied for analysis of the experimental results on the hydrogen combustion that was obtained previously.

The air heater was adjusted and tested in typical operation modes. The temperature of the gas elevation was examined by two different methods. Significant improvement of the measuring system was fulfilled, namely, for the schlieren system, laser absorption system, and chemical station. IR monitoring was included to the list of technique for hot test. The experimental facility PWT-50H was prepared for the hot test. General layout of the facility and arrangement are presented in Fig.2.2.1.

The air heater was conjunct to separate vacuum chamber for the operation mode adjustment. These modes were also tested in regular mounting. The schlieren device was equipped by pulse source of light emission with repetitive rate f>1kHz. Tuning was performed. The workstation for the chemical analysis (CH, CO, NOx, O2, CO2) was delivered and tested.

The air heater adjustment test includes: measurement of gasdynamic and electrical parameters; visualization of the arc operation and of ethylene combustion in the heater, and chemical analysis of exhaust gas.

The chemical analysis of exhaust gases was performed by workstation –ΘPTEC-2C". Methodic of measurements includes exposure after the run and pressure equalization with atmosphere in low-pressure tank (volume V_t=0.7m^3).

The expected result of the heater operation is in the gas temperature elevation. Currently the facility is not equipped by method of direct temperature measurement. Thermocouples can't be utilized due to too fast heating and sequential cooling of the surfaces. Therefore two indirect methods were used for the temperature evaluation: calculations on the base of data on power release, and gasdynamic method based on pressure measurements. The table below presents the data of estimations of the heater operation for two values of fuel mass flow-rate (completeness $\eta=1$), and recalculation of the experimental data at $G_{C2H4}=4.35g/s$, $G_{air}=0.9kg/s$.

Table 2.3.1. Heater operation modes. Models and experiment.

	G_{C2H4}, g/s	G_{air} heater, g/s	ER	W_{el}, kW	W_{comb}, kW	W_{tot}, kW	ΔT, K
Models	5	80	0.93	50	220	270	300
	10	160	0.93	50	440	490	544
Experiment	4.35	65	0.98	55	190	245	272

The efforts were proceeded to study the features of the ethylene plasma-assisted combustion behind wallstep in cold air and at an elevated gas temperature. The modes with effective ignition and combustion were found. At the same time the heating of the air leads to narrowing of concentration limits. The estimations of the combustion completeness were done on the base of comparison with the data of numerical simulations and experimental data on the hydrogen combustion in the same configuration. The previous simulations give the relation between the power deposition and the pressure rise in separation zone. This factor is $\xi \approx (2.4 \pm 0.2)$Torr/kW in a linear part of characteristic. The results on ignition efficiency have the linear part of the dependence of the pressure rise on the fuel mass flow-rate. The grade is $dP/dG \approx 120 Torr \times s/g$, approximately. Using these data it is easy to estimate the thermal effect of the combustion:

$$h = \frac{1}{\xi} \times \frac{\partial P}{\partial G_{fuel}} \approx (50 \pm 5) kJ/g$$

This value is very close to standard heat effect of the ethylene combustion hC2H4=47.5kJ/g. So it can be considered that in a range G_{fuel}=0.16-0.8g/s the combustion efficiency is quite high, not worse that η=0.8. At G>0.9g/s the efficiency drops quickly. Under the air heater operation the efficiency is much lower due to instability of combustion front.

The experiments were carried out on the plasma-assisted combustion of ethylene in cold air and under the heater operation. The dependence of the combustion efficiency on the fuel mass flow-rate was obtained. The energetic threshold of the plasma-assisted combustion was measured for a new scheme of the fuel injection. An effectiveness of the discharge for the ignition is evaluated. A less efficiency is considered for a heated air.

Two types of the combustion instability were described: intensive oscillations and the combustion breakdown. Conditions of appearance and possible mechanisms of development are discussed. The static pressure dependence on fuel mass flow rate is shown in Fig.2.3.1. A general trend is in almost linear behavior for a lean mixture, maximal values under thermal choking, and a combustion breakdown for a rich composition. The effect of breakdown is shown in Fig.2.3.1 as well as the hydrogen injection influence on the pressure distribution itself.

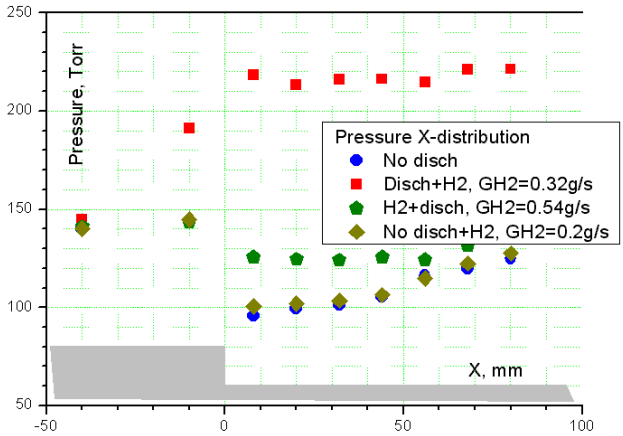

Fig.2.3.1. Effects of fuel injection, and combustion breakdown on the pressure redistribution.

The experiments on liquid hydrocarbon fuel ignition behind wallstep at low and elevated temperature of the air were performed as well. Due to a low efficiency of the fuel ignition the extra efforts were undertaken for the ignition reinforcement by hydrogen or ethylene addition. The kerosene injection to the zone of the hydrogen combustion affects on the radiation intensity, pressure, and the discharge parameters. Two main processes are under competition: a primary flame quenching, and the kerosene combustion. In the geometry behind wallstep the second process is prevailed. It becomes apparent in pressure and discharge‘s voltage increase.

The tests were performed at different fuel mass flow-rate, different geometry of the fuel feeding, different discharge power, and different air temperature. A main attention was paid for the experiments on the ethylene ignition and flameholding behind the wallstep. The test geometry was specified to avoid a thermal choking of the GD channel by means of walls‘ expansion. The ethylene was chosen as hydrocarbon fuel (the hydrogen is too easy to be ignited). The elevated temperature of air was provided by the heater in a range T0=300-620K in quasi-continuous mode and T0≤1100K in pulse mode. To have a better discharge performance as the igniter the location of fuel orifices was assorted. The fuel mass flow-rate and the discharge power release were varied as well. It was demonstrated the reducing of intensity of the fuel combustion at increase of the gas temperature under the experimental conditions. A working hypothesis is that an increase of the temperature leads to intensification of the gas circulation in separation zone and gas exchange between separated zone and main flow.

The 3D Navier-Stokes computational analysis of fuel ignition in cavity and behind wallstep was fulfilled. Extra efforts were done to analyze the effect of the air pollution on the fuel ignition due to air heater operation. The analysis demonstrates that the concentration of water vapors larger than 1% can increase the time of ignition of hydrogen at low temperature noticeably. The addition of CO2 is not so significant. The decrease of the pressure reduces the influence of impurities. Last time the works are popular where a small addition of NO is considered as an important impurity to accelerate the fuel ignition. Our simulations show that the effect appears for the C2H4 and for H2, indeed, but doesn‘t work for CH4, for instance. Significant decrease of the ignition time is observed at temperatures lower than 1300K. At T<1000K the time of ethylene ignition under 1%NO addition appears lower, than for hydrogen-air mixture. So, the effect of NO has to be taken into account very carefully.

The efficiency of plasma ignition was evaluated. As it was considered the energetic type of criterion can be taken for the rough characterization of the ignition efficiency. The most important value of this approach is the power of self-ignition W_{si}, which is a calculated power that has to be released to the gas for predefined induction time of thermal ignition. The physical criterion suggests that the thermal power of self-ignition should be related to a measured power threshold (electrical) of ignition or flame stabilization. The main result was the efficiency can be as high as η=100-300 depending on conditions.

A main result of hydrogen-air CFD simulation is the effect of combustion completeness reduction at the gas temperature increase. The figures below show the dependence of the pressure rise, and combustion completeness on fuel mass flow-rate at three different gas temperature and constant value of the discharge power W_{pl}=5kW.

The model didn‘t predict a thermal choking of the duct and instability of the combustion at rich mixture. At the same time the combustion completeness occurs a bit higher in experiment than under modeling.

The main objective of the spectroscopic measurements during those series of experiments was to find some clear, definite difference between spectral features for two cases: the former is a situation when ethylene is ignited within the discharge region, in the latter ignition does not occur in spite of the ethylene injection into the discharge region. The main spectral features of the discharge emission during its operation within the mixture of air and hydrocarbons are the

different molecular bands, such as CN (B-X violet system), C_2 (Swan band), CH, OH and some other. All these bands are typical for the combustion, but they can be exited by the discharge as well. It means that these bands are clearly seen at the discharge operation in hydrocarbons and air, whether ignition occurs or not and this fact was proved during our previous experiments. The behavior of the atomic lines for the atoms, which are important for combustion, was studied during last experiments instead of the molecular bands. These lines are H_α (656 nm) and O (777 nm). Temperature measurements by passive optical spectroscopy have given a rotational temperature of 3500 K for the measurements by N_2 (second positive system).

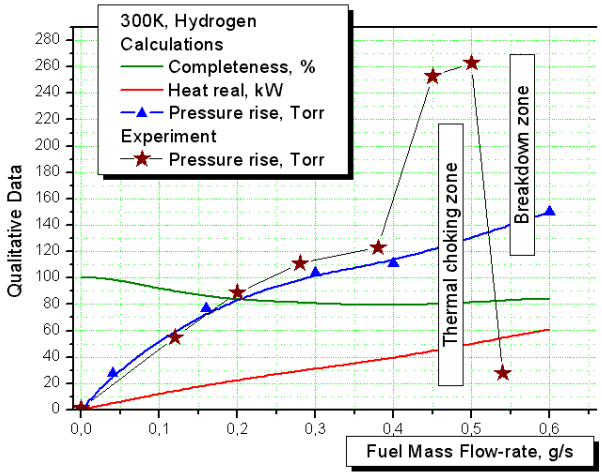

Fig.2.3.2. Pressure rise and combustion completeness as the result of modeling in comparison with experimental data. M0=2, T0=300K, W=5kW.

2.4. Short review of the fourth year efforts.

The forth year efforts were arrowed to the hydrogen and gaseous hydrocarbon fuels ignition and flameholding by transversal surface DC discharge above the plane wall of supersonic duct. This experimental work was supported by the laser-based diagnostic and computational modeling. The analysis of results of four-year work was made in the last quarter.

In the 14th quarter the efforts were arrowed on the proceeding of laser-based diagnostic adjustment for PWT-50H facility. In the 15th quarter the first results were obtained based on laser-based diagnostics, namely: gas temperature in zone located below the combustion area and H2O concentration in the same point. Those measurements were performed for the hydrogen combustion. The gas temperature occurs in a range T_{st}=*900-1100K* and the water vapors partial pressure P_{H2O}=*20-22Torr*. In the 16th quarter the results were obtained for the ethylene combustion and the temperature distribution was measured as well.

During the 16th quarter of the project performance a main work was focused on experiments for discharge based flameholding on the plane wall at elevated gas temperature. During previous efforts (15th quarter) three geometrical modes were considered for the tests: rectangular channel with 20degresses inclination of the bottom wall downstream of zone of interaction, 10degrees inclination of the bottom wall, and 10degrees inclination of the opposite to plasma generator wall. During the 15th quarter of the project two configurations were tested at T0=300K: 20° and 10° of inclination. Now it is concluded that the most correct configuration is the third model because of the actually plane wall in zone of combustion.

The flame front position is sensitive to the fuel flow rate and discharge power. The characteristic points were chosen as the most representative: Pst40 – static pressure in 40mm downstream the electrodes; Pst100, which locates in 100mm downstream; and Pst175, which locates on opposite wall in 175mm downstream. The graphs in Fig.2.4.1 show the dependence of pressure in these points on ethylene flow rate. It is clearly seen that at rich mixture the ethylene is more difficult to be ignited (requiring greater discharge power) and flamefront shifts downstream of the place of interaction. The combustion completeness is reduced as well.

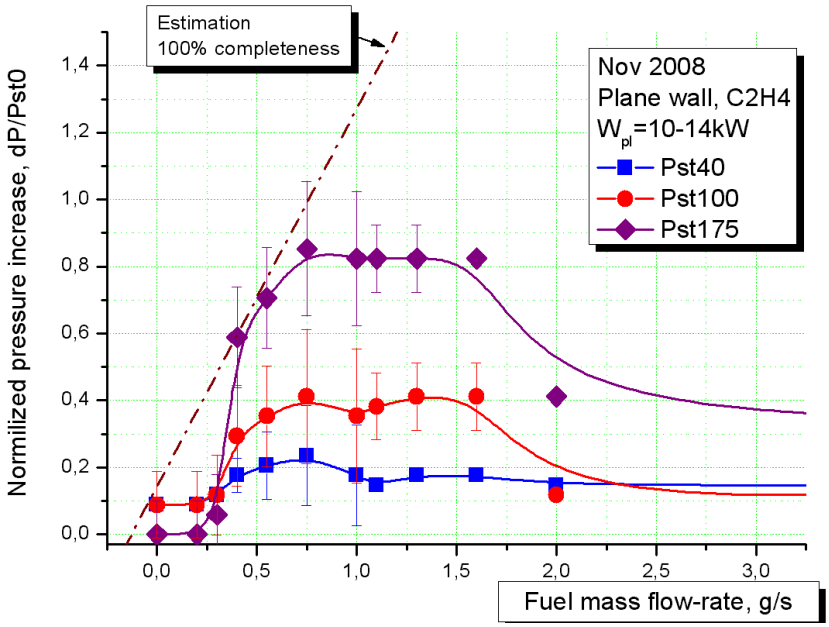

Fig. 2.4.1. Static pressure vs ethylene flow rate in various cross-sections.

As it was found out during the previous work the temperature elevation reduces the discharge abilities for the flameholding. At higher initial flow enthalpy the higher level of the discharge power is required for stable ignition and flameholding. The same effect was observed for the

plane wall configuration. A general rule is that the increase of temperature leads to shift of flamefront downstream.

Distribution of the gas temperature across the channel was measured by means of laser diode absorption spectroscopy (LDAS). At present time the test-molecule is water – H_2O. Two spectral ranges containing absorption lines of H_2O that are suitable for the DWADL have been chosen after analysis of the HITRAN and HITEMP databases – 1.39 μm and 1.41 μm. Method of the measured and theoretical spectra comparison is developed. The method is based on the transformation of the spectra to the images and sequential processing of the images by digital methods.

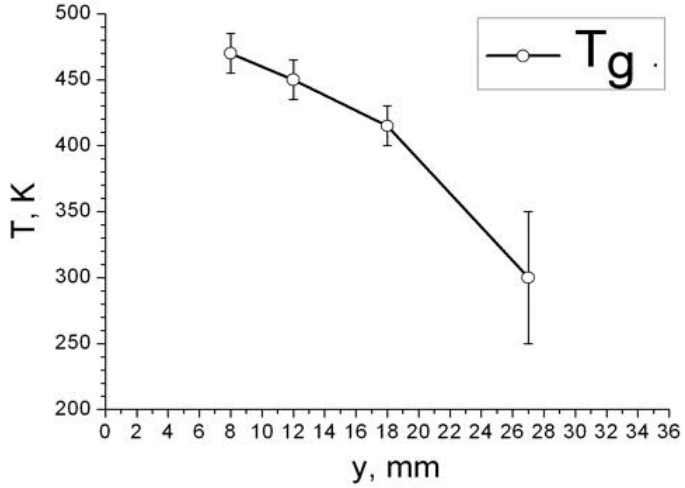

Fig. 2.4.2. Gas temperature vs distance from the wall.

Measurements were carried out in the flame region 170 mm downstream the electrodes. Laser beam was shifted in direction crossing the channel axis within the range 8-27mm from the top wall. It was impossible to make measurements closer to the wall without changing the test section, but these measurements will be done later, after some adjustment of experimental facility. Nevertheless, the trend in the Fig.2.4.2 is clear. Temperature was changing during the run, so the averaging values are presented. A linear part of the temperature distribution has been registered within the measuring region. It is of interest the temperature distribution till the axis of the channel, but there is an unstable shear layer starting from 20 mm (see schlieren images). The accuracy of the measurements in this layer is very low, estimating 100K, as it is shown in the Fig.2.4.2.

2.5. Short review of the fifth year efforts.

The work in 5th year was aimed to study the hydrogen and gaseous hydrocarbon fuels ignition and flameholding by transversal surface DC discharge above the plane wall of supersonic duct under the variation of reduced electrical field. This experimental work was supported by the spatial-resolved laser-based diagnostic to measure the specific rate of the fuel oxidation (prove of the two-stage mechanism of ignition).

In 21st quarter the tests were made on the electrical discharge optimization for the future experiments on plasma-assisted combustion. A new scheme of the laser-based non-intrusive measurements was developed as well. In 22nd and 23rd quarters the experimental work were performed to measure the dynamics of the temperature and water vapor concentration in combustion zone and downstream at the hydrogen and ethylene injection by DLAS. Extra numerical simulations were made to examine the effect of reduced field in plasma of electrical discharge on the ignition time. The results of calculations were analyzed in frames of idea of two-stage mechanism of the plasma-assisted combustion. In 24th quarter the main attention was paid for analysis of data.

Recently two-stage mechanism of Plasma-Assisted Combustion was announced by G. Mungal, M. Cappelli with coauthors for convective flame [1-2], and by S. Leonov, V. Sabelnikov with coauthors for supersonic non-premixed flame [3-4]. The idea may be briefly described as follows: in case of hydrocarbon fueling and low temperature, flame stabilization by non-equilibrium plasma occurs by means of a two-step process. During the first step the plasma induces active radicals production and so-called –preflame" (or fuel reforming in terms of Stanford's team), which may be simplified as production of H_2, CH_2O, and CO. In spite of bright luminescence, this zone does not experience significant temperature and pressure increase. This –preflame" or –cool flame" [5-7] appears as a source of active chemical species that initiates (under favorable conditions) the second step of normal –hot" combustion, characterized by high temperature and pressure rise. Now this idea is promoted as one of the most important features of plasma method for the combustion enhancement.

The major properties of the near-surface quasi-DC electrical discharge were described in previous Reports and papers [8, 9]. The regulation of power release in a range W_{pl}= 3-17kW was performed by means of electrical current change I_{pl}=2-20A. If the current is increased by a factor of 10, the voltage is decreased, but only by a factor of 5. It is resulted in rise of the power in about 2 times. Such a method leads to some variation in the reduced electric field E/N. Usually it is mentioned that non-equilibrium plasma (characterized by higher level of E/N) occurs more effective in terms of fast fuel ignition [11, for example]. In our particular case it should be considered two main factors of successful fuel ignition and flameholding: (1) the discharge power; and (2) length of the discharge filaments (the length reflects a time of interaction). All other factors appeared as much less important. Special experimental series shown a generation of sequence of active zones of reacting gas moved downstream from the place of immediate plasma-fuel interaction that is well seen in Fig.2.5.1. These zones appear as hotbeds of consequent flamefront.

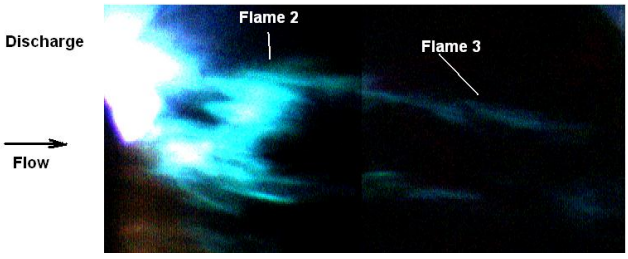

Fig.2.5.1. Discharge appearance at the ethylene injection – reacting gas luminescence in M=2 flow.

Tunable diode laser (DL) absorption spectroscopy (TDLAS) is a widely used spectroscopic technique for the detection of various parameters of heated zones [12-14]. This technique provides remote, non-perturbing measurements of the parameters of a hot zone with time resolution in the μs-ms range depending on the specific experimental conditions. The technique is usually based on the measurements of the ratio of the absorption line intensities of a test molecule. If Boltzmann distribution of the energy levels is established, the ratio of the line intensities depends only on the kinetic temperature of the object.

The parameters of the probed medium are obtained as a result of experimental spectra fitting. In most cases the individual absorption lines are fitted using Voigt profiles. This approach does not require the exact mechanism of line broadening. The temperature is inferred from the ratio of the integrals (or amplitudes) of the selected lines using the ratio calculated from spectroscopic databases. The alternative is the fitting of a whole spectral interval, which includes the selected lines. In this case the spectroscopic parameters of the lines from the databases are used. One should correctly account for different mechanisms and fit experimental line profiles using selected models of line broadening.

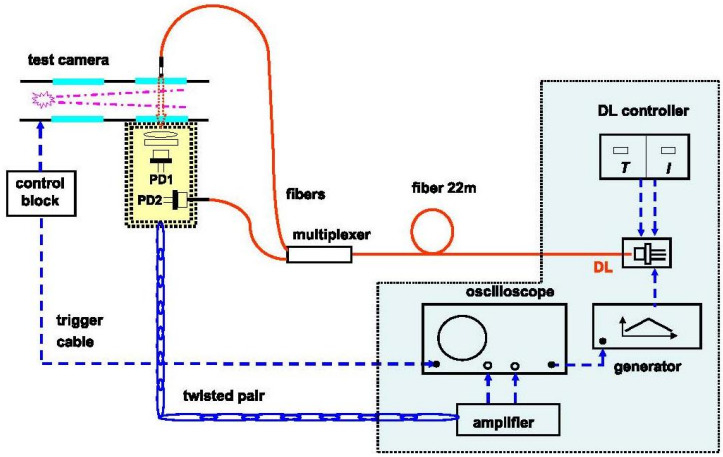

Fig.2.5.2. Scheme of DLAS measurements.

Molecular water was used as a test molecule. Water vapor is one of the major combustion products and key indicators of the extent of combustion and is therefore widely used as a tracer of combustion processes in mixed gas flows. Initially, the optimal TDLAS strategy was developed in laboratory experiments with stable conditions in an evacuated cell filled with the air. The optimized and validated version of the TDLAS technique was then applied to the measurement of the temperature, total gas pressure, and H_2O concentration in a plasma-assisted supersonic combustion flow.

The selection of the specific spectral lines was dictated by several reasons: the energies of low levels should be different, the lines should be reasonably resolved and the spectral interval should be free from lines of other gas components. The following H_2O absorption lines were selected: 7189.344 cm^{-1} (E'' = 142 cm^{-1}), 7189.541 cm^{-1} (E'' = 1255 cm^{-1}), 7189.715 cm^{-1} (E'' = 2005 cm^{-1}). All lines could be recorded in a single scan of the DL wavelength across a $\Delta\lambda\sim$ 1 cm^{-1} spectral interval.

The final version of the experimental set-up is shown in Fig.2.5.2. All parts of the set-up constrained by the dashed line in Fig.2.5.2 were located in the separate room. The DL beam was routed to the chamber via a 22 m-long single-mode fiber (core ∅ 9 μm). Besides this 22m long fiber all other components were the same as in the laboratory experiments: fiber multiplexer, which divided the beam into two channels (signal and reference), end gradient collimators, collecting lens and photodiodes. The optical path inside the test chamber was 7 cm. The DL beam probed a cross-section of about 2 mm within the combustion zone. The collimator of the signal beam was fixed in an optical head, which was solidly mounted at the

input window flange of the chamber. The head could be precisely translated in x-y directions and angularly aligned.

The basic results of study of plasma-assisted flameholding in high-speed flow can be found in publications [3-4, 8-9, 15]. Ignition and flameholding were realized for H_2 and C_2H_4 fuelling on a plane wall by using a transversal electrical discharge at relatively low power deposition (<2% of flow enthalpy). The power threshold for a hydrogen flameholding was measured to be W_{pl}<3kW; with ethylene fuelling it was measured to be W_{pl}≥4kW. The combustion efficiency was estimated and it is found sufficiently high, about 0.9, for both hydrogen and ethylene. The ignition effect of the gas discharge was compared for different levels of the power, power density, and reduced electrical field (characterizing the departure from equilibrium for the discharge).

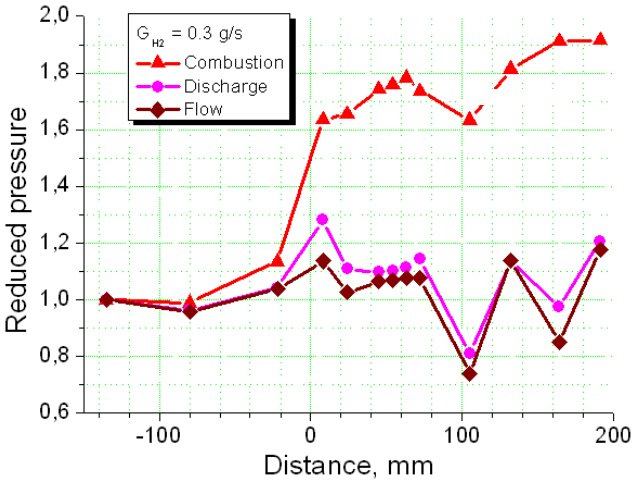

Fig.2.5.3. Evolution of wall pressure. Hydrogen injection, discharge power W_{pl}=8kW. X=0 – electrodes line.

The typical data are presented to clarify the result of interaction. The DLAS measurements were recorded using also the additional window of the test section. The wall pressure distributions in Fig.2.5.3 for hydrogen combustion illustrate details of plasma-fuel-flow interaction. One can conclude that the combustion zone locates not only in immediate vicinity of the zone of discharge and the fuel feeding.

The DLAS measurements were fulfilled in typical operation modes: plasma power was W_{pl}=8kW, hydrogen mass flow rate was G_{H2}=0.3g/s, and the ethylene G_{C2H4}=0.8g/s. The typical absorption spectra are shown in Fig.2.5.3 for ―cold" and ―hot" conditions. They were averaged over 30 scans. In some cases a high signal-to-noise ratio enabled spectral fitting with fewer averaged scans. In reality the fluctuations of gas parameters is observed strong, especially in vicinity of fuel injection place.

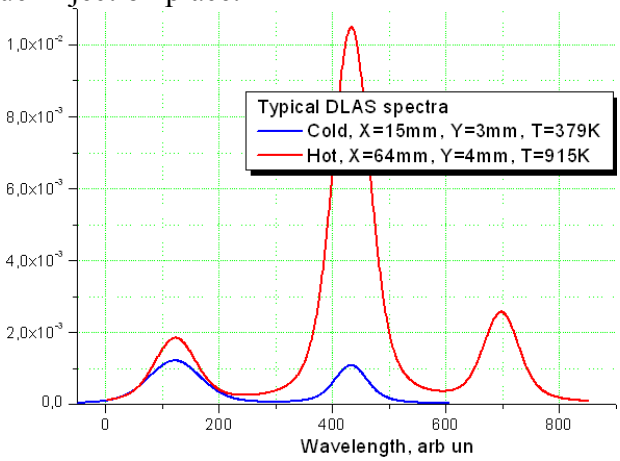

Fig.2.5.3. Typical absorption spectra of water vapors for two zones of flowfield.

The temperature distribution along the combustor obtained as a result of such fitting is shown in Fig.2.5.4. Each point in the figure was obtained in individual run of the facility. The values of the temperature inferred from both slopes coincide reasonably well. The water vapor partial pressure measured in a parallel way is presented in Fig.2.5.5. The estimated precision (statistical error) of the temperature measurements was $\sigma = 40$ K.

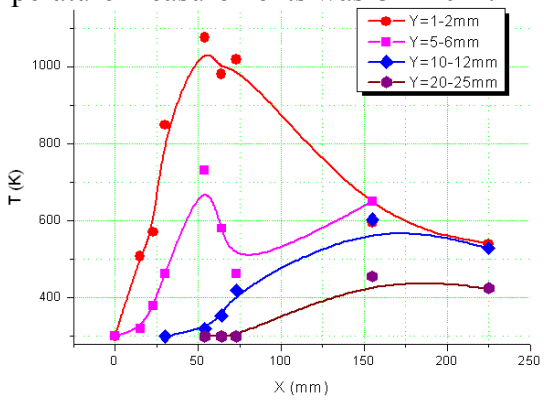

Fig.2.5.4. Temperature distribution measured by DLAS. X axis is along the flow direction. Y is the distance from the wall.

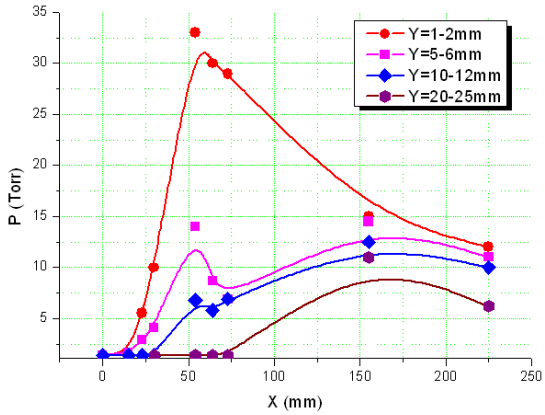

Fig.2.5.5. Water vapor partial pressure in plasma assisted combustor.

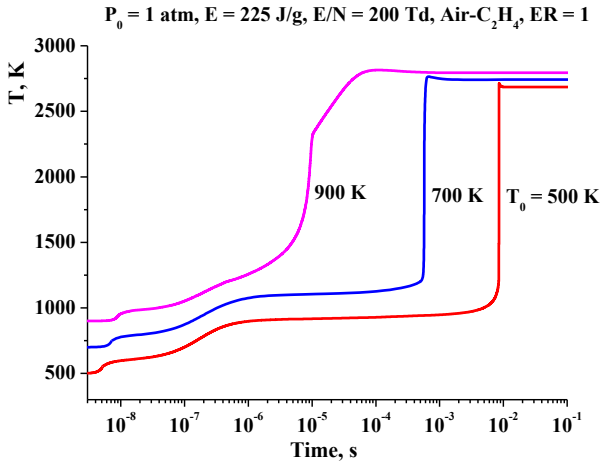

Fig.2.5.6. Calculations: dynamics of gas temperature due to plasma effect on combustible mixture at initial temperature variation. $P_0 = 1$ atm, E = 225 J/g, E/N = 200 Td, Air-C_2H_4, ER = 1.

To explain the above observations, we propose the following two-zone (it reflects the two-stage ignition process) scheme of the plasma assisted flameholding. Zone 1, in which the ~~c~~old" combustion takes place accompanied by plasma-induced fuel conversion and relatively small power release. Note, that the combustion layer in this zone is rather thin. It is actually the shear layer, where the mixing is additionally promoted by the plasma filaments. Despite of high gas temperature here a total heat release is not big. Zone 2, in which the combustion is

completed or almost completed with high energy release. Intensive mixing limits the gas temperature elevation. We emphasize that the plasma is the key element of this scheme: it launches the cold combustion inside of the first zone by generating high amount of active species. The lengths of the first zone in our tests were measured by the schlieren and schlieren-streak technique in the range of from 50mm to 150mm. It corresponds to the induction time range $\tau_{ind}=0.1\text{-}0.3ms$.

The simulations performed proved the two-stage mechanism of plasma-induced ignition as it is shown in Fig.2.5.6. Such a mechanism is appeared mostly at intermediate level of initial gas temperature $T_g=500\text{-}800K$. At higher temperature the thermal mechanism is prevailed concealing the plasma effect.

References to section 2.5.

1. Hyungrok Do, M. Godfrey Mungal, and Mark A. Cappelli ―Jet Flame Ignition in a Supersonic Crossflow Using a Pulsed Nonequilibrium Plasma Discharge", *IEEE Transactions on Plasma Science*, Vol. 36, No 6, Dec 2008, pp. 2918-2923
2. Wookyung Kim, M. Godfrey Mungal, Mark A. Cappelli, ―The role of in situ reforming in plasma enhanced ultra-lean premixed methane/air flames", *Combustion and Flame*, 157 (2010), 374–383
3. Leonov S.B., Carter C., Yarantsev D.A. ―Experiments on Electrically Controlled Flameholding on a Plane Wall in Supersonic Airflow", Journal of Propulsion and Power, 2009, vol.25, no.2, pp.289-298
4. Sergey Leonov, Dmitry Yarantsev, Vladimir Sabelnikov, Electrically Driven Combustion near Plane Wall in M>1 Duct, 3rd EUCASS Proceedings, July 2009, Versailles, France
5. Basevich, V. Ya. Chemical kinetics in the combustion processes. In: ―Handbook of heat and mass transfer". V. 4 (Ed. N.Cheremisinoff), Houston: Gulf. 1990, p. 769
6. Sokolik A. S., ―Self-ignition and combustion in gases", *UFN (rus)*, XXIII, issue 3, 1940, pp.209-250
7. Kim W., Mungal M. G., and Cappelli M. A., ―Formation and Role of Cool Flames in Plasma-assisted Premixed Combustion," *Appl. Phys. Lett.*, vol. 92, 051503, Feb. 2008.
8. Leonov S. B., Yarantsev D. A., Napartovich A. P., Kochetov I. V. ―Plasma-Assisted Combustion of Gaseous Fuel in Supersonic Duct", Plasma Science, IEEE Transactions on Plasma Science, 2006, Volume: 34, Issue: 6, pp.2514-2525.
9. Leonov S. B., Carter C., Savelkin K. V., Sermanov V. N., and Yarantsev D. A., ―Experiments on Plasma-Assisted Combustion in M=2 Hot Test-Bed PWT-50H," 46th AIAA Aerospace Sciences Meeting and Exhibit (Reno, Nevada, USA, 7-10 January 2008), AIAA-2008-1359.
10. M.A. Bolshov, Y.A. Kuritsyn, V.V. Liger, V.R. Mironenko, S.B. Leonov, D.A. Yarantsev, ―Measurements of the temperature and water vapor concentration in a hot zone by tunable diode laser absorption spectrometry", *Appl. Phys. B*, vol. 100, 2010, p. 397.
11. I.V. Adamovich, I. Choi, N. Jiang, J.-H Kim, S. Keshav, W.R. Lempert, E. Mintusov, M. Nishihara, M. Samimy, and M. Uddi, ―Plasma Assisted Ignition and High-Speed Flow Control: Non-Thermal and Thermal Effects", Plasma Sources Science and Technology, vol. 18, 2009, p. 034018
12. C.D. Lindstrom, K.R. Jackson, S. Williams, R. Givens, W.F. Bailey, C.J. Tam, W.F. Terry, AIAA Journal 47, 2368 (2009).
13. S.T. Sanders, J.A. Baldwin, T.P. Jenkins, D.S. Baer, R.K. Hanson, Proc. Combust. Inst. 28, 587 (2000).
14. A. Rousseau, E. Teboul, N. Sadeghi, Plasma Sources Science & Technology 13, 166 (2004).
15. Leonov S. B., Sabelnikov V.A., Yarantsev D. A., Napartovich A. P., Kochetov I. V. ―Plasma-Induced Ethylene Ignition and Flameholding in Confined Supersonic Air Flow at Low Temperatures", Plasma Science, IEEE Transactions on Plasma Science, 2011, February, accepted for publishing.

3. Background.

3.1. Plasma assistance for high-speed combustion.

The properties of electrical discharges strongly depend on the conditions of excitation, flow parameters and characteristics of supplying electromagnetic power. The mechanisms of the plasma of electrical discharges influence on chemical processes in high-speed flow may be considered as follows: fast local heating of the medium; active radicals and particles deposition; shock waves generation; photo-dissociation and ionization; and mixing due to vorticity and turbulence [1-5].

Local heating of the medium leads to intensification of the chemical reactions in these areas and modification of flow structure by means of controlled energy deposition. At a sufficiently large input power, the artificial separation of the flow near wall can be realized. This results in an increase in local residence time and provides a zone of local combustion and the real mechanism of the mixing intensification as well. Deposition of active radicals occurs due to molecular dissociation and excitation by electrons within the electric field and by more complex processes. If the chain chemical reactions are realized, the deposition of active particles may lead to large (synergetic) benefit in reactions‘ rate as well as in the required amplitude of power deposition. Furthermore, generation of local shocks promotes the mixing processes in a heterogeneous medium and initiates chemical reactions due to the heating and pressure rise in shock‘s front zone. The diagram in Fig.3.1.1 illustrates the idea and the contents of Plasma-Assisted Combustion domain in the most simplified form.

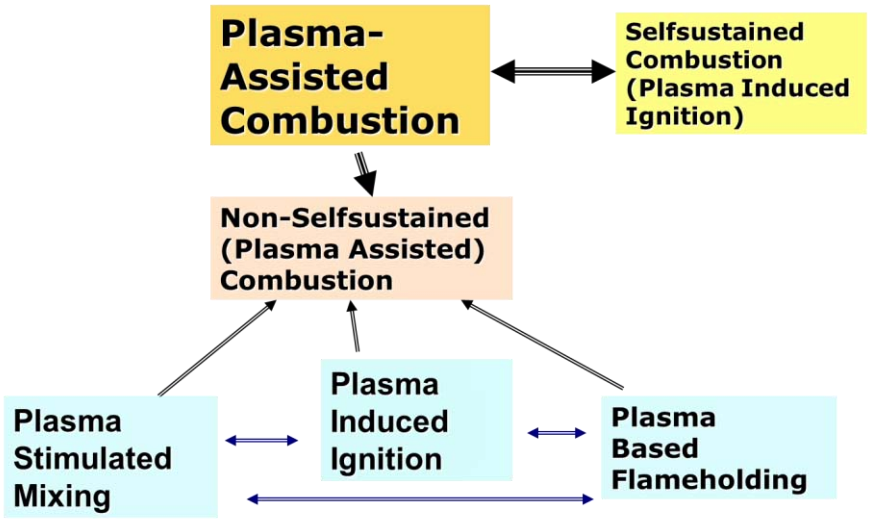

Fig.3.1.1. Diagram of PAC contents.

Last decade several experimental and analytical works have been published on the subject of plasma-assisted combustion. The main objective of those works is to expand the operational field of scramjet to off-design values of Mach number at fixed geometry of gasdynamic duct. A brief review of selected works follows.

The papers [6-7] present nonequilibrium RF plasma assisted combustion experiments in CO-air, ethylene-air, and methane-air flows using FTIR absorption spectroscopy and visible emission spectroscopy. Results of combustion completeness and emission spectroscopy measurements suggest that O and H atoms, as well as OH radicals are among the key species participating in plasma chemical fuel oxidation reactions. Consistent with their previous measurements, the results show the highest fuel oxidation efficiency in lean air-fuel mixtures, as well as significant fuel conversion at the conditions when there is no flame in the test

section. In the latter case, fuel species oxidation occurs in plasma chemical reactions, which are not related to combustion.

In the works [8-10] the numerical simulations of hydrogen-air ignition by a nonequilibrium gas discharge in supersonic flow was considered. The model of the discharge within a chemically-active mixture was developed at the first time. The combustion acceleration effectiveness strongly depends on the initial temperature and energy release. With static temperature of 700K, Mach number *M=2.5,* atmospheric pressure, and power release about 200J/l, the induction time is 3.4 times shorter than with thermal initiation. That calculation was done for the conditions of the actual experiment, described in [11]. Hydrogen and ethylene were the employed fuels.

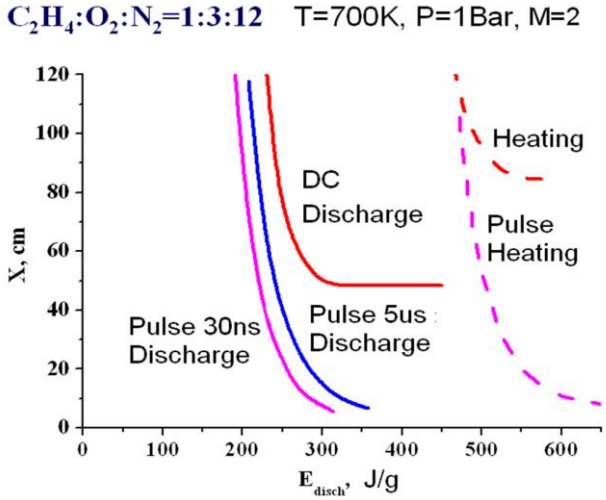

Fig.3.1.2. Results of plasma-chemical simulation. Ignition length vs power deposition by discharge or equivalent amount of thermal energy.

With respect to technical simplicity, combined with low sensitivity to gas composition, one of the discharges was chosen for modeling, namely the transverse glow discharge in high-speed airflow [12-13], which can be considered as a straightforward extension of the conventional low-pressure glow discharge to the regime of high atmospheric pressure. Specific electrode construction, in combination with appropriate gas flow and distributed ballast resistors, stabilize this discharge for many gas mixtures. The measured efficiency for energy deposition into the gas is not less than 90%. A numerical model was developed combining traditional approach of thermal combustion chemistry with advanced description of the plasma kinetics based on solution of the electron Boltzmann equation. This approach allows us to describe self-consistently a strongly nonequilibrium electric discharge in a chemically reacting gas. Our model includes an electron Boltzmann equation solver calculated in parallel with the kinetic equations for charged particles, excited molecular states, ion-molecule reactions and chemical reactions. The effectiveness of chemically active species, produced in a steady state glow discharge, on ignition delay time was studied for mixtures of hydrogen and ethylene with dry air (see Fig.3.1.2), while the effectiveness of pulse-periodic discharge in shortening ignition time was explored for a hydrogen-air stoichiometric mixture only. Here, it was found that the pulse discharge is indeed more effective (shorter ignition time at the same energy input), but the effect is comparatively weak (about 20% difference in required energy input).

Numerous publications were issued by the NEQ-Lab MIPT group, [4, 14-17] and many newer, where an in-depth analysis of plasma-chemical kinetics under the plasma assistance was described. It was found that nonequilibrium, nanosecond-pulse discharge can affect the flame blow-off velocity significantly due to the formation of active radicals. This occurs with an energy input that is negligible in comparison with burner‘s chemical power.

The successful efforts are being performed for plasma-assisted combustion with colleagues at the Air Force Research Laboratory, AFRL. Recent publications [18-21] are devoted to development of a plasma igniter for use in high-speed and high-altitude air vehicles. Such an igniter produces a rich pool of radicals that would drive pre-ignition chemistry leading to ignition. The ignition concept demands nonequilibrium plasma characterized by a high degree of feed-gas dissociation and little direct heating of the gas.

The group of –Applied Plasma Technology" announced some devices for fuel ignition and flame stabilization [22]. The results indicated significant advantages of the selected nonequilibrium plasma generator in comparison with the thermal plasma sources.

An experimental effort—focused on a comparative test of different plasma sources by the criteria of ignition efficiency in high-speed flow—is being carried out by joint Russian team from MSU, CIAM and IGP [23-24].

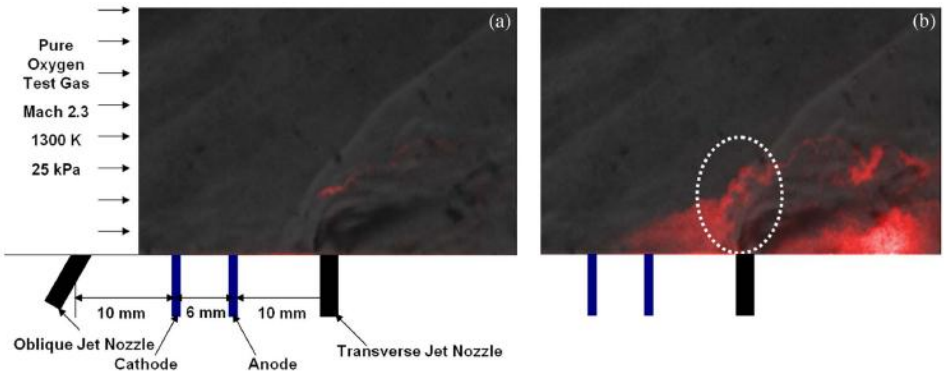

Fig.3.1.3. Schlieren images overlapped with the OH PLIF images: (a) Without and (b) with the pulsed discharge. Supersonic combustion of H2 in pure oxygen freestream (Ma = 1.7-2.4, T_{static} = 900-1300 K, P_{static} = 16-25 kPa). From [25].

A large series of experimental and computational works was performed by group of Mungal-Cappelli of Stanford University for non-premixed fuel-air and fuel-oxygen ignition [25-28], see Fig.3.1.3. These works are accented on mechanism of fuel conversion in plasma and –eool" flame features.

The ONERA efforts are arrowed on premixed flame enhancement by non-equilibrium plasma [29-31].

The experiments on non-premixed fuel ignition in high-speed flow by means co-called plasma torches were performed by groups from Tohoku University and Virginia Tech University [32-33], see Fig.3.1.4. These experiments demonstrate at the first time that the plasma can play role of flameholder being arranged on plane wall of the combustor.

Fig.3.1.4. Fuel jet ignition by the plasma torch.

Several groups have demonstrated ignition of premixed air-fuel composition and flame acceleration by non-equilibrium discharges (see for example refs. 34-36). As a rule in those works the conditions are rather far from practical schemes of high-speed combustion. Some successful tests were performed in high-speed flow as well [37-39].

In the most practical schemes of supersonic combustion, the static gas temperature is too low to provide a short induction time and sufficiently high rate of reactions. The limitations

become stronger if a fuel is not premixed with oxidizer. An increase of gas temperature can be achieved by partial stagnation of the flow or by a heat addition. In the first case an advantage of supersonic combustion is lost. In the second case too much extra energy may be required to be practical. In both cases an efficiency of the thermodynamic cycle drops and more refractory materials must be utilized. It is clear, however, that plasma of electrical discharge is able to ignite fuel-oxidizer mixtures. The problem is to acquire the effect at low levels of average power deposition. For this reason the nonequilibrium, unsteady, and nonuniform modes of discharge operation are under analyses (3-―non" approach).

In particular, plasma generation in the flow results not only in heat and active media production, but also in the modification of supersonic flow structure, including artificial separation, vorticity, etc. The plasma and the recirculation zone are interdependent, which leads to a self-adjustment loop: the plasma modifies the chemistry, which in turn modifies the heat release, which in turn modifies the recirculation zone location, which in turn modifies the plasma parameters, and so on. This feedback is an important feature of active flame control by electrical discharges. In case of hydrocarbon fuel under low temperature conditions, the process of flame stabilization by non-equilibrium plasma occurs in two phases. In the first phase the plasma induces fuel reforming, which results in first approximation in H_2 and CO production. In spite of its bright luminescence, this zone is not associated with significant temperature elevation and pressure increase. This so-called ―cool flame" appears as a source of active chemical species, which initiates (under favorable conditions) the second phase of ―normal" flame characterized by temperature and pressure rise.

The principle of the method of supersonic flameholding and combustion control by plasma of electrical discharge was described earlier; it consists in the following items:

- instead of fixed separation zones based on mechanical elements (wallstep, cavity, pylon, strut, etc.) the area of local separation is being created by near-surface electrical discharge plus fuel jets based on flush-mounted electrodes and orifices;
- the plasma generator and fuel injector are gathered under one single unit utilized for fuel ignition, flameholding, and combustion control;
- the location of this unit along the duct, its activation and switching off, as well as the magnitude of input parameters are chosen based on maximal engine efficiency and controlled by active feedbacks.

Prospectively the use of this method might lead to a reduction of total pressure losses under non-optimal conditions, an enhancement of operation stability and, consequently, to the extension of the air-breathing corridor of scramjet operability,

Last time many international meetings include the plasma-assisted combustion sessions to their schedule. The number of publications grows quickly. At the same time it is clear that some important events/features have not been studied in frames of those works and extra efforts are needed to be done in this field.

References to section 3.1.

1. S. Leonov, V. Bityurin ―Hypersonic/Supersonic Flow Control by Electro-Discharge Plasma Application." 11th AIAA/AAAF International Symposium Space Planes and Hypersonic Systems and Technologies, Orléans, 29 September – 4 October, 2002, AIAA-2002-5209.
2. L. Jacobsen, C. Carter, R. Baurie, T. Jackson ―Plasma-Assisted Ignition in Scramjet", AIAA-2003-0871, 41st AIAA Aerospace Meeting and Exhibit, 6-9 January, Reno, NV, 2003.
3. D. VanWie, D.Risha, C. Suchomel ―Research Issues Resulting from an Assessment of Technologies for Future Hypersonic Aerospace Systems", 42th AIAA Aerospace Sciences Meeting and Exhibit, Reno, NV, 5-8 January 2004, AIAA 04-1357.

4. Starikovskaia S. M., ―Plasma assisted ignition and combustion,‖ J. Phys. D, Appl. Phys., vol. 39, no. 16, pp. R265–R299, Aug. 2006.

5. S. B. Leonov, D. A. Yarantsev , A. P. Napartovich, I. V. Kochetov, ―Plasma-Assisted Chemistry in High-Speed Flow‖, Proceedings of the International Conference on Gas Discharges and their Applications, Xi‘an, China, 11-14 September 2006, paper L18.

6. Ainan Bao, Guofeng Lou, Munetake Nishihara, Igor V. Adamovich ―On the Mechanism of Ignition of Premixed CO-Air and Hydrocarbon-Air Flows by Nonequilibrium RF Plasma‖, AIAA-2005-1197, 43rd AIAA Aerospace Meeting and Exhibit, 10-13 January, Reno, NV, 2005.

7. Lou, A. Bao, M. Nishihara, S. Keshav, Y. G. Utkin, J. W. Rich, W. R. Lempert, and I. V. Adamovich, ―Ignition of premixed hydrocarbon–air flows by repetitively pulsed, nanosecond pulse duration plasma,‖ *Proc. Combust. Inst.*, vol. 31, no. 2, pp. 3327–3334, Jan. 2007.

8. A. Napartovich, I. Kochetov, S. Leonov, ―Study of dynamics of air-hydrogen mixture ignition by non-equilibrium discharge in high-speed flow‖, J. of High Temperature (rus), No. 5, 2005, p.667.

9. I. V.Kochetov, A. P. Napartovich, and S. B. Leonov, ―Plasma Ignition of Combustion in a Supersonic Flow of Fuel Air Mixtures: Simulation Problems,‖ High Energy Chemistry 40 (2006), 98-104.

10. Leonov S. B., Yarantsev D. A., Napartovich A. P., Kochetov I. V. ―Plasma-Assisted Combustion of Gaseous Fuel in Supersonic Duct‖, Plasma Science, IEEE Transactions on Plasma Science, 2006, Volume: 34, Issue: 6, pp.2514-2525.

11. O. Voloschenko, S. Leonov, A. Nikolaev, N. Rogalsky, V. Sermanov, S. Zosimov, ―Experimental study of hydrogen combustion in model supersonic duct‖, International Scientific Conference ―High-Speed Flow: Fundamental Problems‖, Zhukovsky, 21-24 September 2004.

12. Akishev Yu. S., Kochetov I. V., Leonov S. B., Napartovich A. P. Production of chemical radicals by self-sustained discharge in air gas flow. // Proceedings of 5th International Workshop on Magneto-Plasma Aerodynamics for Aerospace Applications, Moscow, IVTAN, April 2003.Yu. S. Akishev, A. A. Deryugin, I. V. Kochetov, A. P. Napartovich, and N. I. Trushkin, J. Phys. D.: Appl. Phys., **26**, 1630, 1993.

14. A. Starikovskii ―Plasma Supported Combustion‖, invited lecture for 30th International Symposium on Combustion, Proceedings of the Combustion Institute, Chicago, 2004. Invited Lecture. P 326 .

15. S. Starikovskaia, I. Kosarev, A. Krasnochub, E. Mintoussov, A. Starikovskii ―Control of Combustion and Ignition of Hydrocarbon-Containing Mixtures by Nanosecond Pulsed Discharges‖, AIAA-2005-1195, 43rd AIAA Aerospace Meeting and Exhibit, 10-13 January, Reno, NV, 2005.

16. I.N. Kosarev, N.L. Aleksandrov, S.V. Kindysheva, S.M. Starikovskaia, A.Yu. Starikovskii, Kinetics of ignition of saturated hydrocarbons by nonequilibrium plasma: CH4-containing mixtures, Combustion and Flame 154, 569-586 (2008).

17. I.N. Kosarev, N.L. Aleksandrov, S.V. Kindysheva, S.M. Starikovskaia, A.Yu. Starikovskii, Kinetics of ignition of saturated hydrocarbons by nonequilibrium plasma: C2H6- to C5H12-containing mixtures, Combustion and Flame 156, 221-233 (2009).

18. M. Brown, R. Forlines, B. Ganguly, C. Campbell, F. Egolfopoulos, ―Pulsed DC Discharge Dynamics and Radical Driven Chemistry of Ignition‖, AIAA-2005-0602, 43rd AIAA Aerospace Meeting and Exhibit, 10-13 January, Reno, NV, 2005.

19. Jacobsen, L. S., Carter, C. D, Baurle, R. A., Jackson, T., Williams, S., Barnett, J., Tam C.-J., Bivolaru, D., and Kuo, S., ―Plasma-Assisted Ignition in Scramjets,‖ Journal of Propulsion and Power, Vol. 24, No. 4, 2008, pp. 641–654. doi:10.2514/1.27358

20. Marcum, S.D. and Ganguly, B.N., ―Electric-field-induced flame speed modification‖, Combustion and Flame, 143 (1), 2005, pp.23-36

21. T. Ombrello, X. Qin, Y. Ju, A. Gutsol, A. Fridman, and C. Carter, "Combustion enhancement via stabilized piecewise nonequilibrium gliding arc plasma discharge," *AIAA J.*, vol. 44, no. 1, pp. 142–150, Jan. 2006.

22. I. Matveev, S. Matveeva, A. Gutsol, A. Fridman "Non-Equilibrium Plasma Igniters and Pilots for Aerospace Application", AIAA-2005-1191, 43rd AIAA Aerospace Meeting and Exhibit, 10-13 January, Reno, NV, 2005.

23. V. Vinogradov, I Timofeev "Initial Study of Different Plasma Discharges in a M=2 Air Flow", AIAA-2005-0988, 43rd AIAA Aerospace Meeting and Exhibit, 10-13 January, Reno, NV, 2005.

24. I.I. Esakov, L.P. Grachev, K.V. Khodataev, V.A. Vinogradov, and D.M. Van Wie, Propane–Air Mixture Combustion Assisted by MW Discharge in a Speedy Airflow, IEEE Transaction on Plasma Science 34 (6), 2497-2506 (2006).

25. H. Do, S-K Im, M.A. Capelli and M.G. Mungal, "Plasma assisted flame ignition of supersonic flows over a flat wall", Combustion and Flame (2010)

26. Hyungrok Do, M. Godfrey Mungal, and Mark A. Cappelli "Jet Flame Ignition in a Supersonic Crossflow Using a Pulsed Nonequilibrium Plasma Discharge", *IEEE Transactions on Plasma Science*, Vol. 36, No 6, Dec 2008, pp. 2918-2923

27. Kim W., Mungal M. G., and Cappelli M. A., "Formation and Role of Cool Flames in Plasma-assisted Premixed Combustion," *Appl. Phys. Lett.*, vol. 92, 051503, Feb. 2008.

28. Wookyung Kim, M. Godfrey Mungal, Mark A. Cappelli, "The role of in situ reforming in plasma enhanced ultra lean premixed methane/air flames", *Combustion and Flame*, 157 (2010), 374–383

29. P. Magre, V. Sabel'nikov, D. Teixeira, A. Vincent-Randonnier (ONERA) "Effect of a Dielectric Barrier Discharge on the Stabilization of a Methane-Air Diffusion Flame", ISABE-2005-1147, 17th International Symposium on Air-Breathing Engines, Munich, Germany, 4-9 September 2005.

30. Vincent-Randonnier, A., and Teixeira, D "Combustion Enhancement and Stabilization by Plasma Discharges: Investigation on the Plasma/Flame Interaction". Proceedings of the International Symposium on Applied Plasma Science, 7, 47-50, (2009)

31. A. Vincent-Randonnier, Combustion enhancement and stabilization: principles of plasma assistance and diagnostics tools, Handbook on Combustion, Vol. 5: New Technologies, Wiley VCH publisher, 125-160 (2010)

32. K. Takita, K. Murakami, H. Nakane, G. Masuya, A novel design of a plasma jet torch igniter in a scramjet combustor, Proceedings of the Combustion Institute 30 (2005) 2843–2849

33. Takita K. Ignition and Flame-Holding by Oxygen, Nitrogen and Argon Plasma Torches in Supersonic Airflow, Combustion and Flame. 2002. V. 128. P. 301.

34. V. V. Naumov, A. P. Chernukho, A. M. Starik, and N. S. Titova, Modeling of plasma-chemical initiation of detonation in a supersonic flow of combustible mixtures Combustion and atmospheric pollution, in Combustion and atmospheric pollution, Ed. G D. Roy, S M Frolov and A M Starik, Moscow: Torus Press, 312-317 (2003).

35. A. M. Starik and N. S. Titova, Possibility of Initiation of Combustion of CH_4-O_2 (Air) Mixtures with Laser-Induced Excitation of O_2 Molecules, Combustion, Explosion, and Shock Waves 40 (5), 499-510 (2004).

36. Pilla, G., Galley, D., Lacoste, D.A., Lacas, F., Veynante, D., and Laux, C.O., "Stabilization of a turbulent premixed flame using a nanosecond repetitively pulsed plasma", *IEEE Transactions on Plasma Science*, 2006, Volume: 34, Issue: 6, pp.2471-2477

37. Fei Wang, J. B. Liu, J. Sinibaldi, C. Brophy, A. Kuthi, C. Jiang, P. Ronney, and Martin A. Gundersen, "Transient Plasma Ignition of Quiescent and Flowing Air/Fuel Mixtures" *IEEE Transactions on Plasma Science*, Vol. 33, No. 2, 2005, pp.844-849

38. J. Liu, F. Wang, L. Lee, N. Theiss, P. Ronney, M. Gundersen, ―Effect of Discharge Energy and Cavity Geometry on Flame Ignition by Transient Plasma", AIAA-2004-1011, 42nd AIAA Aerospace Meeting and Exhibit, 5-8 January, Reno, NV, 2004.

39. Goldfeld M. A., Katsnelson S. S., and Pozdnyakov G. A., ―Plasma initiation of the chemical reactions in a supersonic stream on the example of hydrogen and natural gas combustion reaction," in Proc. 8th Int. Symp. Exp. Comput. Aerothermodynamics Internal Flows, Lyon, France, 2007, p. ISAIF8-0016.

3.2. Discharges for Plasma-Assisted Combustion.

Typical conditions for discharge maintenance in aerospace science: pressure P=0.1-1Bar, velocity of the flow V=100-1000 m/s. Characteristic temperature of gas varies from T=200K (ambient conditions) to T≤2 kK for combustion chamber. As a rule, at such conditions the plasma of electric discharges appears in filamentary form due to instabilities mostly associated with the mechanism of electrical field enhancement in a vicinity of heated plasma channel. At present, there are no reliable universal rules for appearance of any electric discharges at high temperature. Under high pressure and high-speed flow the most types of discharges are nonuniform and nonequilibrium. The high-pressure glow discharge [12-13, previous section] is rather homogeneous one; and high-current longitudinal arc produces the equilibrium plasma. A strong non-uniformity of the plasma inflow renders a chance for significant decrease of required electrical power for predefined effect. This idea is in local multi-points influence with sequential expansion of flame fronts.

Some data for different types of discharges and their merits/drawbacks in plasma assistance for combustion are shown in table below. Here a large domain of non-selfsustained and combined type of electric discharges is not included. These data are averaged and should be considered as quite evaluative.

Discharge type	Typ. power	"+"	"–"
Longitudinal arc	1-100 kW continuous	High temperature	Location in boundary layer, electrodes erosion, low efficiency.
Transverse DC	1-100 kW	Mixing, high temperature	Electrodes erosion, low efficiency, low volume of treatment.
Arc in separation zone	1-100 kW	Mixing, high temperature, auto-adjustment	Location in separation zone.
HF filamentary	1-10 kW	High speed of penetration, mixing, single-electrode.	Low input power, unpredictable position.
HF and MW torch	1-10 kW	Single-electrode or electrodeless	Very sensitive to flow
MW filamentary	0.1-10J/pulse	Electrodeless, high efficiency in radicals generation.	Complex equipment, large breakdown threshold at high pressure.
Laser spark	Wide range	High density of energy deposition.	Small volume of interaction, low efficiency of lasers.
High-pressure glow	1-100 kW, continuous	Large volume, effective in radicals generation.	High level of required power, multi-electrode system is required.
Nanosecond pulse	0.01-1 J/pulse	Effective in radicals generation, high-speed of	Low-pressure application for homogeneous appearance.

discharge		penetration.	
Short-pulse transverse spark	1-100 J/pulse	High density of energy deposition, effective mixing.	Multi-electrode system is required.
Barrier/Corona	1 W/cm^2	Effective in radicals generation.	Location in near-surface layer, low density of energy deposition.

The complete management of the combustion process under any conditions requires a large level of additional energy deposition (in a range of the flow enthalpy) that is out of practical interest. The idea is not related to strong effect of energy release but to gentle control of chemical reactions rate and local multi-ignition. The second direction is to give the gear to force combustor to work under off-design conditions. It may be a temporal mode when the level of required electric energy is not vitally important. Unfortunately, specific information available now is not quite sufficient for proper choice of the discharge type. Our understanding is that there is no versatile solution to a design and method of application of plasma for combustion. Each specific situation has to be considered separately. But it seems clear that the nonequilibrium and nonuniform operation modes are preferable. Our understanding also is that plasma has to be generated ~~–in~~ situ" just in the location of fuel-oxidizer interaction but not by external device.

3.3. Short review of DLAS-related publications.

A variety of optical diagnostic techniques are used for plasma characterization – optical emission spectrometry (OES) [1-3], Thomson scattering (TS) [4-6], coherent anti-stocks Raman scattering (CARS) [7-9], Doppler line broadening [10, 11], etc. These techniques, providing valuable data for specific types of plasma and specific range of plasma parameters, have some limitations. The OES needs instruments with high spectral resolution to obtain well-resolved spectra of the molecular bands. Thomson scattering gives the electron temperature and concentration, which does not coincide with gas temperature in non-thermodynamic equilibrium (non-TDE) conditions. Besides, it works well for hot plasma with high electron number density. Doppler broadening technique works well in case of relatively low plasma density, when the collision broadening does not contribute much in the Voigt profile of a spectral line. CARS technique provides temperature measurements for the broad variety of temperature (up to 3000K) and pressure (above 1 MPa) and successfully used for the diagnostic of different hot zones [9], but the technique needs very sophisticated and expensive laser instrumentation.

Diode laser (DL) absorption spectroscopy (DLAS) is also one of the widely used spectroscopic techniques for detection of the parameters of the hot zones [12-18]. This technique provides remote, non-perturbing measurements of the parameters of a hot zone with time resolution in the μs-ms range depending on the specific experimental conditions. DLAS possesses many attractive features as the diagnostic technique. The spatial coherence of DLs enables to deliver a narrow laser beam to a probing zone without noticeable divergence, which makes it possible remote sensing. In contrast to any version of optical emission-fluorescence technique, DLAS does not need a large solid angle of light collection – all information, which can be deduced from absorption signal, is "frozen" in a narrow laser beam of low divergence. Therefore the thermal emission of an investigated hot zone and laser stray light can be easily eliminated by a set of diaphragms and lenses. As a consequence, the hottest and most dense zones of an object can be probed by DLAS.

If TDE is established the ratio of the intensities of the absorption lines with different energies of low levels depends only on the temperature of an object. Different versions of DLAS can be used. One can measure the ratio of the amplitudes of different absorption lines using different DLs tuned to the selected lines. This approach provides higher temporal resolution but is less accurate [19, 20]. More accurate is the measurement of the ratio of integral line intensities. It can be done by rapid scanning of a single DL over a spectral range

with the selected lines. This approach enables better extrapolation of the baseline and, thus, higher accuracy, but on the price of temporal resolution [21]. The latter version was used in our experiments.

The technically easiest and straightforward version of DLAS is the detection of direct absorption. It works well in case of high signal-to-noise ratio (SNR), when the variations of the baseline cause no serious problems for evaluation of actual line intensity. For weak lines the well-developed wavelength modulation (WM) technique can be applied for reducing low-frequency noise (flicker noise) in the baseline and correcting for nonspecific absorption [22–26].

For remote sensing of the objects with the gas temperatures below 1500-2000 K absorption spectroscopy in near infrared spectral range provides higher sensitivity over OES just because of the higher population of the low energy level of a vibration-rotational transition used for diagnostic. For example, if the temperature of an object is about 1000 K (700 cm^{-1}), Boltzmann factor for the populations of upper and lower levels of a transition around 7000 cm^{-1} (~1.39 μm) is exp (-10) ≈ $4x10^{-5}$. Thus, the DLAS technique is the best choice for the sensing of the post-combustion zone, where the temperature is of the order of 1200 K.

The parameters of the probed medium are obtained as a result of experimental spectra fitting. The efficiency of a particular fitting mode strongly depends on the parameters of the experimental spectra, especially on the signal-to-noise ratio. It means that fitting strategy has to be optimized for the specific experimental conditions. The problem of optimal fitting is especially serious if the baseline is irregular.

References to section 3.3.

1. P.W.J.M. Boumans, Inductively Coupled Plasma Emission Spectroscopy Part 2, Chap. 10, John Wiley & Sons, New York, Chichester, Brisbane, Toronto, Singapore, 1987.
2. G.H. Dieke, H.M. Crosswhite, The ultraviolet bands of OH, J. Quant. Spectrosc. Radiat. Transfer. 2 (1962) 97–199.
3. Se Youn Moon, W. Choe, A comparative study of rotational temperatures using diatomic OH, O2 and N2+ molecular spectra emitted from atmospheric plasmas, Spectrochim. Acta Part B 58 (2003) 249–257.
4. M. Huang, G. M. Hieftje, A new procedure for determination of electron temperatures and electron concentrations by Thomson scattering from analytical plasmas, Spectrochim. Acta Part B 44 (1989) 291-305.
5. M. Huang, K. A. Marshall, G. M. Hieftje, Electron temperatures and electron number densities measured by Thomson scattering in the inductively coupled plasma, Anal. Chem. 58 (1986) 207-210.
6. K. Warner, G. M. Hieftje, Thomson scattering from analytical plasmas, Spectrochim. Acta Part B 57 (2002) 201-241.
7. M. Sperling, B. Welz, J. C. Hertzberg, C. Rieck, G. Marowsky, Temporal and spatial temperature

distributions in transversely heated graphite tube atomizers and their analytical characteristics for atomic absorption spectrometry, Spectrochim. Acta Part B 51 (1996) 897-930.

8. J. Hertzberg, D. Kozlov, C. Rieck, P. Loosen, M. Sperling, B. Welz, G. Marowsky, CARS thermometry in a transversely heated graphite-tube atomizer used in atomic-absorption spectrometry, Appl. Phys. B - Lasers and Optics 61 (1995) 201-205.
9. F. Vestin, M. Afzelius, H. Berger, F. Chaussard, R. Saint-Loup, P.E. Bengtsson, Rotational CARS thermometry at high temperature (1800 K) and high pressure (0.1-1.55 MPa), J. Raman Spectrosc. 38 (2007) 963-968.
10. S.C. Snyder, G.D. Lassahn, J.R. Fincke, C.B. Shaw, R.J. Kearney, Determination of gas-temperature and velocity profiles in an argon thermal-plasma jet by laser-light scattering, Phys. Rev. E 47 (1993) 1996-2005.
11. A. Rousseau, E. Teboul, N. Sadeghi, Time-resolved gas temperature measurements by laser absorption in a pulsed microwave hydrogen discharge, Plasma Sources Sci T 13 (2004) 166-176.
12. M. P. Arroyo, R. K. Hanson, Absorption measurements of water-vapor concentration, temperature and line-shape parameters using a tunable InGaAs diode laser, Appl. Opt. 32 (1993) 6104-6116.
13. M. G. Allen, Diode laser absorption sensors for gas-dynamic and combustion flows, Meas. Sci. Technol. 9 (1998) 545-562.
14. S.T. Sanders, J. Wang, J.B. Jeffries, R.K. Hanson, Diode-laser absorption sensor for line-of-sight gas temperature distributions, Appl. Opt. 40 (2001) 4404-4415.
15. H. Teichert, T. Fernholtz, V. Ebert, Simultaneous in-situ measurement of CO, H2O and gas temperatures in a full-sized coal-fired power plant by near-infrared diode lasers, Appl. Opt. 42 (2003) 2043-2051.
16. X. Liu, X. Zhou, J. B. Jeffries, R. K. Hanson Experimental study of H2O spectroscopic parameters in the near-IR (6940–7440 cm-1) for gas sensing applications at elevated temperature. JQSRT 103 (2007) 565–577.
17. C.D. Lindstrom, K.R. Jackson, S. Williams, R. Givens, W.F. Bailey, C.J. Tam, W.F. Terry, Shock-Train Structure Resolved with Absorption Spectroscopy Part 1: System Design and Validation. AIAA Journal 47, 2368 (2009).
18. C.D. Lindstrom, D. Davis, S. Williams, C.J. Tam Shock-Train Structure Resolved with Absorption Spectroscopy Part 2: Analysis and CFD Comparison (2009), 47, 2379.
19. D.S. Baer, V. Nagali, E.R. Furlong, R.K. Hanson, Scanned- and fixed-wavelength absorption diagnostics for combustion measurements using multiplexed diode lasers, AIAA J 34 (1996) 489-793.
20. S.T. Sanders, J.A. Baldwin, T.P. Jenkins, D.S. Baer, R.K. Hanson, Diode-laser sensor for monitoring multiple combustion parameters in pulse detonation engines, Proc. Combust. Inst. 28 (2000) 587.
21. X. Zhou, X. Liu, J.B. Jeffries, R.K. Hanson, Development of a sensor for temperature and water concentration in combustion gases using a single tunable diode laser, Meas. Sci. Technol. 14 (2003) 1459-1468.
22. J.A. Silver, Frequency-modulation spectroscopy for trace species detection - theory and comparison among experimental methods, Appl. Opt. 31 (1992) 707-717.
23. [23] D.S. Bomse, A.C. Stanton, J.A. Silver, Frequency-modulation and wavelength modulation spectroscopies - comparison of experimental methods using a lead-salt diode-laser, Appl. Opt. 31 (1992) 718-731.
24. C. Schnürer-Patschan, A. Zybin, H. Groll, K. Niemax, Improvements in detection limits in graphite furnace diode laser atomic absorption spectrometry by wavelength modulation technique, J. Anal. At. Spectr. 8 (1993) 1103 - 1107.
25. A.Zybin, C.Schnürer-Patschan, M.Bolshov, K.Niemax, Elemental analysis by diode laser spectroscopy, Trends in analytical chemistry (TrAC), 17, (1998), 513 – 520,
26. V. Liger, A Zybin, Yu.Kuritsyn, K. Niemax, Diode-laser atomic-absorption spectrometry by the double-beam-double-modulation technique, Spectrochim.Acta Part B 52 (1997) 1125-1138.

4. Task 1. Technical Results

4.1. Experimental facility description and updates.

The experimental facility contains the following main parts:

- Supersonic gasdynamic facility PWT-50/PWT-50H;
- Plasma generator and power supply;
- Measuring and data acquisition system.
- Control and synchronization system.

General layout of the experimental facility PWT-50H and arrangement are presented in Fig.4.1.1.

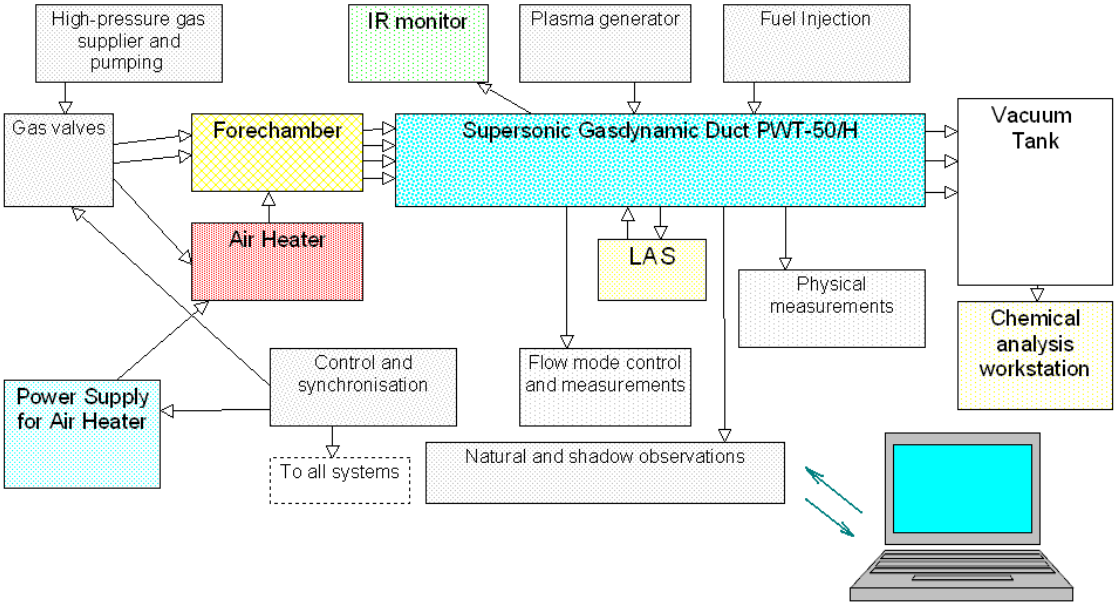

Fig.4.1.1. Layout of the PWT-50/H arrangement.

Table 4.1.1. Technical parameters of the facility PWT-50H.

	PWT-50, 20.05.06	PWT-50H, 20.08.08	PWT-50HL 01.10.10
Test section cross-dimensions, mm	60*72	60*72	60*72
Mach Number	0.1-0.9; 2	2	2, 2.5
Maximal stagnation pressure, Bar	1.0	1.8	2.5
Stagnation temperature, K	300	300-670	300-750
Maximal air mass flow rate, kg/s	<1.0	0.5-1.0	0.5-1.0
Maximal fuel mass flow rate, g/s	<5	0.1-8	0.1-8
Operation time, s	<1	0.3-0.5	1.5
Steady stage duration, s	0.2-0.5	0.15	0.8
Typical power of heater, kW	-	700	700
Maximal thermal power at fuel combustion, kW	300	1000	1000
Maximal power of discharge, kW	10	20	30
Runs per 8 hours, range	10-80	10-30	10-30
Lifetime, runs between services	500	100	200

The experiments were conducted in a short-duration blowdown wind tunnel PWT-50H with a closed test section Y×Z=72×60mm at Mach number of nozzle M=2.0 and 2.5 and stagnation pressure P_0<2.5Bar. The experimental test bed PWT-50H provides the following characteristics of the flow in test section: the Mach number is M=1.9 and 2.35, the static pressure is P_{st}=100-300 Torr, the Reynolds number $Re=(4\div10)\times10^6\times L$, the boundary layer thickness in the testing zone is δ=0.3-0.8 mm, typical gas flow rate through the channel is G=0.6-0.9kg/s, the duration of quasi-stationary phase is 0.2-0.5 s, and the total enthalpy of the flow is H≈200-900 kW (depending on the heater operation). The stagnation temperature of the air was varied in range $T0=300\text{-}700K$. In this experimental series the discharge parameters were varied: discharge current was $Ip\approx50\text{-}5A$, discharge power was $Wp\approx5\text{-}25kW$.

The technical parameters of facility PWT-50H are shown in the table 4.1.1 below in three columns: parameters of PWT-50 without heater, maximal parameters at the heater operation, and the parameters after tanks volume increase. Photo of the PWT-50 is shown in Fig.4.1.2.

Fig.4.1.2. Experimental facility PWT-50.

As a whole the experimental facility PWT-50H was prepared during the first year of the project and was updated step by step depending of specific experimental tasks. A general description of the facility is presented in Final Report dated March 2009. In this Report a short version is shown, which considers the changes made and the most important parameters.

About 45 modifications were made in frames of the project, for example:

- Air heater with power supply, air supply, and fuel supply were designed, manufactured, and tuned;
- Chemical analysis workstation was delivered and adjusted;
- IR monitor was tested and used in some runs;
- Laser absorption spectroscopic system was designed, manufactured, and adjusted;
- Additional air supply pipes for the air heater were installed;
- Place of the fuel injection was changed;
- Sensor of the heater operation was mounted;
- Scheme of synchronization was modified;
- Fuel injection system were modified for simultaneous gaseous and liquid fuels usage;
- Chemical station was updated; a new system for a gas sampling was mounted;
- Heater operation mode was tuned to increase the gas temperature;
- Pressure measurement system was refined;
- Scheme of optical and schlieren measurements was modified;
- etc.

In 5th year of the project the facility was rebuilt to enhance its capabilities. Following main modifications were made:

- New air compressor was installed: higher pressure, higher air production, lower noise;
- Air dryer was installed between the compressor and air tanks;
- Air tanks were increased: V=2m^3 instead V=0.5m^3;
- Extra vacuum tanks were connected to the main one, increasing the volume to V=1.17m^3;
- New nozzle for Mach number M=2.5 was manufactured and tested;
- New optical windows were installed with some inclination to avoid light interference.

Resulting parameters were significantly improved as it is shown in Table 4.1.1 last column.

Gas-Dynamic duct's geometry and parameters. General drawing of the gasdynamic duct is presented in Fig.4.1.3. All parts are made of high-temperature refractory materials. The nozzle was manufactured of Al-Si alloy. The cooling of it is fulfilled by high thermal conductivity to thick walls. Three main requirements have to be taking account at the choice of material for a test section: refractivity, non-conductivity, and ability for machinery.

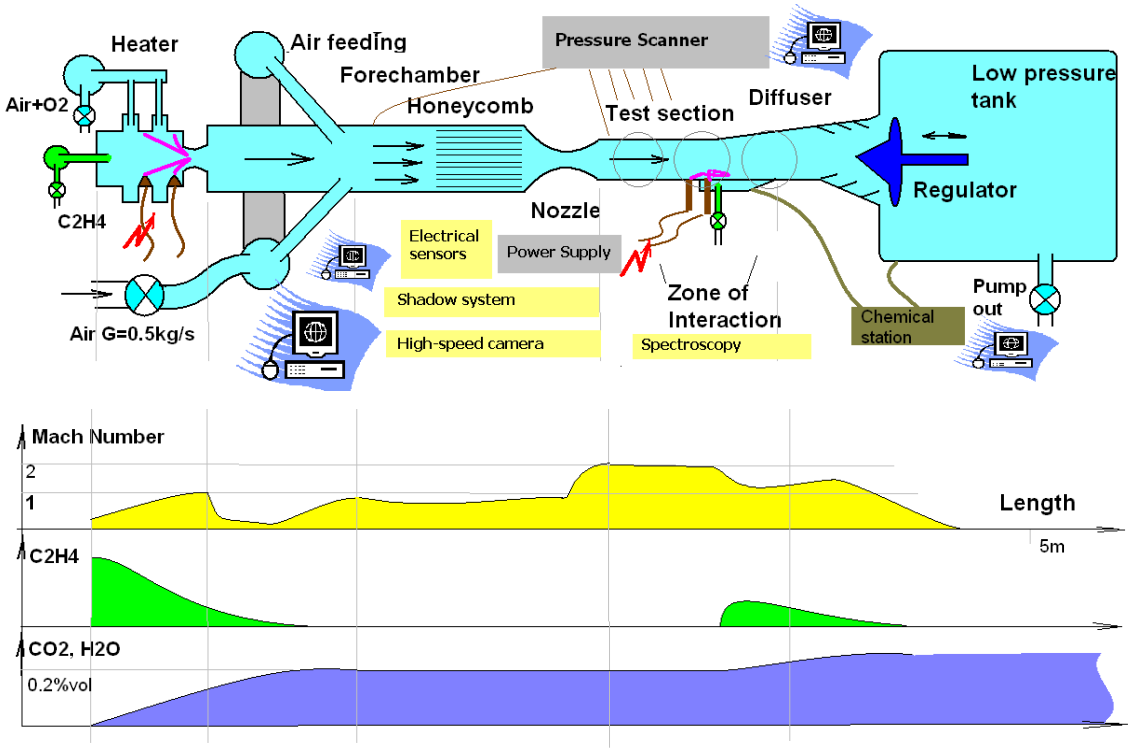

Fig.4.1.3. Gasdynamic duct of experimental facility PWT-50H. General layout, main parameters distribution, and element‘s conjunction.

As a basic material the ceramics was chosen on the base of boron-nitride and silicon oxide composition. This material possesses excellent thermal shock resistance, conductivity, and dielectric constant. It can be machined using standard high speed ~~t~~ool steel” equipment. Machining by grinding may be used if preferred or stringent tolerances are required. Main characteristics:

- Dielectric Strength: 1700V/mil
- Hardness-Knoop 13.5-19kg/mm^2
- Resistivity >10^{14} Ohm-cm
- Loss Tangent @ 8.8 GHz <0.0015
- Dielectric Constant @ RT 4.30
- Thermal Conductivity @ 25°C 27-30 W/m/K
- Open Porosity: <3%.

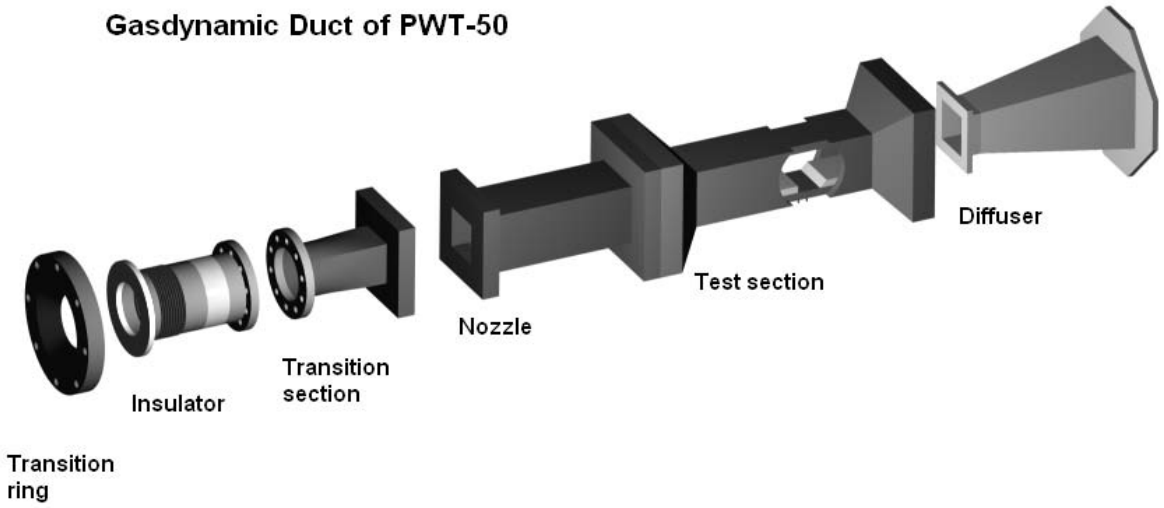

Fig.4.1.4. Draft scheme of the gasdynamic duct.

The system of air feeding consists of two tanks of pumped air with the pressure control. The tanks are connected with the facility‘s forechamber by four lines, which are equipped by EM-controlled valves. Each valve is guided by electronic driver individually. As the result the air feeding is occurred with a regulation of mass flow-rate during the short operation time. The insulator provides electrical and acoustical insulation of the test section from the gas feeding system. Transition section transforms a circular cross-section to a rectangular one at the condition of constant square area. A controlled diffuser is applied between TS and vacuum tank. The regulation is implemented by profiled ring at the diffuser output. Vacuum tank has volume about 1.1m^3 and equipped with automatic overload valve.

Tests' Control. Test sequence includes three phases: preparation of the installation, run itself and data processing. In the most cases not all systems are utilized in the test. It depends on the specific tasks. The data processing occurs, as a rule, after the series of runs during several hours or more.

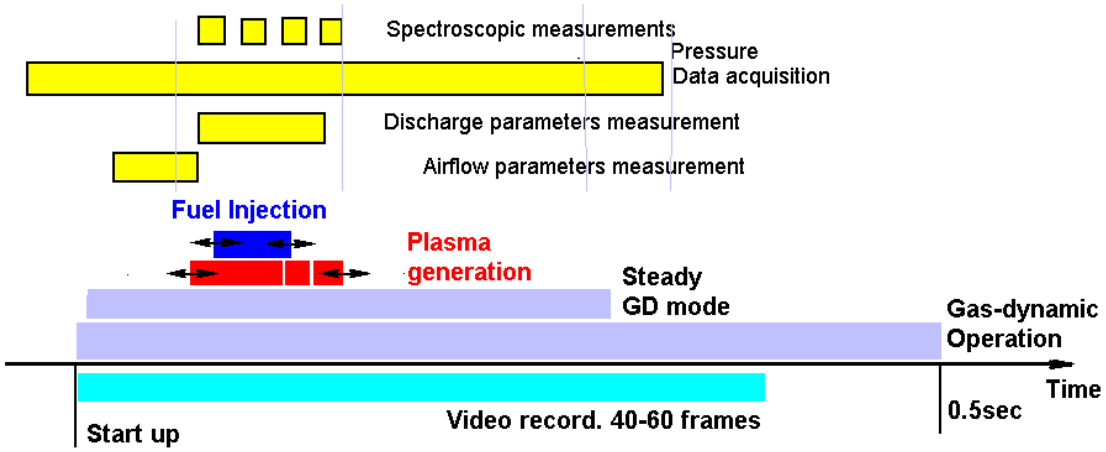

Fig.4.1.5. Typical time diagram of the test.

A time sequence of the typical test is shown in Fig.4.1.5 schematically. Time duration of the discharge operation and the fuel injection can be modified as well as the mutual time position.

Initially the test section had a rectangular cross-section with dimensions 72*72mm. A backwise wallstep, wall cavity, and duct expansion are constructed by one or two wall-attached insertions with a thickness 12mm. Vertical walls have circular windows three on each side, which are made from a quartz glass. Test section has length about 500mm and manufactured from dielectric material. Three variants of the test section arrangement are presented in Fig.4.1.6. These variants were used last two years. The fuel was injected through 5 circular (d=3,5mm) orifices all in a row across the span and inclined at 25 degrees from the normal in the upstream direction. The row of injectors is 15 mm downstream from the row of electrodes, just downstream of the ceramic block; each injector is inline with an electrode in the configuration that includes 5 electrodes. The fuel mass flow rate was balanced between the orifices using a fuel plenum. Fuel injection was started prior to the discharge initiation and was switched off after completion of the discharge. Typically, the fuel injection continued 10-20 ms after the discharge to observe whether the flame was held or extinguished.

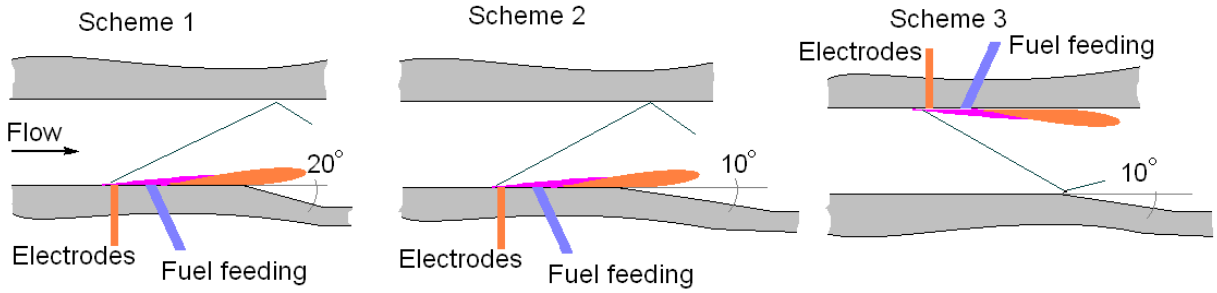

Fig.4.1.6. Test section arrangements.

The parameters of the test section can be summarized as following:

Width of the duct 72mm;

Height of the duct upstream wall-step	60mm;
Depth of the wall inclination (expansion)	12mm;
Distance from electrodes to diffuser	450/300mm;
Diameter of the optic window	120mm;
Material of walls	Nylon-6,6;
Material of insertions	BN/SiO_2;
Material of optic window	quartz;
Material of binder	Nylon 6.6 and Al/Mn/Si alloy.

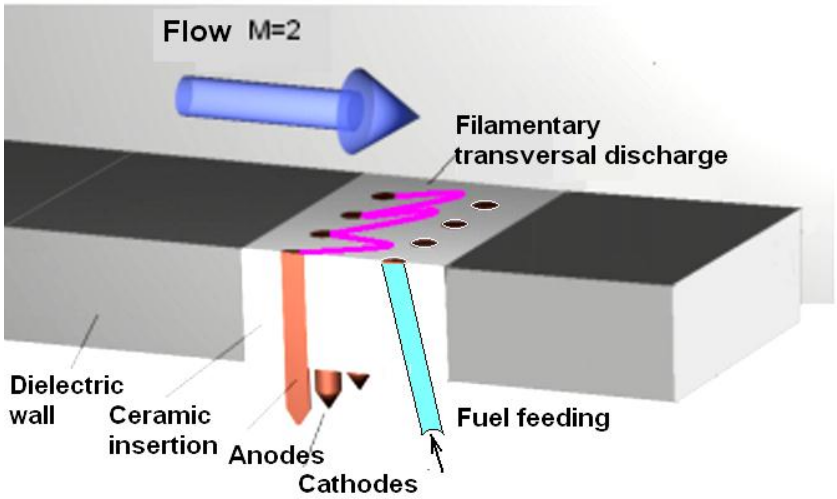

Fig.4.1.7. Basic scheme of electrodes arrangement

The Fig.4.1.7 presents a scheme of electrodes‘ arrangement in case of geometric configuration with plane wall. It consists of insertion made of refractory insulating material. It is flush mounted as well as electrodes themselves. The insertion has the construction with seven or eleven electrodes arranged in one row. The fuel injectors are installed directly on the wall of the test section as it is shown in Fig.4.1.7. They contain a fuel capacitor at 5-6Bar of pressure and fast pulse valve with EM control. The fuel dose and duration of the injection depends on EM pulse duration and the repetition rate. Minimal dose at the single pulse is about 1mg. Maximal mass flow rate is about G_f=8g/sec, typical value is G_f=0.1’ 2g/s.

The photos of the test section (after multiple runs) and the arrangement are presented below in Fig.4.1.8. It is related to Scheme 3 in Fig.4.1.6: discharge on top wall.

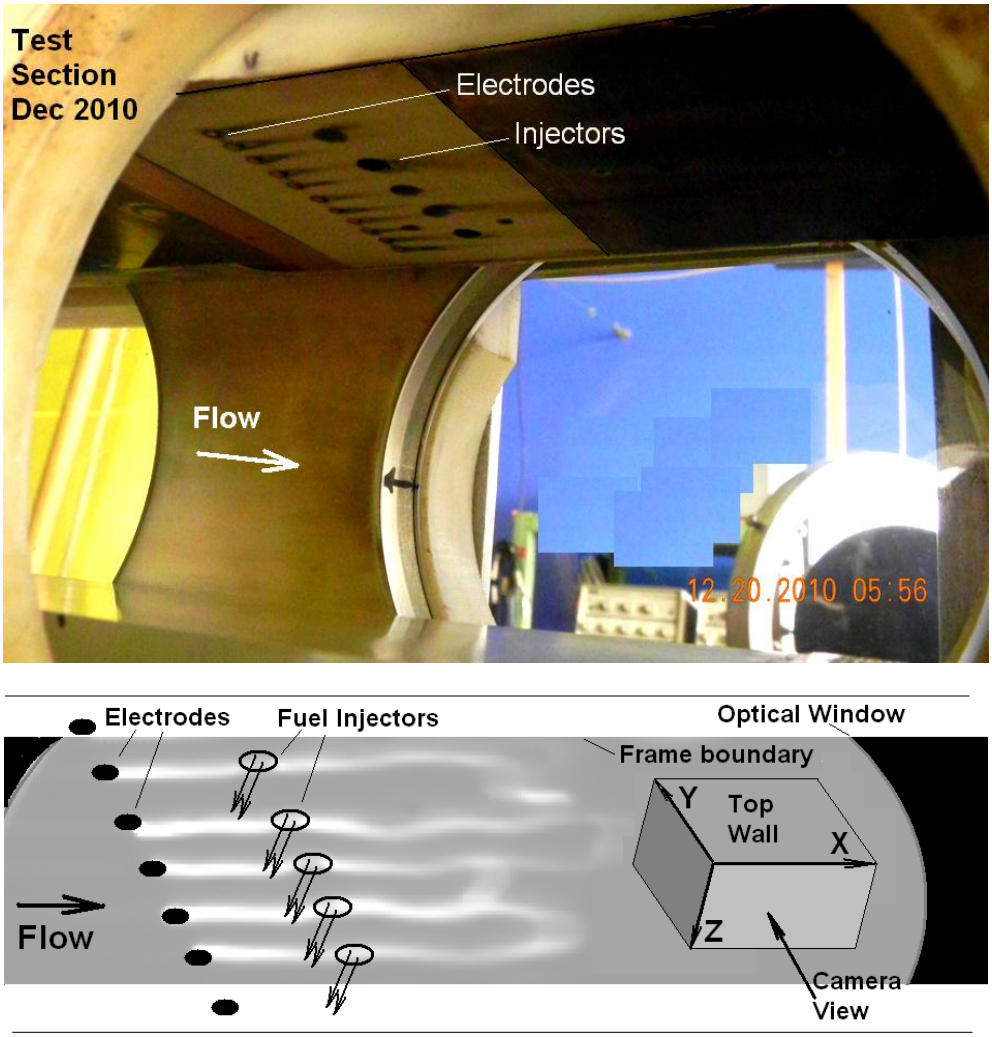

Fig.4.1.8. Test section: electrodes and injectors.

4.2. Measuring system.

The PWT-50H facility test unit is furnished with a number of instruments; use is made of both standard and original methods of measurement and diagnostics of the gas and plasma conditions. Honeywell™ pressure transducers are used to monitor the mode. Time resolution of the transducers is not worse than 0.1 ms. Static pressure is measured in several points on the wall along the channel. The total pressure transducers are connected with Pitot tubes that can be moved across the channel. Placed in the test section of the aerodynamic channel is an absolute pressure transducer for calibration of the system. The pressure profile is measured with the aid of an electronic commutator of pressure transducers for 32 measurement channels, connected to PC through PCMCI interface. The characteristic time of measurement is not worse than 0.3 ms for each channel.

An original shadow (schlieren) device is used to record the flow structure with a possibility of high space- and time- resolution of images. The IR laser diode is used as a light source. The images and shadowgraphs are recorded by a fast digital video camera Basler-A504K at immediate processor control. Use was made of standard and original electric current and voltage sensors, including a symmetrical divider, current shunts, filters with recording in Tektronix TDS-210 and HP-5062 digital oscilloscopes. The oscilloscopes are connected to a data acquisition system via the GPIB serial interface. The data are acquired by the system based on National Instruments™ hardware. The basic software was developed in the LabView© programming language. The synchronization system was built on the base of pulse generators and optical lines of data transmission to avoid electromagnetic noise.

The pressure transducer‘s locations are shown schematically in Fig.4.2.1 for the scheme #3. Actually, the number and position of pressure tabs can be varied from test to test depending of specific task of particular test.

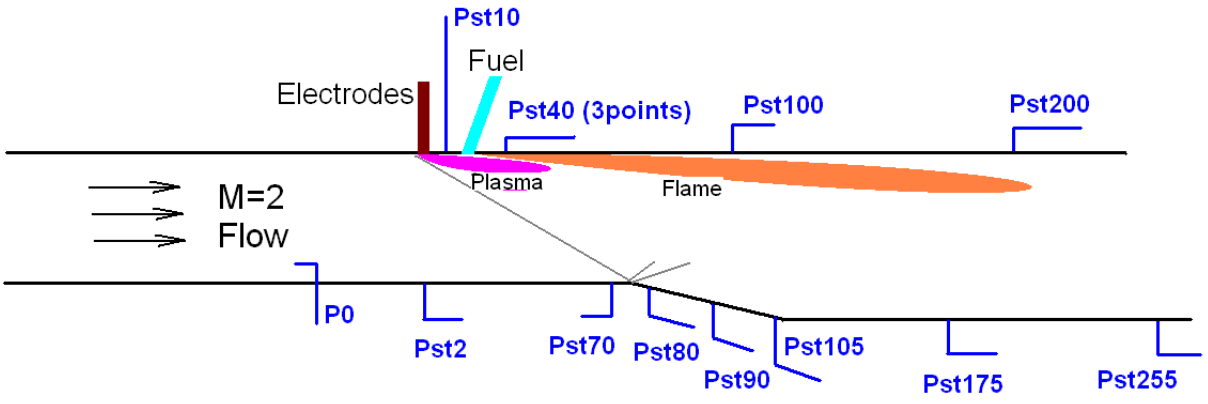

Fig.4.2.1. Layout of the test geometry and arrangement.

The plasma parameters were measured by optical spectroscopy (see Final Report dated March 2009). The measurements of gas temperature and water vapors concentration by DLAS were made based on one-pass scheme, which is shown in Fig.4.2.2 for the Scheme #2 (Fig.4.2.6.).

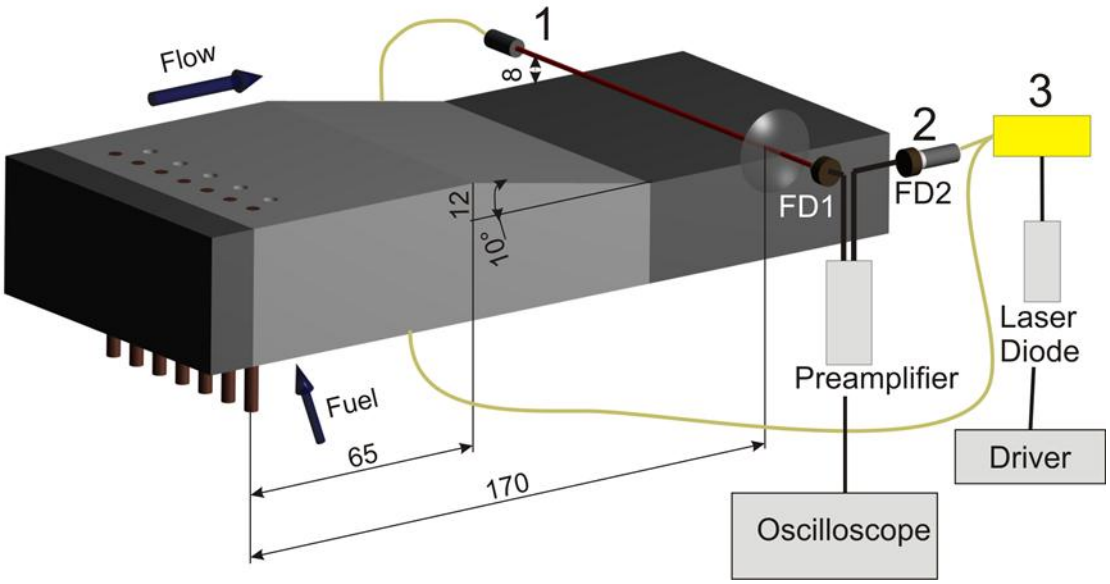

Fig.4.2.2. Draft scheme of DLAS measurements.

4.3. Experimental study of the nonequilibrium discharge effect on effectiveness of plasma-based flameholding over plane wall.

4.3.1. Near surface electrical discharge operational modes. Variation of E/n.

The electrical discharge was excited *transversally* with a scheme that included electrodes arranged across the duct span in a pattern of anode-cathode-anode-cathode-anode; the electrodes are embedded in a refractory ceramic block that provides electrical insulation. Two models were tested: let call them as (1) –7electrodes", and (2) –11electrodes".

The major properties of the near-surface quasi-DC electrical discharge were described in [1-2]. The power supply possesses a steep falling voltage-current characteristic with voltage amplitude at zero-current (at initiation) of about 5 kV. A short time after initiation, the discharge cover the inter-electrodes gap. Furthermore, the arc loops are seen to stretch downstream, following the flow. In general, the loops will elongate, from a direct anode-cathode path, as the conductive path is convected downstream, and the maximum length of the loops is governed by the combination of maximum power supply voltage and inter-electrodes gap. This maximum length of the discharge filament and the gas velocity define the effective frequency of the discharge oscillations. In the most cases this value was *F=10-30kHz* under the experimental conditions. Power release regulation can be realized by the discharge current variation. But this regulation is not linear: when the current is increased, the voltage is decreased, but in less factor, and as a result the power is increased in some degree. Such a method leads to some variation in the reduced electric field, which may be important for understanding of some features of interaction. At low current the discharge is unstable, while at high current, materials erosion can be significant. An increase of the power requires the reduction of the circuits' resistivity that leads to deterioration of the inter-electrodes current auto-regulation.

In this section the data are presented for the flow Mach number M=2.35 and static pressure P_{st}=80Torr. The results for higher static pressure are figured below. The attention is mainly paid for the power release and averaged electrical field. The operation modes include a high-current (low resistivity), high-voltage (non-equilibrium), and all intermediate modes.

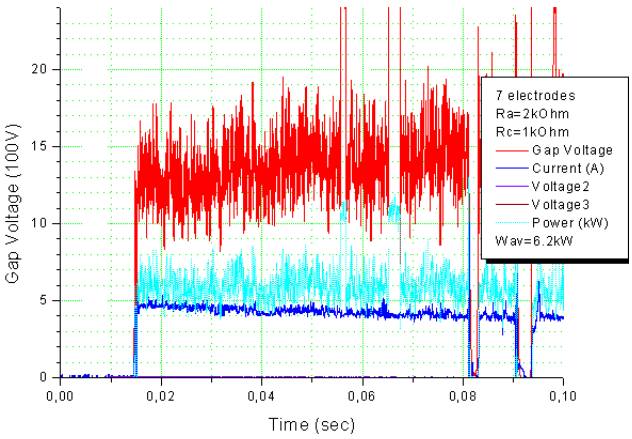

a.

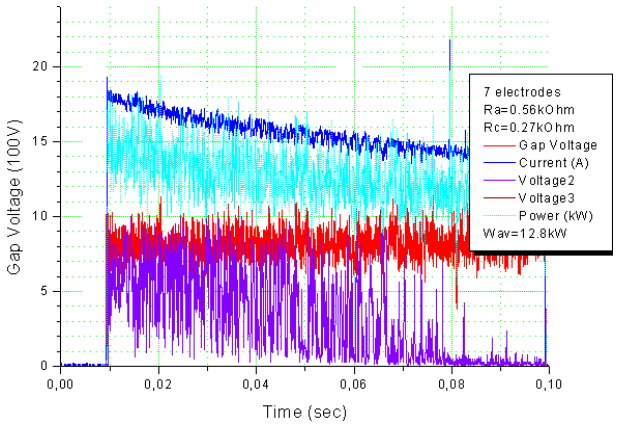

b.

Fig.4.3.1.1. Model 7electrodes. (a) high-voltage mode - unstable operation. (b) high-current mode - plasma contacts the downstream plate.

Typical oscillograms are presented in Figs.4.3.1.1 and 4.3.1.2 for the 7electrodes model. Here and below: gap voltage = U_{pl} is the voltage between 4th and 5th electrodes; current=I_{pl} is the current through all cathodes; voltage3=U3 is the voltage on the downstream copper insertion at R3=500Ohm; power Wav is the averaged power deposition for time t=0.02-0.07sec of operation. The final graph is shown in Fig.4.3.1.2b

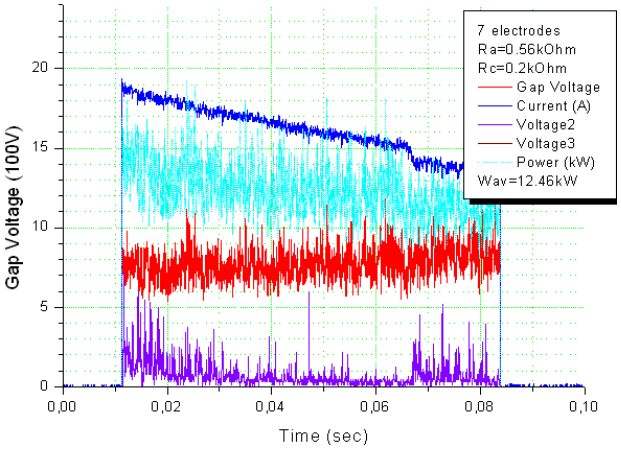

a.

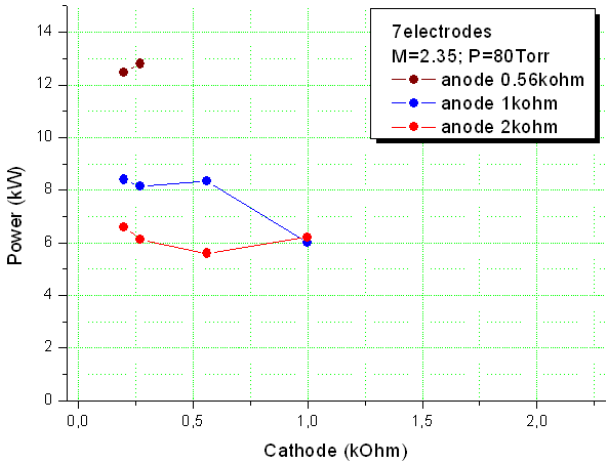

b.

Fig.4.3.1.2. Model 7electrodes. (a) –The best" high-power mode. (b) Resulting data for power deposition.

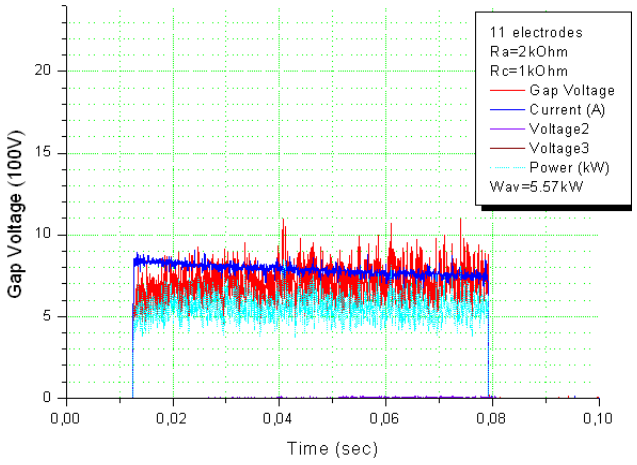

a.

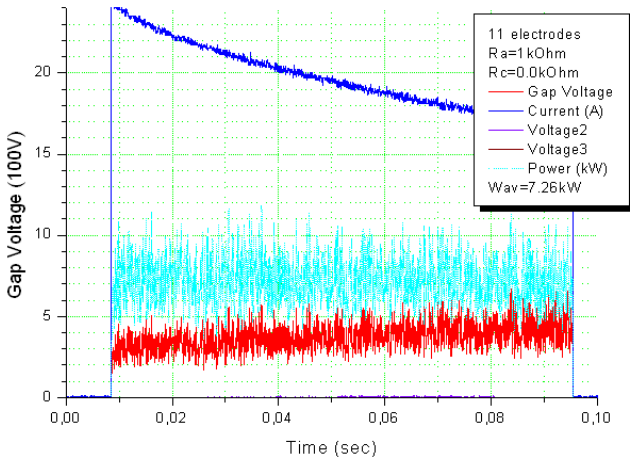

b.

Fig.4.3.1.3. Model 11electrodes. (a) high-voltage mode - stable operation. (b) high-current mode - unstable cathodes operation.

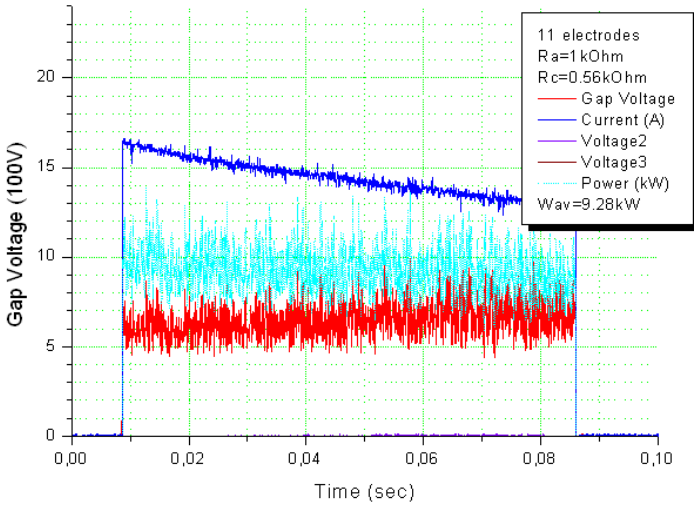

Fig.4.3.1.4. Model 11electrodes. Regular stable mode.

The model 11electrodes was designed taking into account the previous negative experience: zone of stability (anode can‘t be located near a lateral wall), damages for ceramics, and connections to the grounded parts. The same data for the 11electrodes model are presented in Figs.4.3.1.3-4 and Figs.4.3.1.5. This model has demonstrated the best performance among the others in terms of the discharge stability (see also section 4.3.3). The Fig.4.3.1.6 shows zone of regulation of the discharge in this mode. It looked favorable for the future test. The same data for P_{st}=135Torr are presented in Fig.4.3.1.6b. Well seen that the difference is not large. The discharge parameters occur to be very conservative.

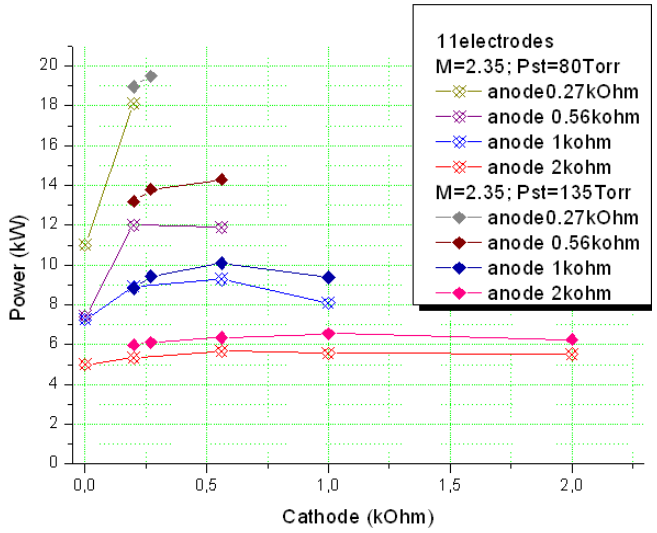

Fig.4.3.1.5. Model 11electrodes. Resulting data for power deposition.

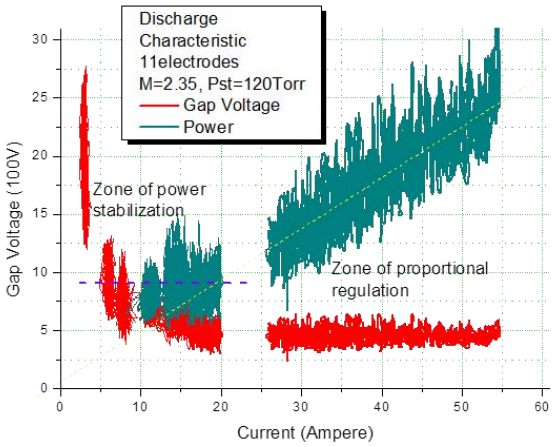

a.

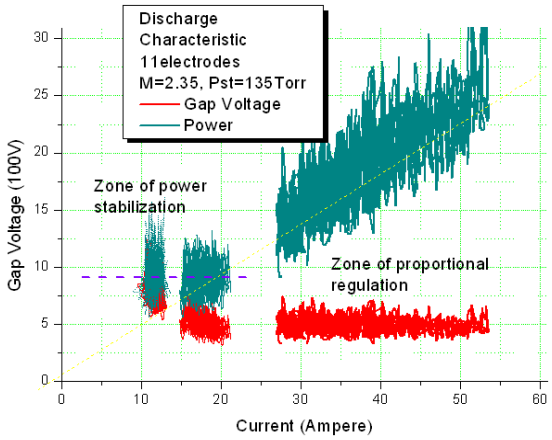

b.

Fig.4.3.1.6. Model 11electrodes. (a) zone of discharge parameters regulation P_{st}=80Torr. (b) zone of discharge parameters regulation P_{st}=135Torr.

Table 4.3.1.1. Discharge characteristics (P_{st}=80-135Torr).

$R_{Anode}+R_{Cathode}$, (kΩ)	Number of electrodes	Power, (kW)	U, (V)	L, (mm)	U/L, (V/cm)
2+0,2	7 P_{st}=80 Torr	5,6	956	38	125
1,1+1	7 P_{st}=80 Torr	6	1102	37	149
1,1+0,56	7 P_{st}=80 Torr	8,4	958	40	119
	11 P_{st}=80 Torr	9,3	650	23	142
	11, P_{st}=135 Torr	9.85	680	21	162

The values of power, voltage and length of the discharge filament for variety of electrodes configuration at some combinations of R_{Anode}+$R_{Cathode}$ are presented in Table.4.3.1.1. Despite voltage and length of discharge filaments decrease with increase of number of electrodes in the same resistance configuration the voltage per unit length changes not significantly.

The following conclusions can be made based on the experimental results obtained in this test series.

- Operational limits of stable discharge are wider for the pattern with bigger number of electrodes. 11electrodes arrangement demonstrates satisfactory characteristics.
- To avoid the discharge breakdown on upstream grounded parts through boundary layer the electrodes near walls must be cathodes.
- Too small cathode resistance in respect of anode resistance leads to unstable discharge.
- Tested configuration allowed to obtain the range of power deposition about W_{pl}=5-25kW.
- The plasma loops are longer in case of 7 electrode configuration on approximately 75%.

As this will be clear later (section 4.3.3) the last conclusion occurs principally important for the fuel ignition and flameholding.

Reference to section 4.3.1.

1. *S. Leonov, D. Yarantsev*, –Near-Surface Electrical Discharge in Supersonic Airflow: Properties and Flow Control", *Journal of Propulsion and Power*, 2008, vol.24, no.6, pp.1168-1181, DOI: 10.2514/1.24585
2. *S. Leonov, V. Soloviev, D. Yarantsev*, –High-Speed Inlet Customization by Surface Electrical Discharge", AIAA-2006-0403.

4.3.2. Spectroscopic observations of ignition dynamics.

Contrary to the method, which was described in previously issued Final Report dated March 2009, combustion zone was visualized by means of high speed color CCD camera with using of low-width band interference filters. The choice of particular filters was defined by the spectra analysis. Figure 4.3.2.1 shows the survey spectra of the discharge luminosity and of the combustion zone (ethylene injection) at the discharge presence. Intensity scales are different here. CN and OH bands are visible at fuel injection and without it due to CO2 and H2O background traces. At the same time the CH band is well visible at hydrocarbon injection into discharge zone and in flame.

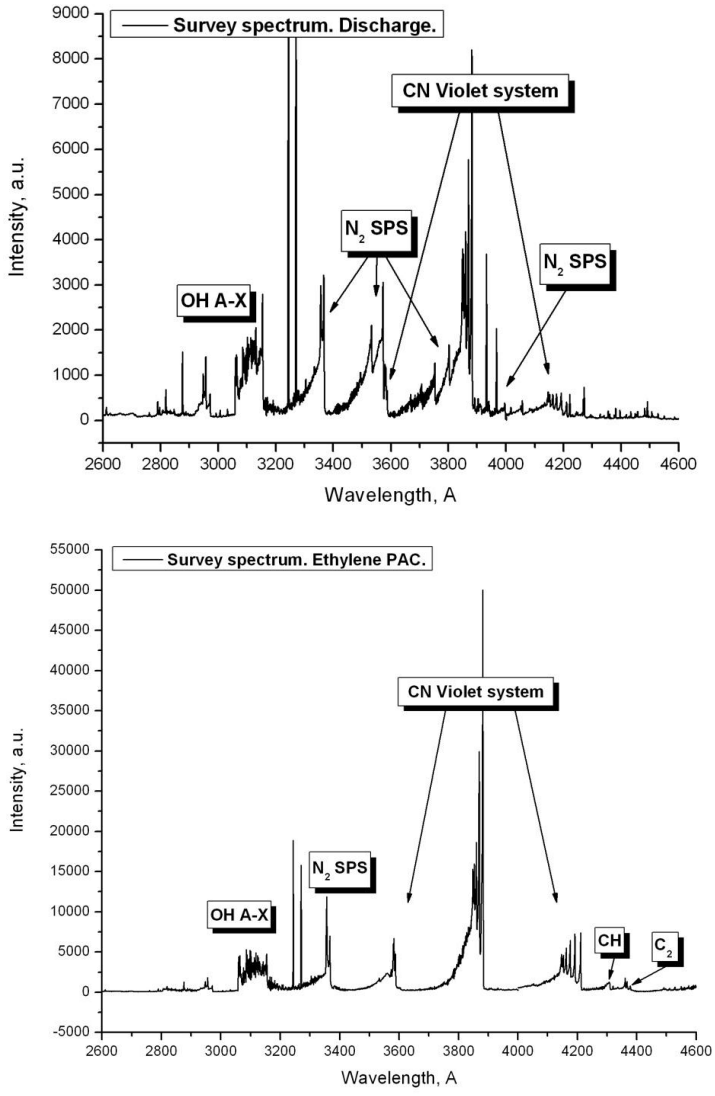

Fig.4.3.2.1. Survey spectra. Spectral zone 260 nm to 460 nm. (a) discharge operation, (b) plasma assisted combustion of ethylene.

Unfiltered images of the zone of discharge-fuel interaction are shown in Fig.4.3.2.2.

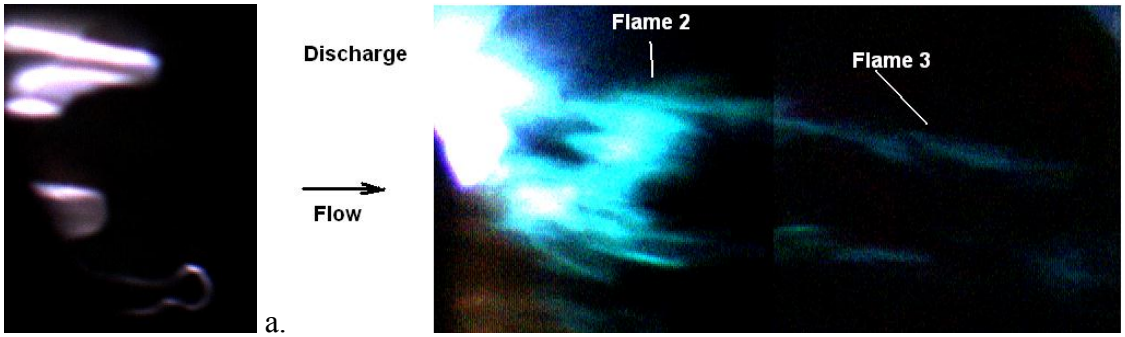

a. b.

Fig.4.3.2.2. Discharge appearance without fuel (a) and at the ethylene injection (b) – reacting gas luminescence in M=2 flow. Exposure 100μs.

Following filters have been applied:

λ=432 nm – CH (A-X) band. The emission of this band is not overlapped by others and this band is specific one for the discharge operation in hydrocarbons. Emission was registered from the area 20-90 mm downstream the electrodes. It can be recognized easily in the figure below (Fig.4.3.2.3), that emission of discharge's filaments becomes much higher in this spectral region in case of ethylene injection. Moreover, it is seen that there is low intensity luminosity downstream the discharge cords. This luminosity is related to the combustion. It is the question why the secondary growth of the CH luminosity was not detected.

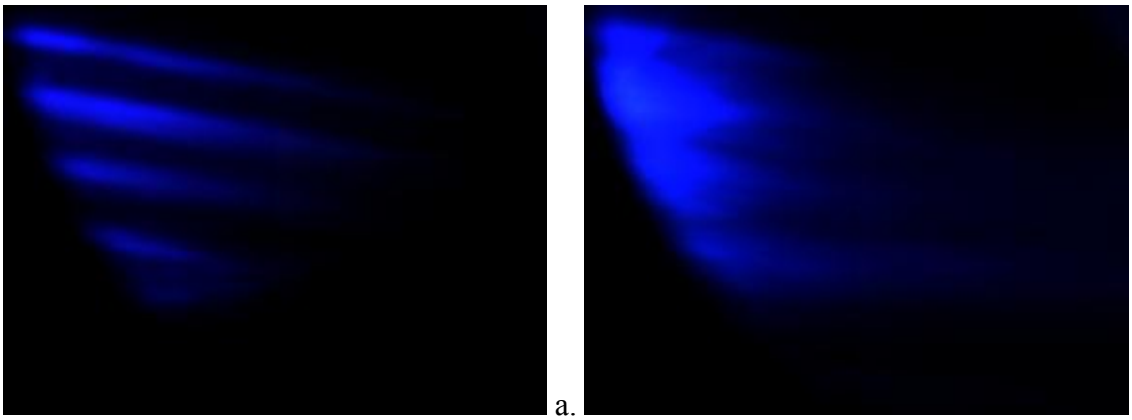

a. b.

Fig.4.3.2.3. Discharge and zone of plasma-assisted combustion visualization in CH band. (a) discharge operation without fuel; (b) discharge at the ethylene injection. Exposure 1ms.

λ=515 nm – C_2 Swan band. Swan band is typical both for combustion and for the discharge operation in ethylene. Intensity of this band is higher than CH band and images become more bright. It is seen rather bright plume downstream the discharge filaments that is similar to CH visualization.

Frame exposure affects the picture quality in high-speed flow: longer frame means less detailed image.

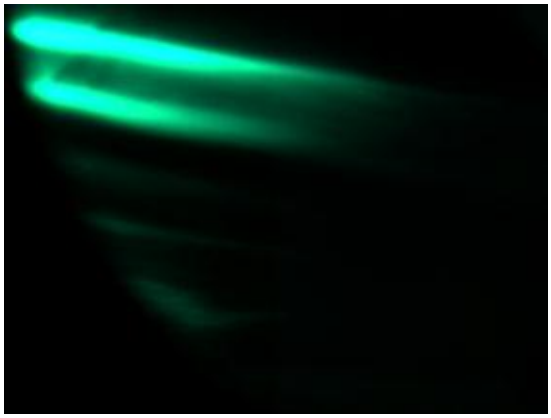
a.
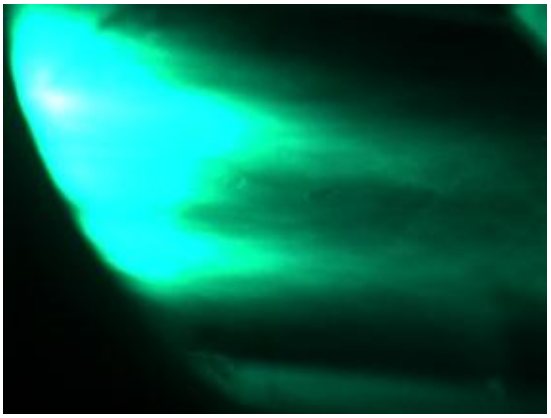
b.

Fig.4.3.2.4. Discharge and zone of plasma-assisted combustion visualization in C_2 band. (a) discharge operation without fuel; (b) discharge at the ethylene injection. Exposure 1ms.

Usually it was mentioned that non-equilibrium plasma (characterized by higher level of E/N) occurs more effective in terms of fast fuel ignition. In our particular case it should be considered two main factors of successful fuel ignition and flameholding: (1) the discharge power; and (2) length of the discharge filaments (the length reflects a time of interaction). All other factors appeared as much less important. Special experimental series shown a generation of sequence of active zones of reacting gas moved downstream from the place of immediate plasma-fuel interaction that is presented in this section. These zones appear as hotbeds of consequent flamefront.

4.3.3. Specific limitations for plasma-based flameholding in case of hydrocarbon fuel.

Optimization of the discharge mode. During the last year the experimental work has been performed to find out the more optimal electrodes geometry. 11 electrodes arrangement has been tested and compared with 7 electrodes. The main conclusion was the following: operational limits of stable discharge are wider for the pattern with bigger number of electrodes. Then the experiments on plasma assisted combustion of hydrogen were fulfilled and it was shown that hydrogen combustion intensity (pressure magnification) is not less than one for the 7 electrodes configuration. On the contrary, combustion intensity was negligibly low when ethylene was injected in experiments that have been performed in 7 electrodes configuration. It is clear that the reason is the increasing of the number of electrodes because it was the main changing of the experimental configuration in comparison with successful ethylene ignition obtained previously. Additional series of experiments have been fulfilled last time in order to find the difference between two electrodes configurations in terms of hydrocarbon fuel combustion and to ignite the ethylene.

The main idea of this experimental series based on dependence of discharge filaments‘ length on distance between electrodes. Shorter distance causes the shorter length of the filaments due to lower value of the breakdown voltage, Fig.4.3.3.1. The assumption was made that the length of the discharge filament is critically important for the ignition and flameholding of the ethylene.

Several electrodes‘ configurations have been tested. All of them were based on the 11 electrodes arrangement. Changing of the configuration was made by simple commutation of power supply.

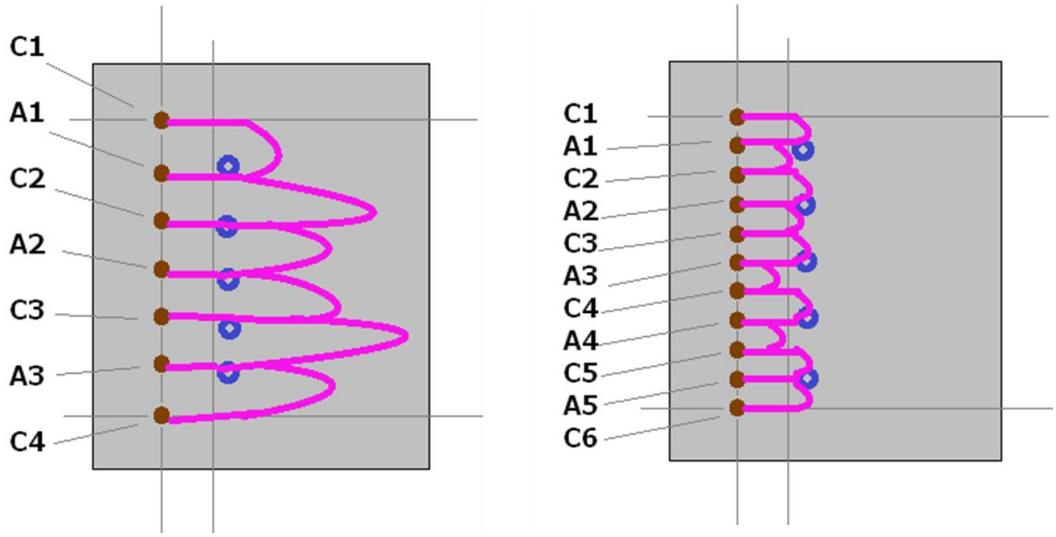

Fig.4.3.3.1. Discharge filaments length depending on electrode gap.

1st configuration was an attempt to find a compromise between stability of the configuration with bigger number of electrodes and long filaments generation in the configuration with smaller number of electrodes. Electrode system consisted of the following electrodes: 1c, 2a, 4c, 6a, 8c, 10a, 11c. The electrodes arrangement and photo of discharge operation at the ethylene injection in supersonic flow are shown in Fig.4.3.3.2 at Rc = 1 kOhm, Ra= 0.56 kOhm.

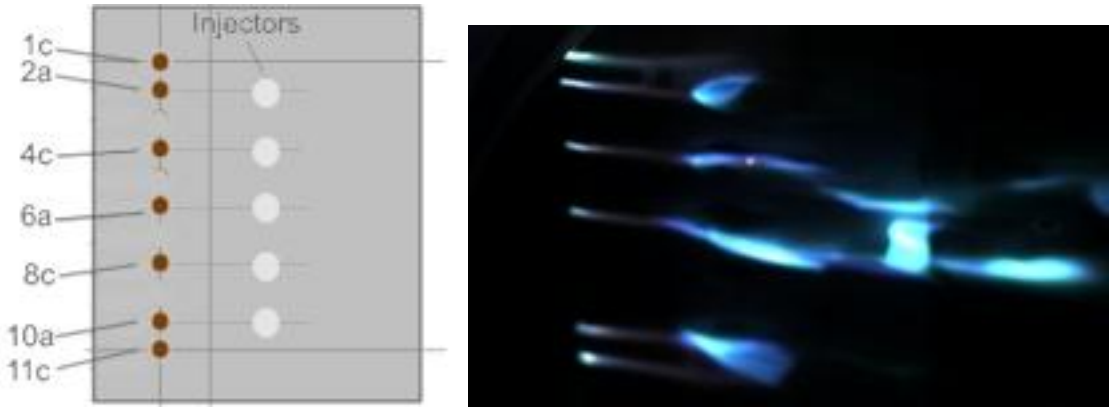

Fig.4.3.3.2. 1st electrodes configuration and photo of discharge operation.

End filaments of the discharge were very stable but three middle electrodes work rather unstable, usually only one pair of the middle electrodes work at the same time as it is seen in Fig.4.3.3.2. Indeed, the distance between middle electrodes occurs even longer than it was for the 7 electrodes configuration and such behaviour of the middle discharge loops looks quite reasonable. Combustion of ethylene was observed for such configuration by the schlieren visualization and by the pressure distribution measurements but it was just short flash that appears from time to time. Increasing resistance of the end electrodes (cathodes) up to 1.1 kOhm caused to a bit more stable behaviour of the middle electrodes but it was insufficient to obtain a stable combustion.

2nd configuration that had been tried consists of 5 electrodes: 2c, 4a, 6c, 8a, 10c. This configuration occurred very unstable for any combinations of the resistances due to rather big distance between electrodes. One important feature of the discharge behaviour for such a configuration has been found out. Discharge breakdown always occures through the injection system if the working electrodes are posed in front of the injection holes along the flow direction, Fig.4.3.3.3. Each injector was connected through the tube to the general volume that was installed out of the test section for experimental arrangement that was tested previously. Then, during the modification of the electrodes plate this volume was mounted into the electrodes plate itself. It has been done to siplify the sealing of the test section (one hole instead

of five). As a result the path through the injection system became short enough for the discharge to breakdown. So, such injection system occurres to be unsuitable one.

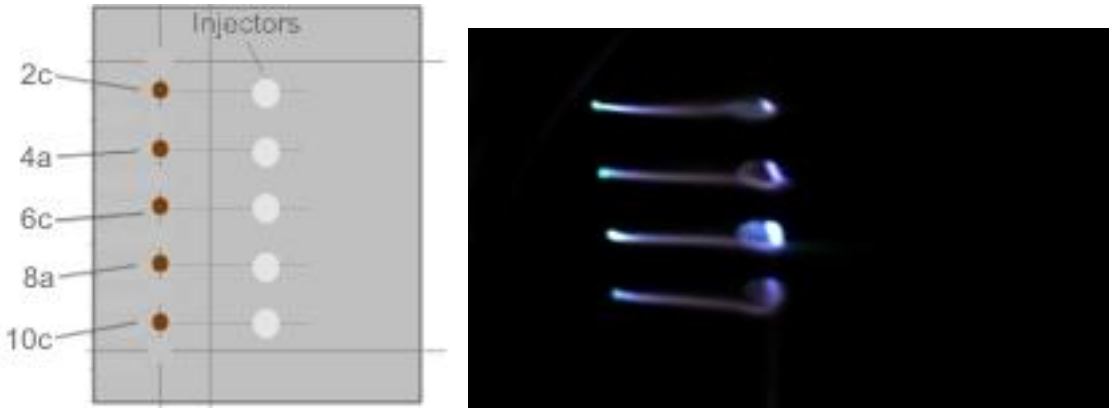

Fig.4.3.3.3. 2nd electrodes configuration and photo of discharge operation.

3rd configuration included following electrodes: 1c, 2a, 4c, 5a, 7a, 8c, 10a, 11c, Fig.4.3.3.4. The behaviour of the discharge was the same as for the 11 electrodes configuration: short stable discharge loops. No ethylene combustion has been obtained.

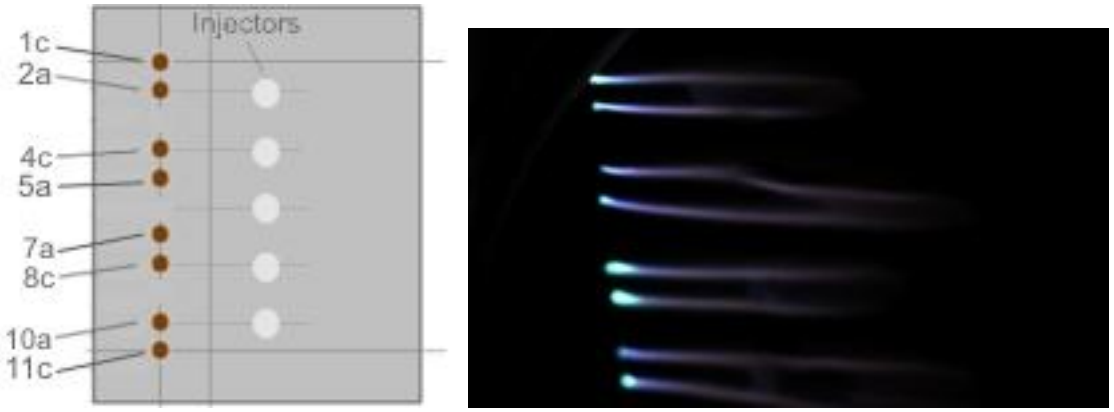

Fig.4.3.3.4. 3rd electrodes configuration and photo of discharge operation.

4th configuration posesed the same distance between electrodes as the 2nd configuration but working electrodes were the odd ones in order to prevent the breakdown through the injection system: 1c, 3a, 5c, 7a, 9c, 11a, Rc = 0.56 kOhm, Ra = 1 kOhm, Fig.4.3.3.5. Discharge loops became rather long for such configuration. Sometimes breakdown occurs through the injection system but it happens rarely and never during the injection of the ethylene. As a result stable intensive combustion of the ethylene had been obtained for this electrodes arrangement.

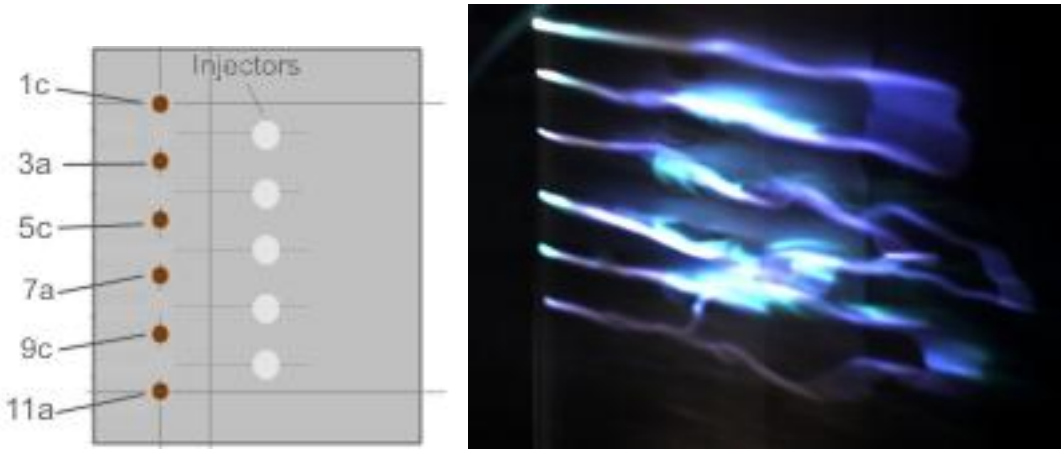

Fig.4.3.3.5. 4th electrodes configuration and photo of discharge operation.

Intensity of the ethylene combustion was even higher than one obtained during previus efforts. Pressure distribution and schlieren photo for the case of successfull combustion are shown in the Fig.4.3.3.6.

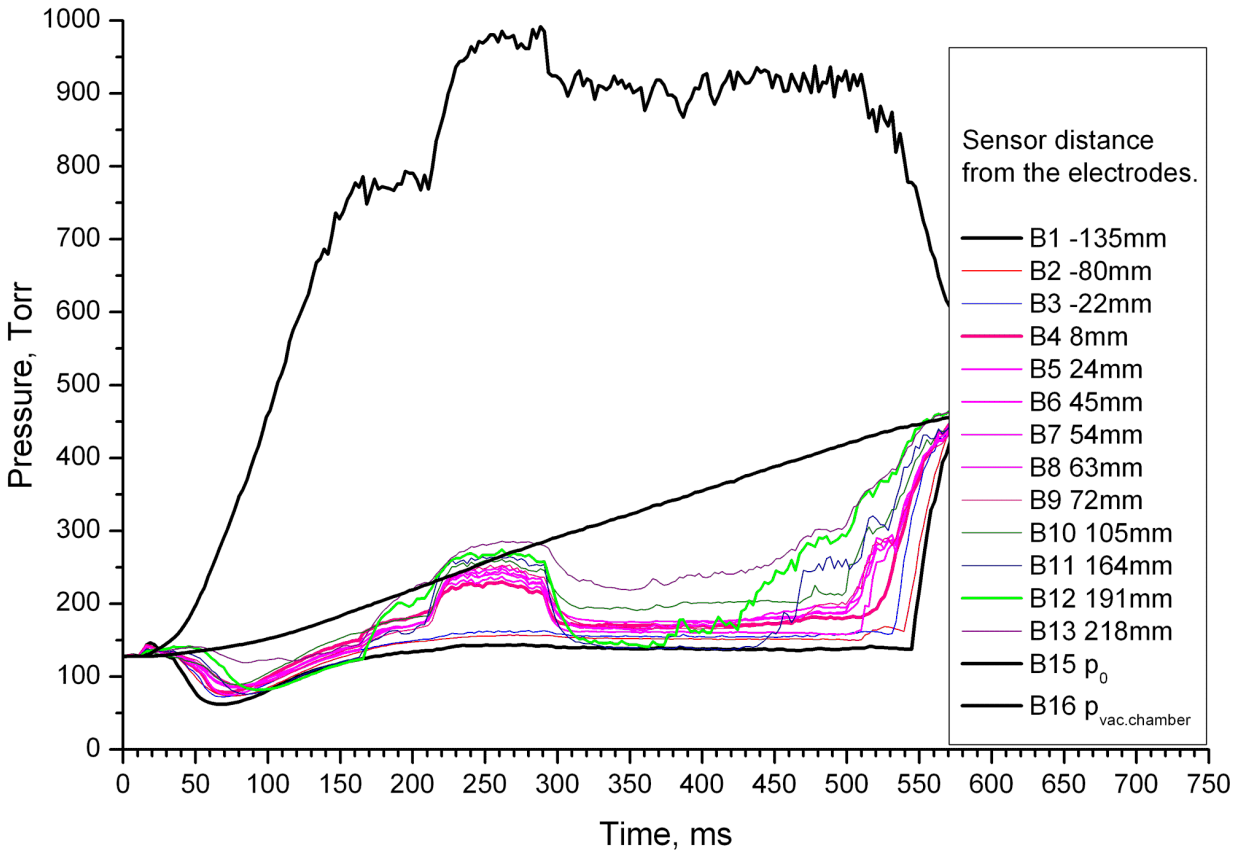

Fig. 4.3.3.6a. Pressure dynamics and distribution at the ethylene combustion.

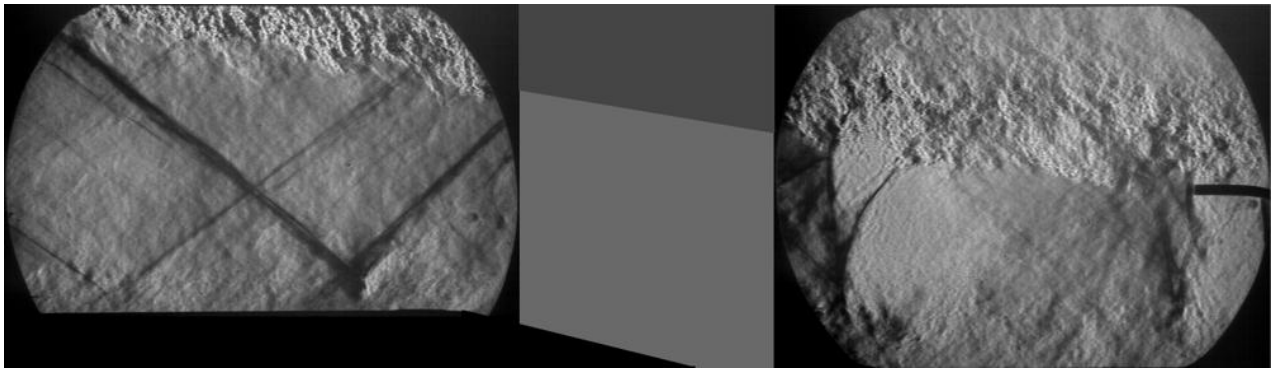

Fig. 4.3.3.6b. Schlieren visualization of the ethylene combustion. G_{C2H4}=1.3g/s

Combustion mode with thermal choking of the flow was not observed for this experimental arrangement that is similar to the previous experiments with ethylene combustion.

Concluding this section it may be stated that there is one main specific limitation for plasma-based flameholding in case of hydrocarbon fuel for this experimental approach: the length of the discharge filaments is very important feature of the discharge – if filaments shorter than some value, ethylene is not ignited. Distance between electrodes also influances on another discharge feature, namely on the reduced electrical field. The longer distance between electrodes the more nonequilibrium state of discharge is realised that may be usefull for combustion enchancement. Note, that the discharge length is roughly proportional with a time of interaction of the discharge with the air-fuel particular portion.

4.3.4. Refined results on plasma-assisted combustion of hydrogen and ethylene in M=2 flow.

The basic results of study of plasma-assisted flameholding in high-speed flow can be found in publications [1-3]. Ignition and flameholding were realized for H_2 and C_2H_4 fuelling on a plane wall by using a transversal electrical discharge at relatively low power deposition (<2% of flow enthalpy). The power threshold for a hydrogen flameholding was measured to be W_{pl}<3kW; with ethylene fuelling it was measured to be W_{pl}≥4kW. The combustion efficiency was estimated and it is found sufficiently high, about 0.9, for both hydrogen and ethylene. The ignition effect of the gas discharge was compared for different levels of the power, power density, and reduced electrical field (characterizing the departure from equilibrium for the discharge). Here it was found that the effectiveness of the flameholding is determined primarily by the level of power deposition, and secondarily by the length of plasma filaments (time of interaction), thirdly by the power density, and the last by the other factors. In this experiment the effect of reduced electrical field was not an important factor. In comparison with hydrogen fuelling, a main difference with ethylene fuelling was that thermal choking was not observed, even at the maximum discharge power of W_{pl}>10 kW. Furthermore, the completeness of the ethylene combustion decreases with increased fuel mass flow rate.

The data on pressure distribution at hydrogen and ethylene injection and for variety of the discharge parameters (power, E/n, polarity) were obtained and processed. An example of the data is shown below to clarify the result of interaction. The most parameters are pointed in capture. The schlieren pictures and the DLAS measurements were recorded using also the additional window of the test section. The optimized geometrical configuration was considered for the tests: rectangular channel with 10 degrees inclination of the opposite to plasma generator wall because of the actually plane wall in zone of combustion. The scheme and pressure tabs arrangement were described in section 3.2.

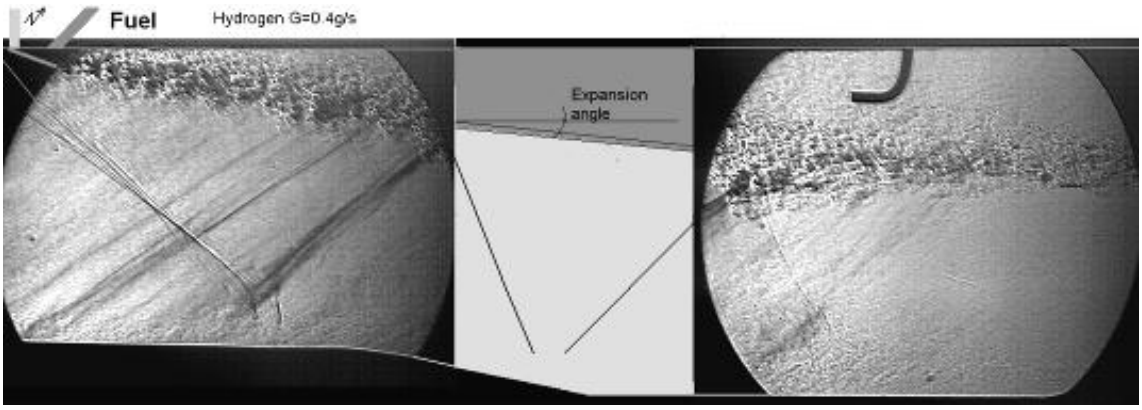

Fig.4.3.4.1. Combined from two windows schlieren image of hydrogen combustion.

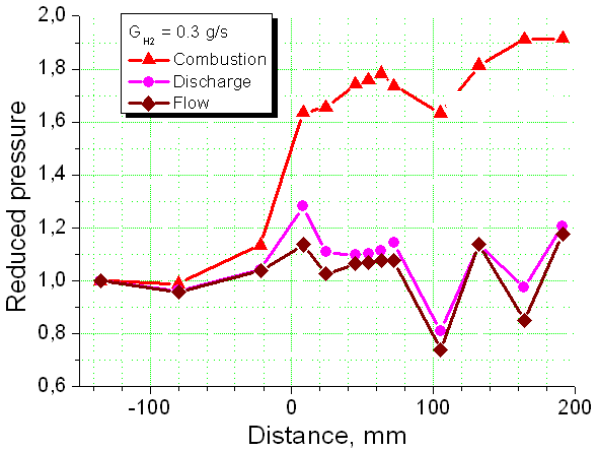

Fig.4.3.4.2. Evolution of wall pressure. Hydrogen injection, discharge power W_{pl}=8kW. X=0 – electrodes line.

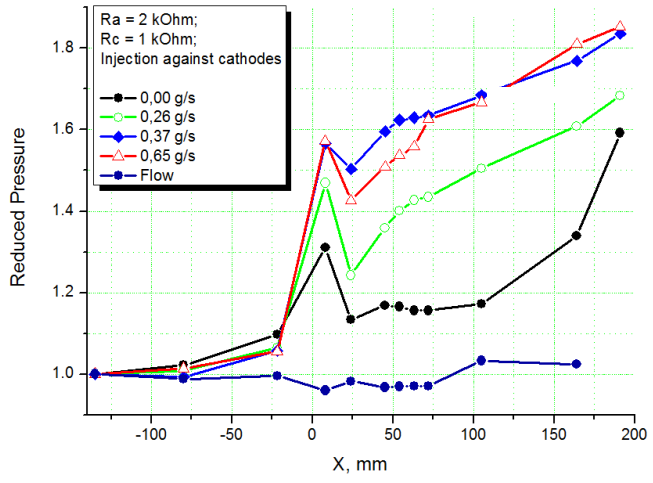

a.

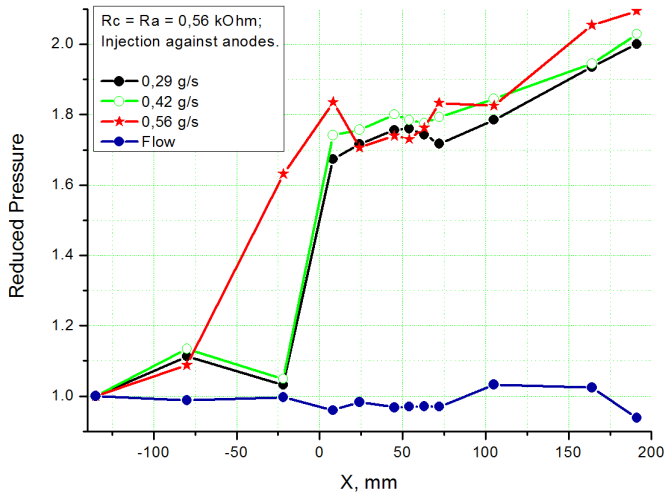

b.

Fig.4.3.4.3. Evolution of wall pressure. Hydrogen injection, discharge power W_{pl}=4.5kW (a) and W_{pl}=9kW (b). X=0 – electrodes line.

Schlieren images in Fig.4.3.4.1 and wall pressure distributions in Fig.4.3.4.2 for hydrogen combustion illustrate details of plasma-fuel-flow interaction. The electrodes configuration in this test geometry for the hydrogen injection was tested in 11electrodes + 5 fuel injectors

arrangement. One can conclude that the combustion zone locates not in immediate vicinity of the zone of discharge and the fuel feeding. The result is sensitive to plasma power deposition and fuel mass flow rate as it is demonstrated in Fig.4.3.4.3. The same data are presented below for the ethylene combustion. The red line in Fig.4.3.4.4 shows a sample of section for DLAS measurements.

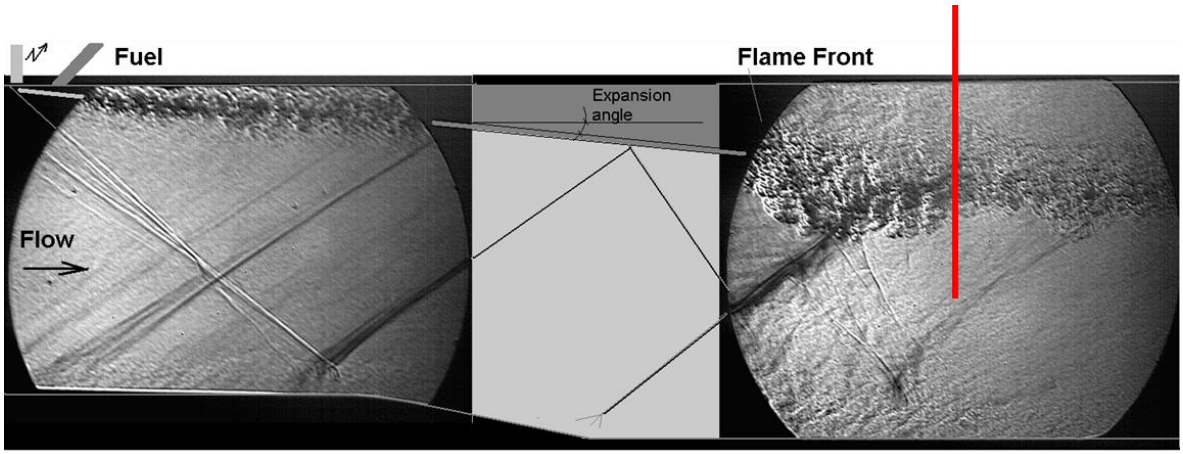

Fig.4.3.4.4. Typical schlieren pictures of ethylene combustion.
Combination of images from two windows.

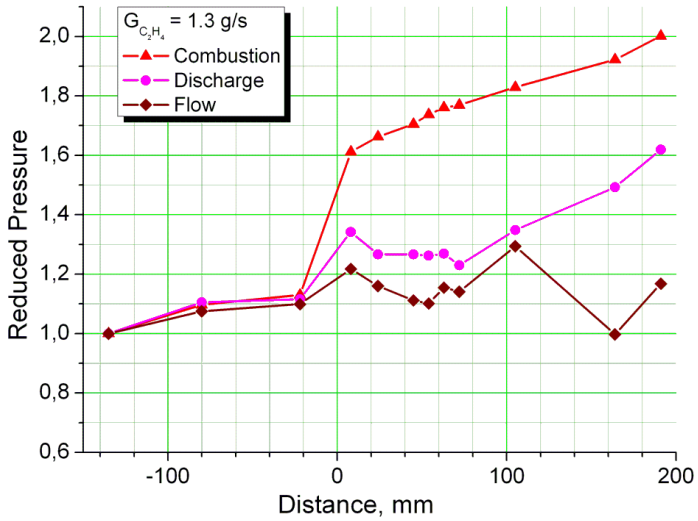

Fig.4.3.4.5. Evolution of wall pressure. Ethylene injection G=1.3g/s, discharge power W_{pl}=8.4kW. X=0 – electrodes line.

The DLAS measurements were fulfilled in typical operation modes: plasma power was W_{pl}=8-8.5kW, hydrogen mass flow rate was G_{H2}=0.3g/s, and the ethylene G_{C2H4}=1.3g/s. As was already pointed out the developed technique and algorithm of data acquisition give the line-of-sight values for the temperature and H_2O concentration. In reality both parameters

fluctuates along the optical path inside the test section. It means that the line-shapes and widths of water molecules depend on the coordinate along the beam.

High signal-to-noise ratio enabled spectral fitting with fewer averaged scans. The temperature distribution along the combustor obtained as a result of such fitting is shown in Fig.4.3.4.6. Each point in the figure was obtained in individual run of the facility. The values of the temperature inferred from both slopes coincide reasonably well. The water vapor partial pressure measured in a parallel way is presented in Fig.4.3.4.7. The uncertainty of the temperature evaluation associated with the experimental errors and fitting procedure was estimated basing on the results database. Estimated precision (statistical error) of the temperature measurements was $\sigma = 40$ K.

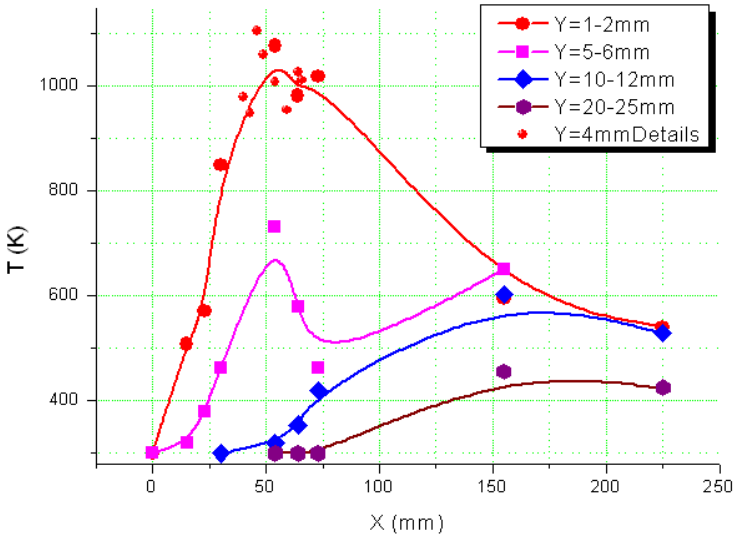

Fig.4.3.4.6. Temperature distribution measured by DLAS at H2 injection.
X axis is along the flow direction. Y is the distance from the wall.

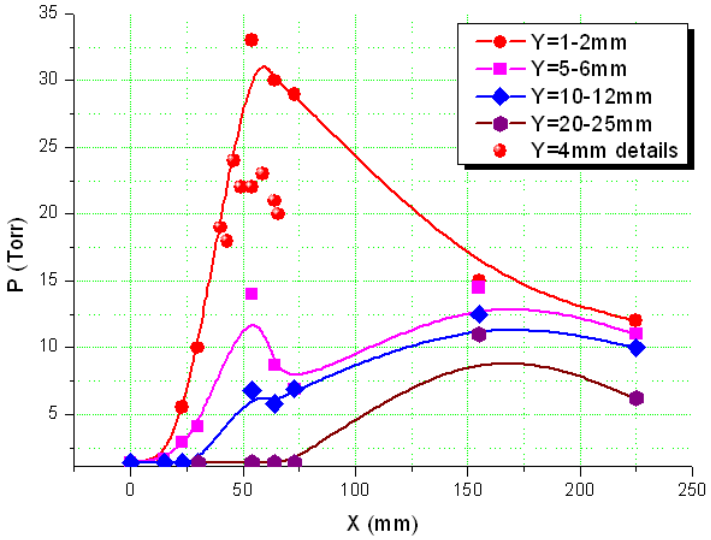

Fig.4.3.4.7. Water vapor partial pressure in plasma assisted combustor at H2 injection.

The data for the ethylene ignition and flameholding are presented in Figs.4.3.4.8-4.3.4.9. The effect of two-stage pattern is well seen.

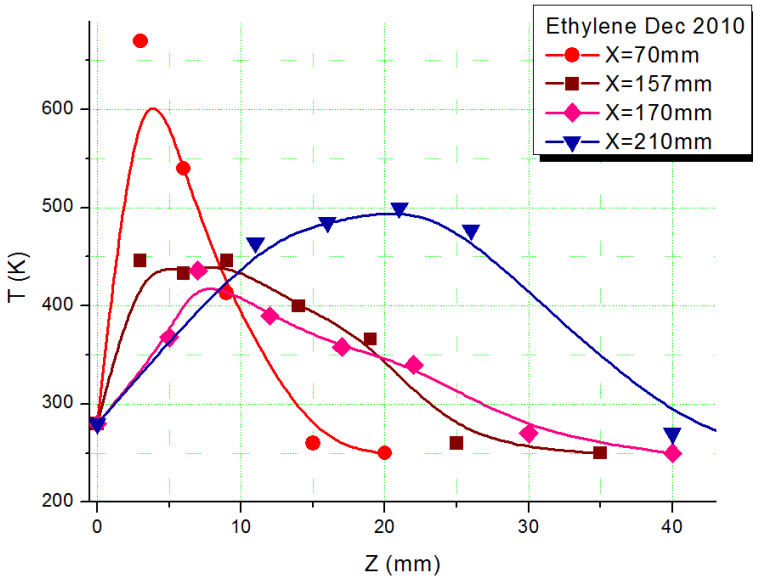

Fig.4.3.4.8. Temperature distribution measured by DLAS at C2H4 injection.
X axis is along the flow direction. Z is the distance from the wall.

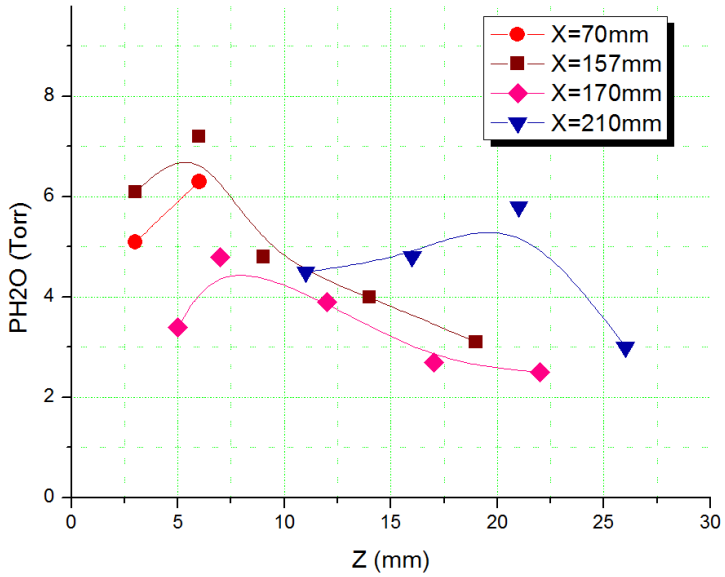

Fig.4.3.4.9. Water vapor partial pressure in plasma assisted combustor at C2H4 injection.

To explain the above observations, we propose the following two-zone scheme of the plasma assisted flameholding (it reflects the two-stage ignition process). Zone 1, in which the ~~–~~cold" combustion takes place accompanied by plasma-induced fuel conversion and relatively small power release. Note, that the combustion layer in this zone is rather thin. It is actually the shear layer, where the mixing is additionally promoted by the plasma filaments. Despite of high gas temperature here a total heat release is not big. Zone 2, in which the combustion is completed or almost completed with high energy release. Intensive mixing limits the gas

temperature elevation. We emphasize that the plasma is the key element of this scheme: it launches the cold combustion inside of the first zone by generating high amount of active species. The lengths of the first zone in our tests were measured by the schlieren and schlieren-streak technique in the range from 50mm to 150mm. It corresponds to the induction time range τ_{ind}=0.1-0.3ms.

References to section 4.3.4.

1. Leonov S.B., Carter C., Yarantsev D.A. ―Experiments on Electrically Controlled Flameholding on a Plane Wall in Supersonic Airflow", Journal of Propulsion and Power, 2009, vol.25, no.2, pp.289-298
2. Sergey Leonov, Dmitry Yarantsev, Vladimir Sabelnikov, Electrically Driven Combustion near Plane Wall in M>1 Duct, 3rd EUCASS Proceedings, July 2009, Versailles, France
3. Leonov S. B., Sabelnikov V.A., Yarantsev D. A., Napartovich A. P., Kochetov I. V. ―Plasma-Induced Ethylene Ignition and Flameholding in Confined Supersonic Air Flow at Low Temperatures", Plasma Science, IEEE Transactions on Plasma Science, 2011, February, accepted for publishing.

5. Task 2. Technical Results

Diagnostics development and analytical support.

The following parameters of the gas and plasma have to be measured during the tests:

- Gas temperature, averaged and local values, T_g;
- Distribution of static and stagnation pressure, P_o, P_{st};
- Optical spectra of the excited molecules N_2, CN, OH, CH;
- Temporal evolution of optical lines OH, CH, etc.;
- Plasma energetic parameters;
- Dynamics of the ignition processes by video-records and shadow photos;
- Relative concentration of important gas species.

Several diagnostic‘s methods are quite standard. They were described in Final Report on Project #3057p dated March 2009. A few methods applied are well known but their application requires extra efforts for adjustment for specific conditions of the test. As a rule each group of experimentalists improves such technique and procedure of data processing. In case of current project the most specific information was obtained by passive optical spectroscopy and active absorption laser spectroscopy. Features of experimental approach, which complicate the issue, are: short time of run, strong inhomogeneity of object studied, numbers of simultaneous processes and species in interaction volume.

At the present time an optical diagnostics of flames is the main experimental method for getting some qualitative information on the gas kinetics that are compared with combustion models. In particular, development of laser spectroscopic methods has resulted in the significant progress in the field of combustion investigation. Modern optical methods of the flame investigation possess high temporal and spatial resolution. It allows determining of the two-dimensional arrays of variety of reacting medium parameters. The most appropriate methods were chosen by such criteria as equipment accessibility, simplicity of use, and importance of the information that is given by them.

5.1. Measurements of reactant gas parameters distribution in area of plasma-gas interaction and combustion zone by laser-based non-intrusive diagnostics.

One of important goals of this Project was the development of DLAS technique for the contactless measurements of the parameters of a plasma-assisted supersonic combustion flow at the PWT-50H facility in the Joint Institute for High Temperature RAS. Molecular water was used as a test molecule. Water vapor is one of the major combustion products and key indicators of the extent of combustion and is therefore widely used as a tracer of combustion processes in mixed gas flows. The main problems to be solved in the frame of this Project were:

1. Development of the experimental DLAS instrumentation adjusted to the experiments at PWT-50H facility;
2. Optimization of the recording scheme to the conditions of PWT-50H facility with high level of electric and acoustic noises;
3. Optimization of the algorithm for fitting the experimental spectra in the case of an irregular baseline;
4. Measurements of the temporal and spatial distribution of the temperature and water vapor concentration in different combustion zones.

5.1.1. DLAS – method description.

The basic equation of absorption spectroscopy is the Bouguer-Beer-Lambert law. The general exponential form of the law can be expanded for the case of low absorption to the form

$$I_\nu = I_{\nu,0} \exp\left[-S(T)g(\nu - \nu_0)\, N\, L\right] \approx I_{\nu,0} - I_{\nu,0}\, S(T)g(\nu - \nu_0)NL\,, \qquad (1)$$

where I_ν is the intensity of the monochromatic radiation with a frequency ν (см$^{-1}$) transmitted by an absorbing medium of length L (cm), ν_0 (см$^{-1}$) is the frequency of the line center, S (cm/mol) is the line strength (integral intensity), g (cm) is the normalized line-shape function, N (cm^{-3}) is the number density of H_2O molecules. The line strength S depends on temperature while the line-shape function depends on temperature, pressure, gas composition and the mechanisms of line broadening. For pressures of about an atmosphere the line-shape is usually approximated by a Voigt profile. The typical absorption line width of the simple molecular components in mixing gas flows and flames is of the order of 0.1 cm^{-1} (3 GHz). Thus, single-mode DLs with typical line-widths ~ 10-50 MHz can be treated as monochromatic light sources and Eq. (1) can be used for evaluation of the experimental data with high precision.

The line strength $S(T)$ depends on temperature in the form:

$$S(T) = S(T_0)\frac{Q(T_0)}{Q(T)}\exp\left[-\frac{hcE''}{k}\left(\frac{1}{T}-\frac{1}{T_0}\right)\right]\left[\frac{1-\exp(hc\nu/kT)}{1-\exp(hc\nu/kT_0)}\right], \qquad (2)$$

where $Q(T)$ is the partition function, E'' is the lower state energy of the quantum transition, k is Boltzmann's constant, $S(T_0)$ is the line strength at a reference temperature T_0, h is Planck's constant and c is the speed of light.

The ratio of the line strengths of two different transitions depends only on the temperature and, assuming the second bracket in Eq. (2) is equal to unity, can be written in the form:

$$R = \left(\frac{S_1}{S_2}\right)_T = \left(\frac{S_1}{S_2}\right)_{T_0}\exp\left[\frac{hc\Delta E}{k}\left(\frac{1}{T}-\frac{1}{T_0}\right)\right], \qquad (3)$$

where ΔE is the energy difference between the lower levels of the selected transitions. Thus, from simultaneous measurement of the absorption at different lines one can deduce the temperature of a medium and from the measurement of the absolute absorption line intensity one can deduce the concentration of the absorbing species, provided that the spectroscopic parameters of the selected transitions are known.

For uniform media Eq. (1-3) give the actual temperature and concentrations. For non-uniform media path-integrated temperature and concentration can be calculated from the absorption spectra. The line strengths and broadening parameters for many transitions at ambient temperatures are well known.

One of the most serious problems of the diagnostics of non-steady-state processed by absorption spectroscopy with diode lasers (DLAS) is the fluctuations of the base line. These fluctuations are caused by several mechanisms:

- random amplitude modulation of diode laser (DL) intensity caused by modulation of the injection current during the wavelength scanning,
- strong scattering of the DL beam by the fluctuations of the refractive index in non-stationary gas flows,
- interference effects of the coherent DL radiation at the optical surfaces (cell windows, color filters, focusing optics etc.),
- temperature fluctuations of the active layer of the semiconducting chip of DL.

Due to non-stationary variations in plasma/reacting gas parameters and the processes of combustion the fluctuations of the base line have a stochastic character. Strong base line fluctuations complicate significantly fitting of the experimental absorption spectra of a test molecule with the simulated one, and in this way increase the errors of the evaluation of temperature and pressure in the combustion zone by DLAS technique.

Dominant part of the work on right signal extraction was related with the improvement of the electronic scheme of the recording system and development of the specific methods to decrease the influence of base line fluctuations on the results of DLAS measurements. The differential detection scheme was designed and tested. It was done in such a way, that the output signal should be zero (in fact - minimal), when there was no absorption of water molecules in the detection channel.

Simplified scheme of the first cascade is shown in Fig.5.1.1.1. The differential signal is the photocurrent generated at the common point of an operational amplifier OpAmp1. In this point the currents of the signal and reference photodiodes are combined, the polarity of the currents being opposite. To compensate the variations of the signal‘s photocurrent, which are not caused by H_2O absorption (intensity ramp, low frequency random amplitude modulation, technical noise etc.), the currents must be well equalized in both channels. It is done by tuning the differential current to zero, when there is no H_2O absorption in the signal channel. A pair of matched MAT04 transistors (Analog Devices, Inc.) automatically equalizes both channels. As

a result / H_2O

absorpt

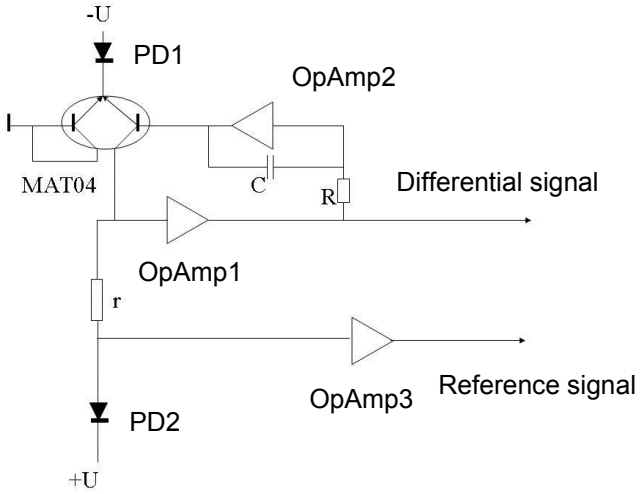

Fig.5.1.1.1. Scheme of the first cascade of electronic. PD1 – photo-detector of the signal channel, PD2 – photo-detector of the reference channel, OpAmp1,2,3 – operational amplifiers.

The reference signal is the signal proportional to the instant value of DL intensity. This signal is used for evaluation of the temperature channel according to Beer-Lambert law. This signal is collected from the resistor "r" (see Fig.5.1.1.1) in the circuit of PD1 and amplified by OpAmp3. Both signals were recorded by the two-channel digital oscilloscope Agilent 54621A, digitized for further processing and transferred to the PC.

Verification of DLAS.

First experiments at IADT-50 facility in the Joint Institute for High Temperature (RAS) have demonstrated the potentials of DLAS technique for contactless measurements of the parameters of hot zone. At the next step one needed the verification of DLAS technique. It was done in the laboratory experiments in the absorption cell with controllable parameters of the absorbing layer. Special absorbing cell was designed, in which temperature and total pressure of air could be maintained and regulated. Both parameters were independently measured by the commercial sensors. A simplified scheme for the laboratory cell used for DLAS verification is shown in Fig.5.1.1.2.

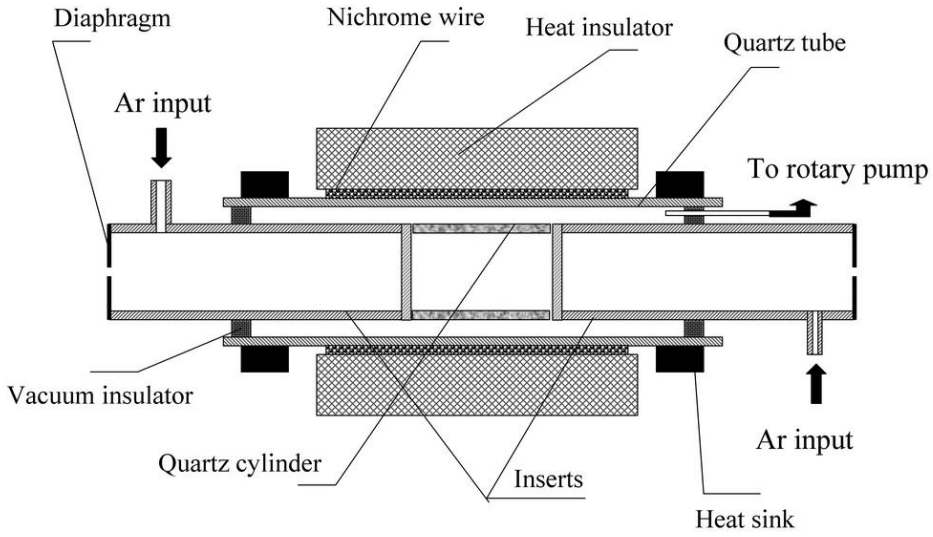

Fig.5.1.1.2. Experimental cell (see explanations in text)

The cell was made of a quartz tube (60 cm long, inner diameter 32 mm, wall thickness 3 mm) inserted in an electrically heated cylindrical oven. The absorbing air layer was formed by a quartz cylinder (10 cm long, outer diameter 22 mm) pressed between quartz windows attached to two cylindrical inserts (50 cm long, outer diameter 22 mm). The planes of both end surfaces of the cylinder were tilted slightly with respect to the optical axis. In this way the volume inside the cylinder was connected to the volume of the gap between the inserts and the main tube. The inserts were fixed inside the main tube by vacuum insulators. The space between the inserts and tube could be pumped out by a rotary pump through a metallic needle. The cell was heated by a Nichrome wire fixed on the central part of the main tube. In order to provide a uniform temperature profile along the absorbing layer, the oven was 4 times as long as the central quartz cylinder, 40 cm. This ratio provided the temperature profile from the central part to the end of the absorbing layer (10 cm) of – 20K for the maximal temperature of 1300K. The cell temperature can be varied from 300K to 1300K.

To minimize DL absorption by laboratory air outside the central part of the cell the cylindrical inserts were continuously blown up with a stream of pure argon. The temperature of the absorption air layer was measured by a commercial thermocouple PS2007 (Instrument Specialists Inc., USA) fixed inside the main tube close to the central cylinder containing the absorbing air. The air pressure of the absorbing layer was maintained or changed by a rotary pump and an input valve (not shown in Figure) and measured by a pressure sensor G16K (BOC Edwards, UK).

An example of the experimental spectra fitting is presented in Fig.5.1.1.3. Two different fitting methods were compared. The first one is the common profile fitting method, in which each absorption line is fitted separately using different kinds of modeling line profile. The following theoretical line shapes were used: Voigt function with independent Gaussian and Lorentzian parts (VP), Voigt profile with equal Gaussian width for both lines and different Lorentzian widths (VPEG), and a Rautian profile (RP), which takes into account Dicke narrowing.

Part of the spectra with two lines for an air temperature ~1000 K is shown in the upper trace of the Fig.5.1.1.3, the residuals for two fitting algorithms – Spectrum Fitting (SF) and Voigt Profile Fitting with equal Gaussian width (VPEG) are shown below.

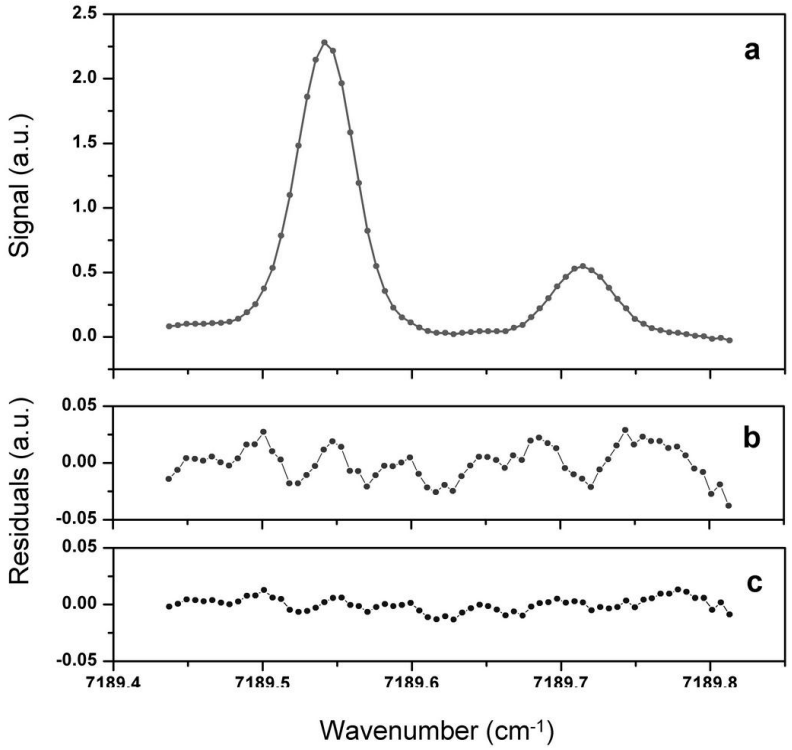

Fig.5.1.1.3. Example of the experimental line fitting. a) H_2O absorption lines 7189.541 cm^{-1} and 7189.715 cm^{-1}. The points are the experimental values, solid line is the best fitting. b) residual (difference between experimental and theoretical spectra for SF model; c) residual for VPEG model.

In Fig.5.1.1.4 temperatures derived from DL spectra using different fitting procedures are plotted versus temperatures measured by the thermocouple. It is noteworthy that the minimal residual is obtained for the VPEG (Fig.5.1.1.3c), but this model gives a large deviation of the evaluated temperatures from temperatures measured by the thermocouple, particularly for temperatures above 1000 K (Fig.5.1.1.4). For this temperature magnitude the variations of the

baseline were more pronounced from scan to scan as compared to the temperature range (300-800) K. It can be explained by the increased fluctuations of the DL beam inside the cell caused by higher temperature gradients. The SF model shows larger minimal residual, but provides better accuracy (Fig.5.1.1.4). This algorithm was selected as the optimal one for the experiments at the IADT-50 facility within the Project.

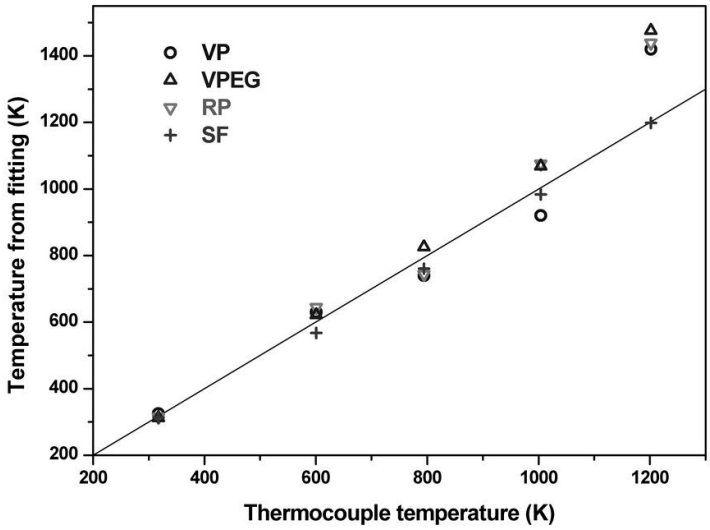

Fig.5.1.1.4. Temperature evaluated by TDLAS vs temperature measured by thermocouple.

5.1.2. DLAS - spectra processing.

5.1.2.1. Primary processing of the non-stationary absorption spectra

In the experiments considered the hydrogen and ethylene were used as the fuel. The water vapor concentration was high enough to detect direct absorption with the appropriate SNR. Two one-dimension files with 2×10^6 points each were detected in a single run. The full registration time was 500ms. The first file contains about 600 scans of differential signals, the second one about 600 scans of the incident DL intensities, detected in the second channel. The raw data detected in the first 250 ms of a single run are presented in Fig.5.1.2.1. The aerodynamic parameters of this run were: static pressure in pre-mixing zone, 130 Torr, fuel mass flow rate G_f 0.5 g/s.

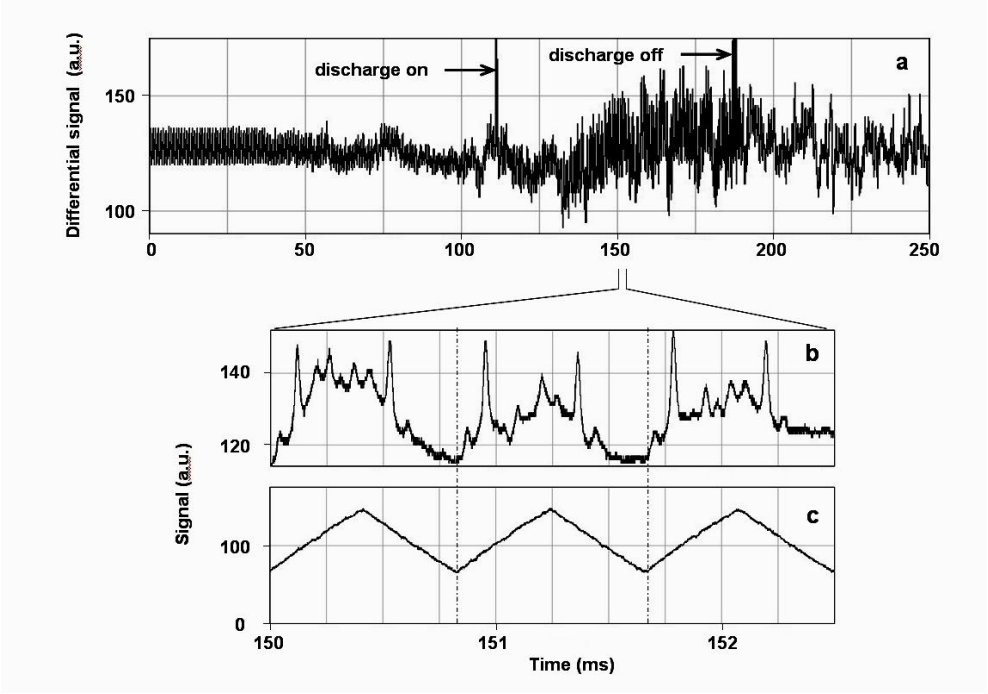

Fig.5.1.2.1. Fuel – hydrogen. a) Trace of the first 250 ms of a run (differential output), b) fragment of this run corresponding to three round-trip scans of DL wavelength, c) the saw tooth DL intensity variation during these scans (second output of the scheme).

The times of plasma on and off are indicated in Fig.5.1.2.1. The run and the oscilloscope scan are started by a trigger pulse. 30 ms after the start, the air valve opens and 20 ms later the gas flow reaches the supersonic regime (M=2). 120 ms after the start the discharge is ignited, the fuel (in this case hydrogen) is injected and the combustion process starts. At about 190 ms the discharge is off and the combustion ends.

In each scan the DL intensity varies during the round-trip cycle of wavelength tuning due to injection current modulation and the water vapor absorption. Short fragment of 3 scans (about 2.5 ms) is presented in Fig.5.1.2.1b. This fragment corresponds to about middle of the run. Fig.5.1.2.1c shows 3 corresponding scans of DL intensity registered in the second channel. These temporal profiles of DL intensity were used to infer temperature and water concentration.

In the initial step of data processing the file in Fig.5.1.2.1a was transformed into a 2D image. This procedure greatly simplified the general overview of the data and selection of the most important periods of the combustion process. In the following steps only the periods containing important information were processed. The algorithm used for the digital processing of the 2D images is based on the ImageJ software with open source code [2]. This algorithm enables comfortable visual presentation of the experimental data and significantly reduces the processing time. The result of such processing of the file from Fig.5.1.2.1a is shown in Fig.5.1.2.2.

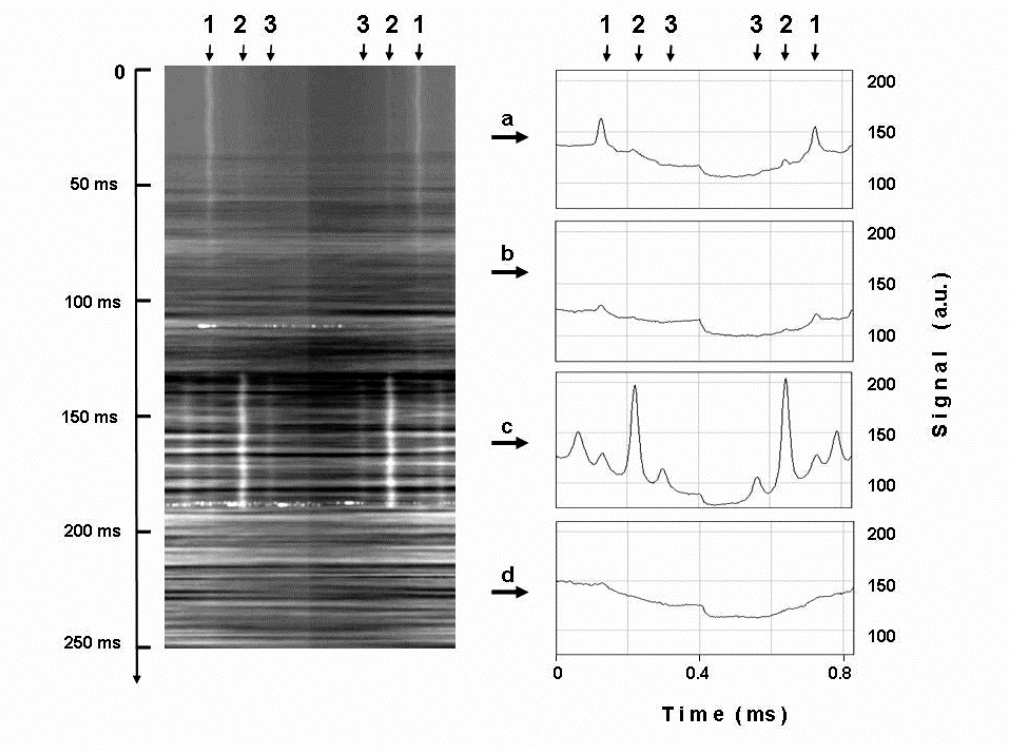

Fig.5.1.2.2. 2D image of the raw data (left) and H_2O absorption lines integrated over 30 scans (right). The time intervals (a-d) correspond to different stages of the. The spectral lines used for processing are labeled by numbers. Line attribution: (1) – 7189.344 cm^{-1}, (2) – 7189.541 cm^{-1}, (3) – 7189.715 cm^{-1}.

Fig.5.1.2.2a shows a 2D image of the differential signals detected during the first 250 ms of the run. The 2D image is constructed from the individual successive scans. In each scan the DL

intensity varies according to the variation of the injection current (linear ramp) and H_2O absorption when the DL wavelength coincides with the wavelength of the absorption line. In this way the H_2O absorption spectra is registered in each scan. In the image presented in Fig.5.1.2.2a the frequency v of DL radiation changes from left to right (x axis). During first half of the scan v decreases with the increase of DL injection current and vice-versa during the second half. All scans are arranged one below the previous one with the number of the scan n increasing from top to bottom (y axis). The interval of DL frequency tuning (axis x) is about $1cm^{-1}$, the full duration of one scan is about 830 μs, the duration of the presented part of the scans (axis y) is about 250 ms. The software allows one to select and process any part of the image (time interval) and to average any number of scans.

In the experiments with plasma-assisted combustion the baseline exhibited much stronger variations, as compared to the laboratory experiments, during one scan and from scan to scan because of strong turbulence in the probed volume. The dark horizontal lines in Fig.5.1.2.2a are the result of strong deviation of the DL beam from the adjusted trajectory in a particular scan (or scans).

The absorption lines are well seen in the 2D image as the light vertical stripes. The different phases of the combustion evolution, denoted by the letters (a-d) can be distinguished. Fig.5.1.2.2 right presents the H_2O absorption spectra reconstructed from the 2D image in Fig.5.1.2.2 left. These spectra are the result of averaging over 30 scans in four different characteristic intervals of the run. During the time interval labeled by ***a*** in Fig.5.1.2.2 the zone of observation is filled with air at room temperature. The "cold" line 7189.344 cm^{-1} is well seen both in the image and in the spectra (Fig.5.1.2.2). At the end of the interval ***a*** air flow reaches the supersonic regime, which results in a decrease of the gas temperature to ~ 200K. The temperature drop causes freezing of water vapor. As a result, the intensity of the water absorption spectra starts to decrease and after approximately 20-30 ms disappears, which is clearly seen both in the image and spectra in Fig.5.1.2.2 (interval ***b***). About ~ 110 ms after the beginning the discharge is ignited and ~ 20 ms later the fuel is injected. The combustion process starts at this moment and the temperature rapidly increases. The temperature increase is well illustrated by the appearance of the H_2O "hot" lines: 7189.715, 7189.541 and 7189.199 cm^{-1}. In the same period the "cold" line 7189.344 cm^{-1} dramatically decreases. This structure of the spectra remains over a time interval of ~ 50 ms when the combustion is sustained (interval ***c*** in both figures). After the plasma is switched off the combustion rapidly ends and the water lines disappear (interval ***d***). During this time interval the conditions of the supersonic flow are similar to those during interval ***b***.

Note, that in the described experiments the deviations of the DL beam inside the chamber, variations of total and local concentration of water molecules, beam attenuation (scattering) due to aerosol formation inside the combustion zone and the tail of the flame were much stronger as compared to the laboratory experiments. Because of this the variations of the differential signal and variations of the baseline from run to run were rather strong. To keep the signal within the dynamic range of the ADC we had to decrease the amplification of the electronic system and, hence, the effective dynamic range of the absorption signal recording to about 5 bits (compare to 8 bits in the laboratory experiments). This loss of the linear dynamic range was partly compensated by the short time of digitizing of the used ADC (250 ns). The fast response of the ADC enabled to cut off high frequency noises by a low-frequency digital filter applied at the first step of data processing. As a result, each point of the reduced file was an average of 16 raw points. In this way the level of effective digitization was improved to 7-bit.

5.1.2.2. Evaluation of the hot zone parameters

All absorption lines detected and processed in our experiments were weak enough to use the linear approximation in Eq. (1). The differential signal Y_i at a frequency ν_i detected by the recording system can be rewritten in the form:

$$Y_i = \alpha I_{0i} \sum_j S_j(T) g_j(\nu_i - \nu_{0,j}) NL + b_i + \varepsilon_i , \qquad (4)$$

where α is the coefficient of amplification of the electronics, ν_{0j} is the center of the absorption line j, b_i presents the baseline and ε_i is the residual (difference) between the experimental and simulated spectra. All other parameters are denoted for Eq. (1).

Two different fitting methods were compared. The first one is the common profile fitting method in which each absorption line is fitted separately using different kinds of modeling line profile. We tried the following theoretical line shapes: Voigt function with independent Gaussian and Lorentzian parts (VP), Voigt profile with equal Gaussian width for both lines and different Lorentzian widths (VPEG), and a Rautian profile (RP) [3], which takes into account Dicke narrowing. Parameters characterizing line profiles (center, area, width and so on) were adjustable. The baseline was approximated by the polynomial $b_i = \Sigma k_n Q_{in}$, with k_n – fitting parameters, Q_{in} – orthogonal polynomial. A polynomial rank of 2 or less was used. The temperature was determined from the ratio of the areas under two fitted lines by comparing this ratio with the theoretical one.

The second approach was spectrum fitting (SF), in which the experimental spectrum was fitted to a theoretical one calculated using spectral databases. The fitting was started with the matching of the maxima of the selected lines to the tabulated reference values. Linear scanning of the DL wavelength with time during a scan was assumed. At the next step physically reasonable values of the initial temperature T and total pressure P were selected and a theoretical spectrum in the region of interest was calculated using spectroscopic parameters from the HITRAN 2008 database [1] and partition function Q(T) from the SPECTRA database [4]. Then, using the nonlinear least-squares Nelder-Mead method [5] the values of temperature and total pressure were found from the best fit of experimental spectra, e.g., from the minimal value of $\sqrt{<\varepsilon_i^2>}$.

For the run shown in Fig.5.1.2.2 fitting gave a temperature of the probed zone of T=1050 K, and a water vapor concentration (partial pressure) of 21 Torr. The developed model provided fitting with $\sqrt{<\varepsilon_i^2>} \sim 0.4\%$. In this example a linear polynomial was used for the baseline.

The DLAS technique and algorithm of data acquisition give the line-of-sight values for the temperature and H_2O concentration. In reality both parameters fluctuates along the optical path inside the camera. It means that the line-shapes and widths of water molecules depend on the coordinate along the beam. The used technique can only provide ~~–a~~veraged" line shapes and infer ~~–a~~veraged" temperature and water concentration. It is well known that in any gas flow in a closed compartment there exists a wall layer of cold gas. The results of the preliminary investigations of the combustion zone structure by a shadowgraphic technique gave a rough estimation of this layer to about 2-3 mm. We did not account for this layer in our model.

To detect the variations of the parameters along the beam one needs to probe the combustion zone in the perpendicular direction and/or to use much more complex multi-beam scheme. Note, that Abel inversion technique cannot be used in our case because of irregular fluctuations of *T, P, N* distribution from scan to scan.

The total pressure in the zone was estimated from the width of the broadened lines. Broadening of the absorption lines by air and self-broadening by H_2O molecules were taken into account using [1]. The coefficient of water self-broadening is 5-6 times greater than the coefficient of water line broadening by air. Accounting for self-broadening provided an accurate value of the total pressure in the probed zone P = 200 Torr, which is in quite reasonable agreement with the value ~ 210 Torr measured by the membrane pressure meter incorporated in the test chamber. The model overestimated the total pressure (about 270 Torr) when self- broadening was ignored.

5.1.2.3. Improvement of the linearity of DL wavelength tuning.

The above described results have discovered an extra source of errors in estimation of the gas temperature and water concentration by DLAS technique. To improve the S/N ratio the scan averaging has to be used. It was found that DL wavelength tuning is not linear within full range of the scan. The wavelength profile does not exactly fit the linear profile of the DL injection current. Because of this the position of the absorption lines maxima are not the same at the rising and falling parts of the triangle profile of the injection current.

The linearity of the DL wavelength tuning was examined using the Fabry-Perrot etalon. The F-P spectra proved much better linearity at the falling part of the full scan. The new generator for injection current scanning was designed. The initial symmetric triangle form, used in the experiments at IADT-50 was replaced by the asymmetric saw-tooth form with rapid rising and slow falling parts. With this new generator the absorption spectra were detected for further processing only at falling part of the scan. The time diagrams of the old and new profiles are shown in Fig.5.1.2.3.

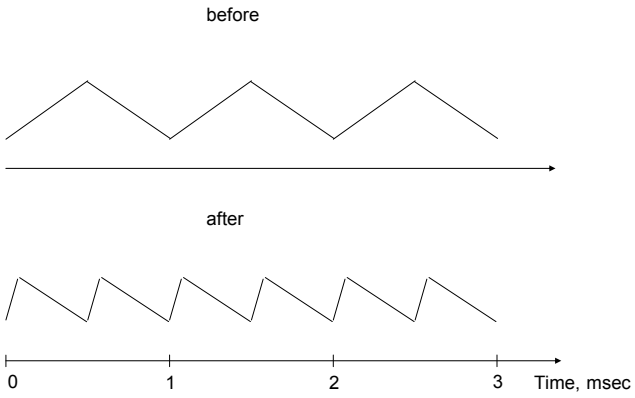

Fig.5.1.2.3. Old and new injection current time profiles.

Besides, the uncertainty of the beginning of the successive scans in one-two bits was originated by the lack of rigid synchronization of the beginning of the injection current scan and the beginning of signal conversion in the oscilloscope ADC. These random variations provided the effective line width broadening during the scans averaging. To improve the synchronization the new home-made generator for the DL current scanning was designed for the experiments at PWT-50H facility. The generator was triggered by the 5-Volt master pulse

of the oscilloscope, which is used for calibration. The output of this signal is located at the front panel of the oscilloscope.

References to section 5.1.2.

1. L.S. Rothman, D. Jacquemart, A. Barbe, et al., The HITRAN 2004 molecular spectroscopic database, J. Quant. Spectrosc. Radiat. Transfer, 96 (2005) 139-204; HITRAN website: http://www.cfa.harvard.edu/hitran//
2. W. Burger, M.J. Burge, Digital image processing: An algorithmic approach using Java, Springer, 2008; ImageJ website: http://rsb.info.nih.gov/ij/
3. S. G. Rautian, I. I. Sobelman, Usp. Fiz. Nauk 90, 209 (1966) [Sov. Phys. Usp. 9, 701 (1967)].
4. SPECTRA website: http://spectra.iao.ru
5. J.A. Nelder, R. Mead, Computer Journal 7, 308 (1965).

5.1.3. Result of measurements by laser absorption spectroscopy

The most experiments on PWT-50H facility was performed with the new version of DL tuning. Note, that the duration of the scan was about two times shorter (~416 μs), as compared to above described version of triangle profile of the injection current (830 μs). The example of the transient absorption spectra recorded with this version of DL tuning is shown in Figure5.1.3.1. In this run the mixture of ethylene and hydrogen was used as the fuel.

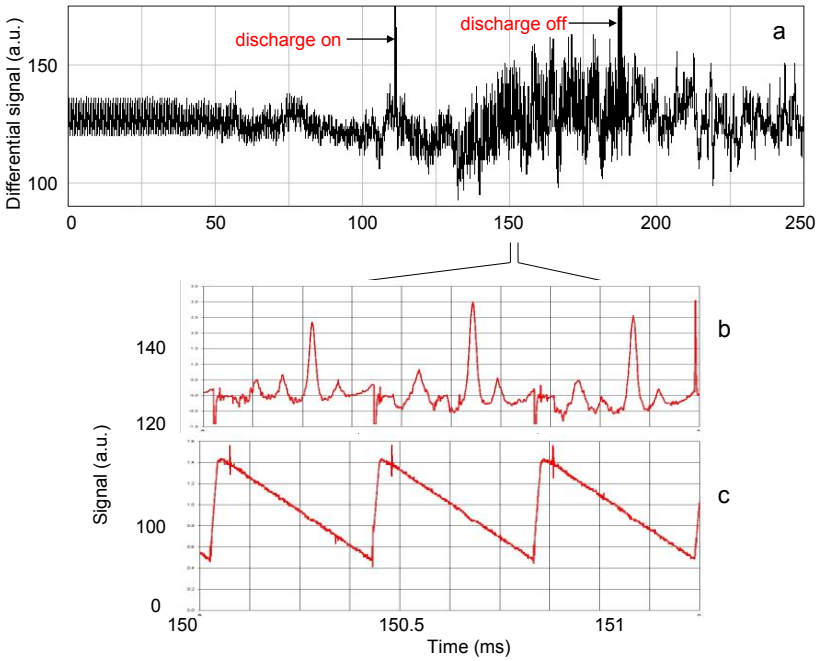

Fig.5.1.3.1. Fuel – mixture of ethylene and hydrogen. a) Oscilloscope trace of the first 250 ms of a run (differential output), b) fragment of this run corresponding to three round-trip scans of DL wavelength, c) the saw tooth DL intensity variation during these scans (second output of the electronic scheme).

The structure of the spectra is very similar to the spectra described above (see Fig.5.1.2.1). Visual difference is the temporal profile of DL tuning during a scan and appropriate difference in the symmetry of the spectra. Main physical difference – lower temperature of these runs will be discussed below.

The 2D-images and according spectra, similar to presented in Fig.5.1.2.2, are shown in Fig.5.1.3.2. One can point out serious difference between the processes in pure hydrogen and mixture of ethylene and hydrogen (Fig.5.1.3.2). In latter case the traces of water vapor are seen during full duration of the process. It may be interpreted in different ways. One explanation is higher spatial concentration of the hot gas in a kind of stratus(es) and larger volume with ~~–~~cold" vapor, not involved in the gas stream.

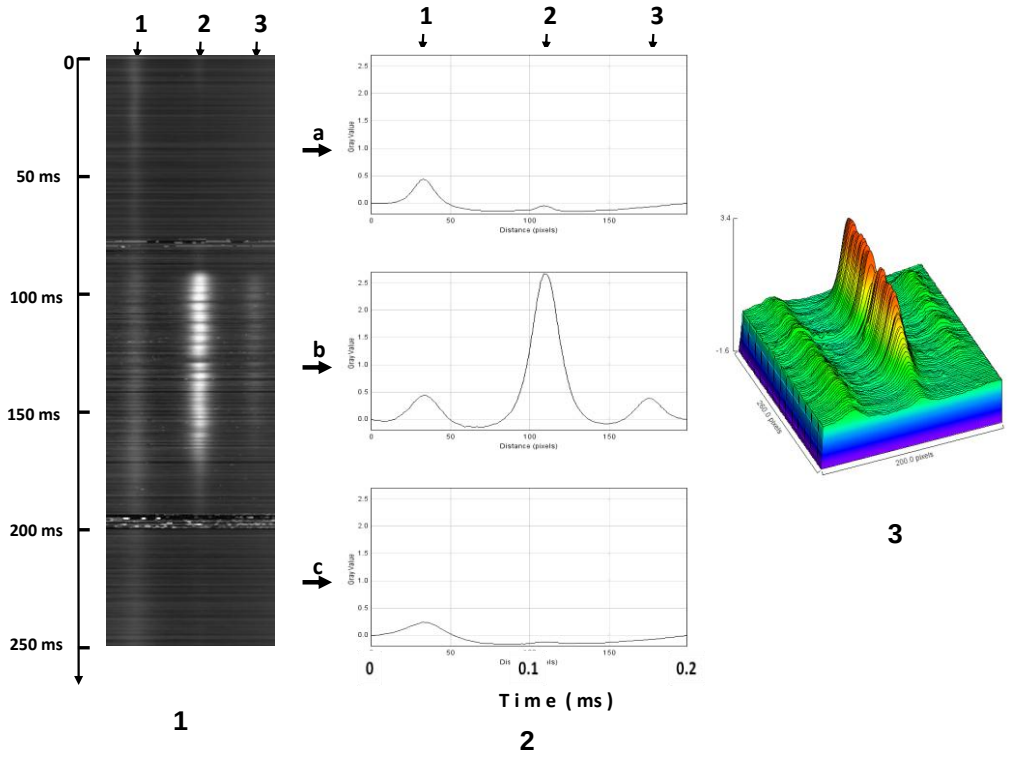

Fig.5.1.3.2. (1) - 2D image of the raw data, (2) - H_2O absorption lines integrated over 100 scans, (3) - 3D image of the stage (b) of the run. The time intervals (a-c) correspond to different stages of the run. Line attribution is the same as in Fig.5.1.2.2.

Generally, the sight-of-light absorption of the DL beam is the sum of the absorption in a part with ~~–c~~old" gas and in a hot layer. Probably, in PWT - 50H facility hot zone is more concentrated as compared to the previous versions and the contribution of the cold gas absorption to the light-of-site signal is more pronounced. Another argument for this hypothesis is relative stable intensity of the ~~–c~~old" line, which is also noticeably differs from the situation in pure hydrogen (see Fig.5.1.2.2). Relatively constant intensity of the ~~–c~~old" line during the cycle can be also explained by higher contribution of the cold gas to total signal. Note, that narrow line-width of this cold line undoubtedly proves the fact that gas inside the chamber with low total pressure is responsible for the absorption signal. The water vapors in ambient laboratory atmosphere would provide much broader line.

The analysis of the experimental absorption spectra detected on IADT-50 and their data processing were performed in two steps. For the quick semi-quantitative estimation of the gas temperature the special software for preliminary processing was designed. More precise data were obtained at the next step using the developed program of the transient spectra fitting.

Firstly, the file of raw data is transformed into a 2D image. This procedure greatly simplifies the general overview of the data and selection of the most important periods of the combustion process. In the following steps only the periods containing important information are processed. The algorithm used for the digital processing of the 2D images is based on the ImageJ software. The example of such processing of the run 5 from 30.06.2010 is shown in Fig.5.1.3.3.

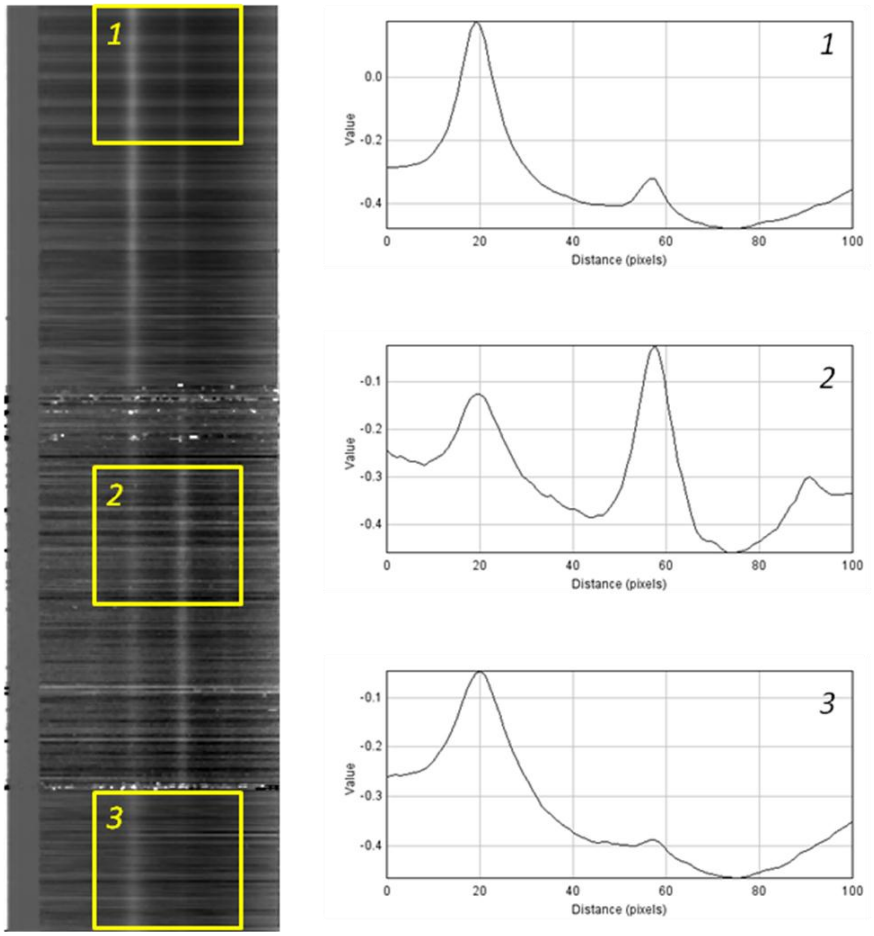

Fig5.1.3.3. 2D image of a particular run (left) and experimental spectra integrated over 100 diode laser scans of the same run (right). Fuel – ethylene.

Left figure shows a 2D image of the absorption spectra detected during the first 300 ms of the run. The 2D image is constructed from the individual spectrum in successive scans. In each scan the diode laser (DL) intensity varies according to the variation of the injection current (linear ramp) and H_2O absorption when the DL wavelength coincides with the wavelength of the absorption line. In the image presented the frequency v of DL radiation increases from left to right (x axis). All scans are arranged one below the previous one with the number of the scan n increasing from top to bottom (y axis). Thus constructed picture presents a 2D image of the time development of the absorption spectra of the probed zone. The interval of DL

frequency tuning (axis *x*) is about 0.8 cm^{-1}, the full duration of one scan is about 830 μs, the duration of the presented part of the scans (axis *y*) is about 300 ms. The software allows one to select and process any part of the image (time interval) and to average any number of scans.

The absorption lines are well seen in the 2D image as the light vertical stripes. The different phases of the combustion evolution, denoted by the digits (***1-3***) can be distinguished. Right figures present the H_2O absorption spectra reconstructed from the 2D image in the left figure. These spectra are the result of averaging over 100 scans in three different characteristic intervals of the run. During the time interval labeled by ***1*** the zone of observation is filled with air at room temperature. The ~~c~~old" line 7189.344 cm^{-1} and ~~w~~arm" line 7189.541 cm^{-1} is well seen both in the image and in the spectra. About ~ 110 ms after the beginning the discharge is ignited and ~ 20 ms later the fuel is injected. The combustion process starts at this moment and the temperature increases. The temperature increase is well illustrated by the increase of the H_2O ~~w~~arm" line 7189.541 cm^{-1} and appearance of the ~~h~~ot" line 7189.715 cm^{-1}. In the same period the ~~c~~old" line 7189.344 cm^{-1} decreases. This structure of the spectra remains over a time interval of ~ 50 ms when the combustion is sustained (interval ***2*** in both figures). After the plasma is switched off the combustion rapidly ends and the water temperature decreases (interval ***3***).

The potentials of the designed software for the fast quasi-on-line evaluation of the transient absorption spectra are presented in Fig.5.1.3.4.

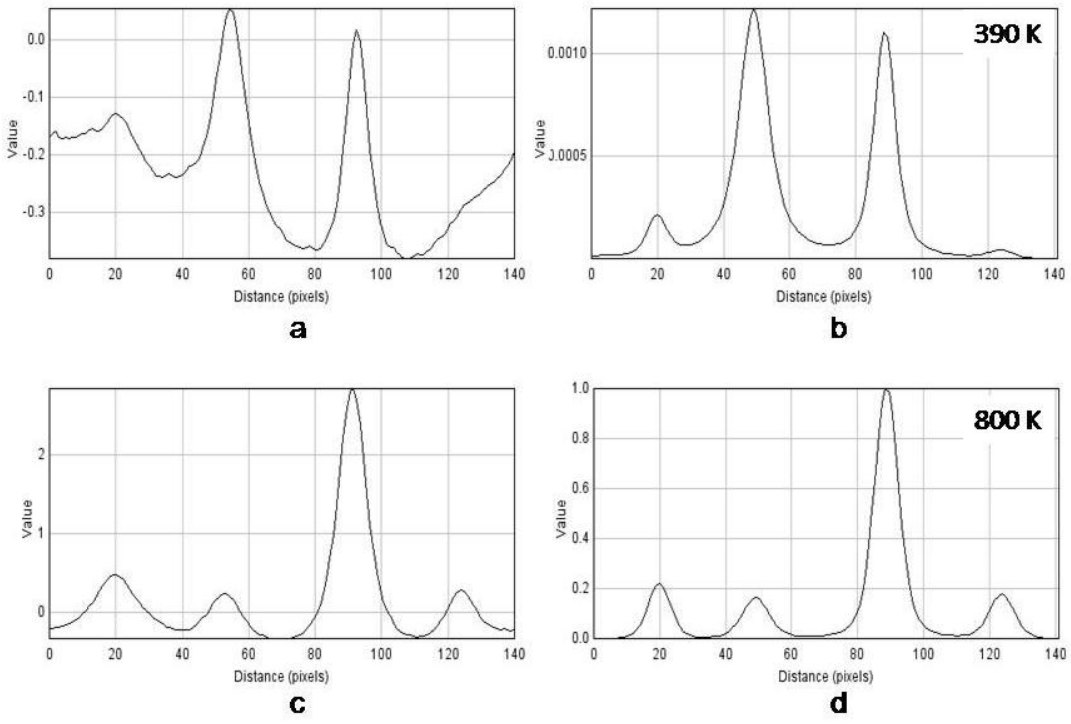

Fig5.1.3.4. Experimental (a, c) and simulated (b, d) absorption spectra.

The software designed allows on-line simulation of the H_2O absorption lines for a given static pressure and any gas temperature. After each run both experimentally detected and simulated spectra are displayed on the PC. An operator just smoothly varies the temperature for simulated spectra using function keys on the computer keyboard and visually compares amplitudes of the experimental and simulated lines. At this stage the influence of the variations of total pressure and concentration of water vapors on line broadening is not taken into consideration and gas temperature is estimated only by the ratio of the line amplitudes, but not by the integrals.

This fast on-line evaluation of the gas temperature greatly simplifies the optimization of the experimental parameters of the IADT-50 set-up. The spectra shown in Figure 2 were detected for two different regimes – (a) pure ethylene fuel – run 10 from 07.07.2010 and (c) mixture ethylene-hydrogen – run 12 from the same date. Evidently, the structure and relative intensities of the absorption lines dramatically differ for two regimes, which results in quite different estimated temperatures – 390 K and 800 K, respectively.

More precise off-line evaluation of the gas parameters are conducted at the second stage. The spectra detected were processed using the software developed for explicit evaluation of the gas parameters. Main ideas of the algorithm are described above. Full processing was provided for the time interval from 166 ms to 208 ms (DL scans from 400 to 500) from the beginning of the run. For all experimental parameters tested for ethylene combustion the gas temperatures did not exceed 500 K, thus for precise temperature evaluation the "low temperature" lines 7189.344 cm^{-1} and 7187.541 cm^{-1} were used. The temperature and water vapor concentration inferred from the spectra in Figure 1 (time interval ***2***) were 485 K and 5×10^{16} cm^{-3}, respectively.

The representative set of the measurements of temperature and water vapor concentration by DLAS technique are summarized in following tables. The parameters of gas flow in different zones downstream the igniting electrodes were inferred from the experimental absorption spectra using the developed fitting procedure. The data from HITRAN-2008 base were used.

Table5.1.3.1. Fuel - **hydrogen**

Temperature and concentration of the H_2O. Results obtained using two ~~–e~~old" lines: v_1=7189.34 cm^{-1}, v_2=7189.54 cm^{-1}.

x – horizontal coordinate of the probing zone from the electrodes; z – vertical coordinate of the probing zone from the top wall of the aerodynamic duct; α – distance from the electrodes to the vertex of the window angle. For Window 2 – 10 mm, for Window 3 – 160 mm.
Beam crosses the duct in horizontal plane at some angle, so the position of the exit is shifted from the entrance by 10 mm. It means that median x-coordinate of the beam is defined by the following equation: $x = \alpha + x_{exit} \pm 5mm$

1) Section Window 2, point 10: **x** = 10mm + 10mm – 5mm = **15mm**.

z, mm	1		2	3	4	5	6
	13.05 run 1	13.05 run 2	13.05 run 3	13.05 run 4	13.05 run 5	13.05 run 8	13.05 run 9
T, K	475	508	469	379	359	332	320
P_{H20}, Torr		1.9	1.6	1.5	1.4	1.6	1.4
n, 10^{16} cm^{-3}		3.6	3.4	3.9	3.8	4.6	4.3

2) Section Window 2, point 09: **x** = 10mm + 18mm – 5mm = **23mm**.

z, mm	1	5	7
	12.05 run 20	12.05 run 22	12.05 run 23
T, K	571	379	331
P_{H20}, Torr	5.8	2.9	2.2
n, 10^{16} cm^{-3}	10	7.5	6.5

3) Section Window 2, point 08: **x** = 10mm + 25mm – 5mm = **30mm**.

z, mm	1	4		5	6	8
	12.05 run 13	12.05 run 14	12.05 run 15	12.05 run 16	12.05 run 17	12.05 run 18
T, K	664	448	419	462	380	313
P_{H20}, Torr	10	4.4	5.4	4.1	3.1	1.4
n, 10^{16} cm^{-3}	15	9.4	12	8.5	7.8	4.3

4) Section Window 2, point 07: **x** = 10mm + 39mm + 5mm = **54mm**.

z, mm	3		6	8
	12.05 run 3	12.05 run 4	12.05 run 12	12.05 run 8
T, K	951	1142	732	477
P_{H20}, Torr	31	33	14	6.8
n, 10^{16} cm^{-3}	29	27.5	18	14

5) Section Window 2, point 11: **x** = 10mm + 49mm + 5mm = **64mm**.

z, mm	6	8	10	12
	13.05 run 12	13.05 run 13	13.05 run 14	13.05 run 15
T, K	580	440	354	347
P_{H20}, Torr	3.6	5.8	1.2	1.0
n, 10^{16} cm^{-3}	6.0	13	3.3	2.8

6) Section Window 2, point 03: **x** = 10mm + 58mm + 5mm = **73mm**.

z, mm	1	6
	04.05 run 04	04.05 run 07
T, K	1018	462
P_{H20}, Torr	29	6.9
n, 10^{16} cm^{-3}	28	14

7) Section Window 3, point 02: **x** = 160mm + 00mm - 5mm = **155mm**.

z, mm	1	6	11	16	21	26	31
	30.04 run 13	30.04 run 15	30.04 run 20	30.04 run 21	30.04 run 22	30.04 run 23	30.04 run 24
T, K	595	650	603	516	440	472	328
P_{H20}, Torr	15	15	13	8	4.5	11	8.5
n, 10^{16} cm^{-3}	25	23	20	15	9.9	3.2	2.5

8) Section Window 3, point 01: **x** = 160mm + 60mm + 5mm = **225mm**.

z, mm	2	7	12	17	22	27	32
	30.04 run 3	30.04 run 4	30.04 run 5	30.04 run 6	30.04 run 8	30.04 run 11	30.04 run 12
T, K	**540**	**576**	**529**	**473**	**425**	**353**	**300**
P_{H20}, Torr	12	13	10	9	6.2	4.7	1.5
n, 10^{16} cm^{-3}	22	21	19	19	14	13	4.9

Table 5.1.3.2. Fuel-**hydrogen**

x – horizontal coordinate of the probing zone from the electrodes; z – vertical coordinate of the probing zone from the top wall of the aerodynamic duct;

1). z = 4 mm. Distribution of the H_2O parameters at constant z along the x-axis.

x, mm	40	43	46	49	54	59	64	66
Run №	3	4	5	6	7	8	9	10
Averaging range, scans	350-400	350-400	350-400	350-400	350-400	350-400	350-400	350-400
T, K	978	947	1105	1058	1007	953	1025	1010
P_{H20}, Torr	19	18	24	22	22	23	21	20
n, $10^{16}cm^{-3}$	19	18	21	20	21	23	20	19
P_{total}, Torr	200	190	155	141	161	181	154	146

2) z = 4 mm; x = 64 mm. H_2O parameters at one point depending on fuel mass flow.

Δp, Torr	0,0075	0,15	0,25	0,32
Run №	12	18	19	20
Averaging range, scans	350-400	321-470	320-327	321-324
T, K	1061	800	1040	1245
P_{H20}, Torr	16	12	26	37
n, $10^{16}cm^{-3}$	15	15	23	29
P_{total}, Torr	135	170	108	97

Table 5.1.3.3. Fuel - **ethylene** (June 2010 – ~~c~~old" combustion)

x – horizontal coordinate of the probing zone from the electrodes; z – vertical coordinate of the probing zone from the top wall of the aerodynamic duct;

1) x = 40 mm.

z, mm	2	3	4	5	6
	30.06 run 5	30.06 run 2	30.06 run 6	30.06 run 7	30.06 run 8
T, K	485	427	386	345	284
P_{H20}, Torr	2.5	2.2	2	1.6	1
n, 10^{16} cm^{-3}	5	5	4.9	4.4	3.4

2) x = 163mm.

z, mm	4	9	14	19	24
	30.06 run 18	30.06 run 20	30.06 run 21	30.06 run 23	30.06 run 24
T, K	363	359	350	329	294
P_{H20}, Torr	3.1	2.7	2.7	2.5	1.8
n, 10^{16} cm^{-3}	8.2	7.2	7.5	7.4	5.8

3) x = 220 mm.

z, mm	2	3	4	6	8	10	12	14
	30.06 run 10	30.06 run 11	30.06 run 12	30.06 run 13	30.06 run 14	30.06 run 15	30.06 run 16	30.06 run 17
T, K	379	382	379	369	360	340	312	299
P_{H20}, Torr	3.3	3,3	2.9	3.1	2.8	2.7	2	2.1
n, 10^{16} cm^{-3}	8.5	8.4	7.4	8.1	7.4	7.8	6.1	6.9

4) z = 4 mm.

x, mm	40	50	60	70	158	168	178	188	198
	28.06 run 09	28.06 run 08	28.06 run 06	28.06 run 04	22.06 run 08	22.06 run 09	22.06 run 11	22.06 run 13	22.06 run 14
T, K	348	374	406	424	376	375	374	360	365
P_{H20}, Torr	1.6	1.9	2.1	2.6	2.3	2,3	2.2	2.1	2.2
n, 1016 cm-3	4.5	4.9	5	5.9	5.8	5,9	5.8	5.7	5.9

5) z = 4 mm.

x, mm	40	50	60	70	158	168	178	188	198
	28.06 run 09	28.06 run 08	28.06 run 06	28.06 run 04	22.06 run 08	22.06 run 09	22.06 run 11	22.06 run 13	22.06 run 14
T, K	348	374	406	424	376	375	374	360	365
P_{H20}, Torr	1.6	1.9	2.1	2.6	2.3	2,3	2.2	2.1	2.2
n, 10^{16} cm^{-3}	4.5	4.9	5	5.9	5.8	5,9	5.8	5.7	5.9

6) **z = 5 mm**.

x, mm	16	21	26	36	46
	28.06 run 13	28.06 run 14	28.06 run 15	28.06 run 16	28.06 run 17
T, K	284*	346*	369	420	459
P_{H20}, Torr	1*	1.3*	1.5	1.8	2.1
n, 10^{16} cm^{-3}	3.5*	3.6*	3.9	4.1	4.3

7) **z = 7 mm**.

x, mm	40	50	70
	28.06 run 10	28.06 run 11	28.06 run 12
T, K	260 253*	287 254*	315 297*
P_{H20}, Torr	.65 .79*	.54 .8*	1.1 1.1*
n, 10^{16} cm^{-3}	2.4 3*	1.8 3*	3.4 3.5*

8) z = 8 mm.

x, mm	158	168	178	188	198
	23.06 run 08	23.06 run 04	23.06 run 03	23.06 run 02	23.06 run 01
T, K	387 387*	383 386*	382 381*	381 378*	368 370*
P_{H20}, Torr	2.4 2.6*	2.8 2.7*	2,9 2.9*	2.8 2.8*	3.1 3.1*
n, 10^{16} cm^{-3}	5.9 6.5*	7 6.8*	7.4 7.4*	7.1 7.2*	8 8.1*

9) z = 14 **mm**.

x, mm	178	188	198
	23.06 run 17	23.06 run 15	23.06 run 12
T, K	362 357*	365 366*	357 356*

P_{H20}, Torr	2.6 2.7*	2.6 2.7*	2.9 3*
n, 10^{16} cm^{-3}	6.8 7.2*	7 7*	7.9 8*

10) z = 20 **mm**.

x, mm	178	184	184 z=26 mm
	23.06 run 21	23.06 run 19	23.06 run 20
T, K	302 301*	314 314*	282 280*
P_{H20}, Torr	2 1.9*	2 2*	1.4 1.3*
n, 10^{16} cm^{-3}	6.5 6*	6.1 6.2*	4.7 4.6*

Table5.1.3.4. Fuel - **ethylene** (November 2010); X=210mm

Z, mm	11	11	11	16	16	21	26
	25.11 run 04	25.11 run 05	25.11 run 06	25.11 run 07	25.11 run 08	25.11 run 10	25.11 run 12
T, K	484	464	450	485	425	500	477
PH20, Torr	3.9	4.8	5.2	6.1	3.6	5.8	3
n, 10^{16} cm^{-3}	8.2	10	10.9	12.1	6.2	10.9	6.4

Example of the spectra processing is shown in Fig.5.1.3.3 for the last data, see Table 5.1.3.4.

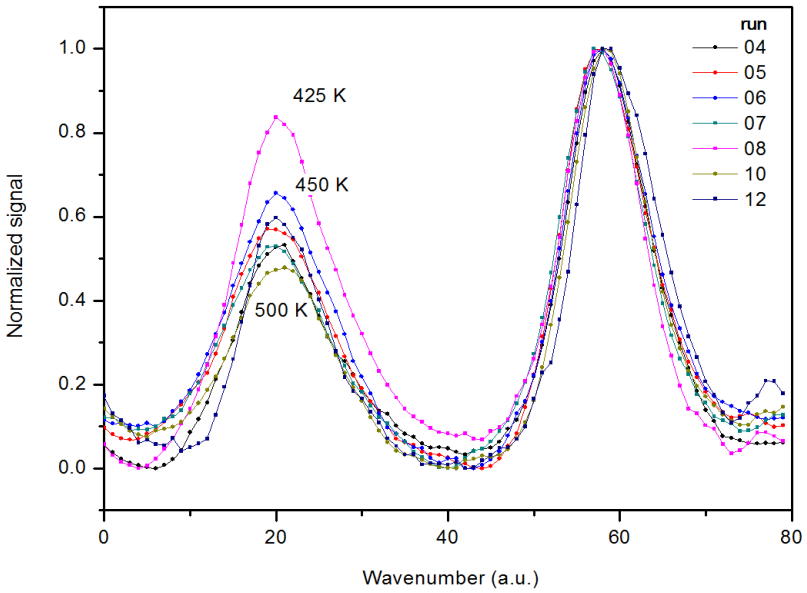

Fig.5.1.3.3. Spectra of the H_2O molecule in the 7189.15-7189.65 cm^{-1} region, normalized to the amplitude of the line at 7189.541 cm^{-1}.

Table5.1.3.5. Fuel - **ethylene** (December 2010); X=170mm

Z, mm	22	17	12	7	7	5
	10.12 run 04	10.12 run 05	10.12 run 06	10.12 run 07	10.12 run 08	10.12 run 09
T, K	340	358	390	436	375	368
P_{H20}, Torr	2.5	2.7	3.9	6.3	3.3	3.4
n, 10^{16} cm^{-3}	7.1	7.2	9.6	14	8.5	8.8

Example of the spectra processing is shown in Fig.5.1.3.4 for the last data, see Table 5.1.3.5.

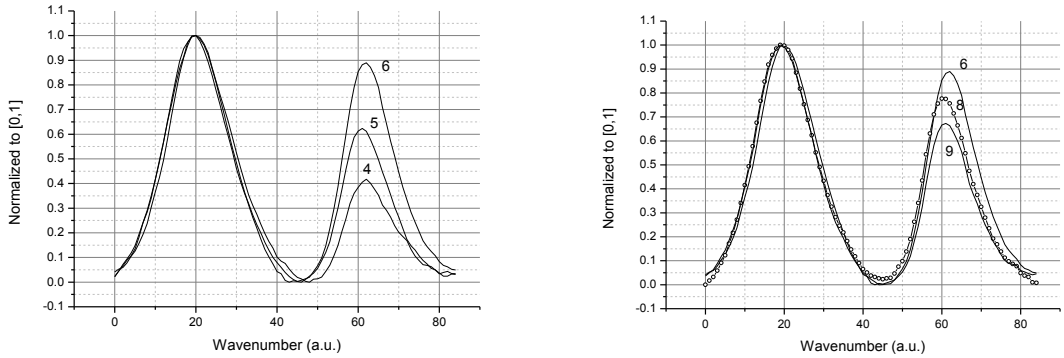

Fig.5.1.3.4. Spectra of the H_2O molecule in the 7189.15-7189.65 cm^{-1} region, normalized to the amplitude of the line [0,1].

Table 5.1.3.6. Fuel - **ethylene** (December 2010); X=157mm

z, mm	3	6	9	14	19
Run №	13.12 3	13.12 4	13.12 6	13.12 7	13.12 8
T, K	446	433	446	400	366
P_{H20}, Torr	6.1	7.2	4.8	4	3.1
n, 10^{16}cm^{-3}	13	16	10.4	9.6	8.2

Table 5.1.3.7. Fuel - **ethylene** (December 2010); X=70mm

z, mm	3	6	9		z=3; x=55
Run №	14.12 3	14.12 5,7	14.12 9		14.12 12
T, K	670	540	413		520
P_{H20}, Torr	5.1	6.3			4.7
n, 10^{16}cm^{-3}	7.5	13			8.6

5.1.4. Some ideas about Y-inhomogeneity of gas parameters

As was already pointed out the developed technique and algorithm of data acquisition give the line-of-sight values for the temperature and H_2O concentration. In reality both parameters fluctuates along the optical path inside the test section. It means that the line-shapes and widths of water molecules depend on the coordinate along the beam. The used above technique can only provide –averaged" line shapes and infer –averaged" temperature and water concentration. But in the case of exothermic reaction in the supersonic flow we obtain some separated zones with different temperatures because the mixing of zones is slow and temperature equalization is taking a place significantly downstream of the measuring point.

As the first approach a two-zone model could be applied for an analysis of Y-distribution of the gas temperature. The experimental spectrum $f_{sum}(x)$ obtained in this case is approximately the sum of –hot" and –cold" zones spectra with some coefficients k_h and $k_c=1-k_h$: $f_{sum}(x)=k_h \times f_h(x)+(1-k_h)\times f_c(x)$, and the total width of hot zone is the $k_h \times 72mm$ (72 mm is the width of combustor). Hot spectrum has three peaks (see Fig.6a), therefore we have two ratios of line's amplitude, which is enough to describe the spectra and find the temperature. Not each pair of ratios can be associated with definite temperature.

The –cold" spectrum is known and the difference between $f_{sum}(x)$ and $(1-k_h)\times f_c(x)$ can be found easily. Then the k_h can be determined in range from 0 to 1 by accurate fitting of experimental and simulated spectra. Because of three peaks spectrum is used in experiments it makes possible to divide spectrum to –cold" and –hot', find the temperature of the –hot" part of the flow, and determine the total width of this area.

The typical normalized absorption spectra and calculated model spectra in case of hydrogen are shown in Fig.5.1.4. Results obtained for X=15mm and Z=2mm give for hydrogen experimental –hot" temperature ~450K, but it is only averaged across the combustor temperature value. After recalculation the –hot" temperature value ~1300K was found, coefficients k_h was approximately 0.2. This example shows that it is very important to find recalculated –hot" spectrum from experimental –hot" and –cold" spectra, because there is significant difference between measured averaged temperature and the temperature of heated (–hot") zone.

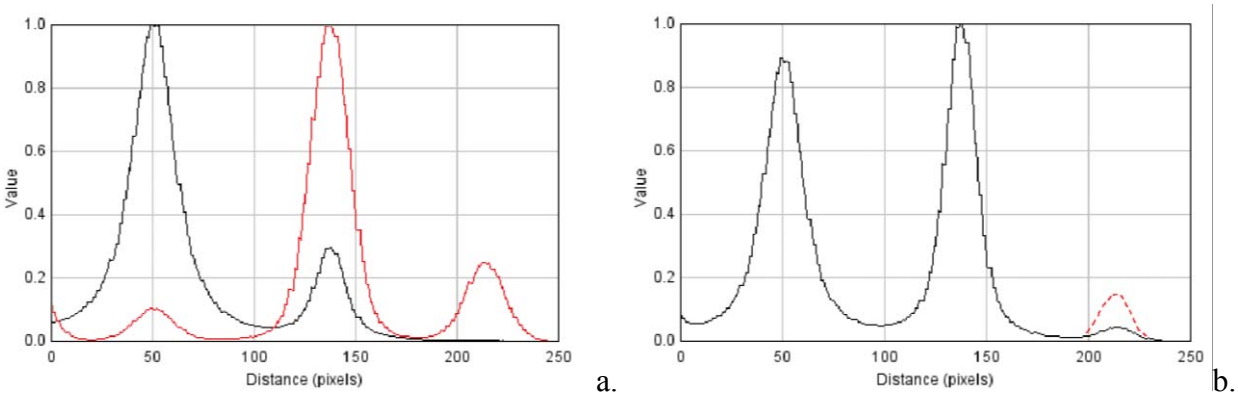

Fig.5.1.4. a – ―cold" experimental (black) 310K and ―hot" calculated (red) 1300K spectra.
b – ―hot" experimental (black with red) and nearest model (black) 450K spectra.

Reference to sections 5.1.3 - 5.1.4.

1. ―Control of Flow Structure and Ignition of Hydrocarbon Fuel in Cavity and behind Wallstep of Supersonic Duct by Filamentary DC Discharge", *Ed. S. Leonov*, Project ISTC-EOARD-JIHT RAS #3057p, The 4th year Report, March, 2009.
2. Leonov S. B., Carter C., Savelkin K. V., Sermanov V. N., and Yarantsev D. A., ―Experiments on Plasma-Assisted Combustion in M=2 Hot Test-Bed PWT-50H," 46th AIAA Aerospace Sciences Meeting and Exhibit (Reno, Nevada, USA, 7-10 January 2008), AIAA-2008-1359.
3. M.A. Bolshov, Y.A. Kuritsyn, V.V. Liger, V.R. Mironenko, S.B. Leonov, D.A. Yarantsev, ―Measurements of the temperature and water vapor concentration in a hot zone by tunable diode laser absorption spectrometry", *Appl. Phys. B*, vol. 100, 2010, p. 397.

5.2. Analytical and Computational support.

Analysis of two-stage scheme of plasma-enhances combustion.

5.2.1. Numerical analysis of nonequilibrium plasma effect on fuel ignition.

This section describes the method and basic results of simulation of fuel ignition by non-equilibrium plasma. With respect to technical simplicity, combined with low sensitivity to gas composition, one of the discharges was chosen for modeling, namely: transverse glow discharge in airflow [1-4], which can be considered as a straightforward extension of the conventional low-pressure glow discharge to the regime of high atmospheric pressure. Specific electrode construction, in combination with appropriate gas flow and distributed ballast resistors, stabilize this discharge for many gas mixtures. Experimentally achieved efficiency for energy deposition into the gas is not less than 90%.

A numerical model was developed combining traditional approach of thermal combustion chemistry with advanced description of the plasma kinetics based on solution of electron Boltzmann equation. This approach allows us to describe self-consistently strongly non-equilibrium electric discharge in chemically unstable (ignited) gas. Our model includes an electron Boltzmann equation solver calculated in parallel with kinetic equations for charged particles, excited molecular states, ion-molecule reactions and chemical reactions. Effect of chemically active species produced in the discharge on ignition delay time was studied for conditions of steady state glow discharge for mixtures of hydrogen and ethylene with dry air, while effectiveness of pulse-periodic discharge in shortening ignition time was explored for hydrogen-air stoichiometric mixture only.

Simplified schematic of combustion sell is shown in Fig.5.2.1.1. Calculations were performed for the supersonic flow with Mach number $M=2.5$, static pressure $P_{st}=1Bar$, static temperature $T=700K$, distance along flow up to 90cm for the hydrogen and ethylene mixed with dry air at varied energy input into the gas flow for stoichiometric compositions.

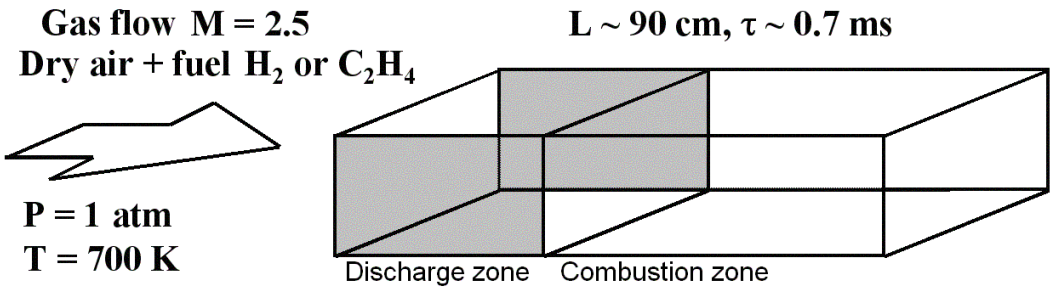

Fig.5.2.1.1. Simplified schematic of combustion cell.

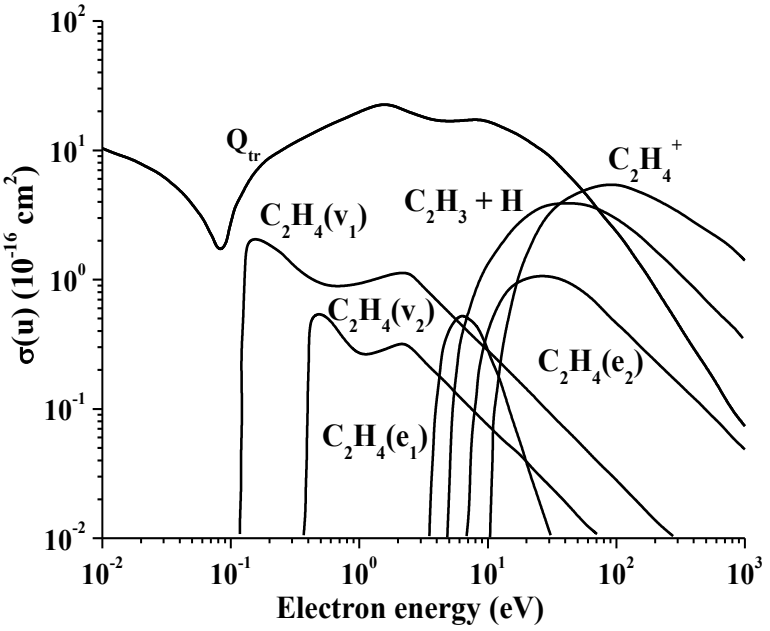

Fig.5.2.1.2. Electron scattering cross sections for C_2H_4.

The numerical model includes a system of kinetic equations for gas and plasma species, both charged and neutral. Ion heating in electric field resulting in increase of their temperature was taken into account, too. Rate coefficients for processes involving electrons were calculated from parallel solution of electron Boltzmann equation in a two-term approximation. In numerical simulations evolution of a gas portion transported by the flow was followed. Most calculations were done in suggestion of constant density. To prove those results in some cases the variation of gas-dynamic parameters along flow was taken into account as 1-D model. Numbers of reactions were (H2/C2H4): 26/30 processes involving electrons [5], 108/105 ion-molecular reactions [5], 92/294 neutral chemistry reactions [6], 51/80 total amount of species. The existing database for electron scattering cross sections was extended to include electron scattering processes for ethylene molecules. The selected cross sections are shown in Fig.5.2.12. Two vibrational modes and two electronic excited levels are included in the model. Single-channel dissociation and electron-impact ionization are considered, as well.

An effect of energy input variation is illustrated in Fig.5.2.1.3 for the ethylene-based mixture. As expected, the higher is the energy input, the shorter is the ignition time. Thermal and discharge ignitions were induced by depositing equal amounts of energy for the same time into the gas flow. The reduction of the ignition time at discharge initiation in comparison with thermal heating is clearly seen in Fig.5.2.1.4 for hydrogen and ethylene-air mixtures. In accordance with expectation the hydrogen requires considerably less value of energy deposition.

Along with cw glow discharge ignition of mixtures fueled by hydrogen, numerical simulations were made to evaluate in what degree the pulse discharge is more effective for initiation of combustion. Generally speaking, it is clear that pulse discharges can realize higher values of E/N parameter when production of radicals in plasma is more effective. However, to hold flame in the supersonic duct it is necessary to realize pulse-periodic operation of the discharge. It is important to compare time-averaged characteristics of steady current and pulse-periodic discharges. For such studies we select for numerical simulations of reasonably short pulse discharges technically available in the range of a few microseconds. It was assumed that the discharge area extends uniformly over the transverse width of the gas dynamic duct and some size along the flow. The energy input in one pulse was varied. As a reference points, ignition times were calculated also for the thermal initiation with the same energy input as in the discharge. It was considered that the pulse discharge is indeed more effective (shorter ignition time at the same energy input), but the effect is comparatively weak (about 20% difference in required energy input).

The simulation of pulse discharge gives some extra benefit in terms of power release. The Table 5.2.1 presents the data obtained by simulations in the most condensed form.

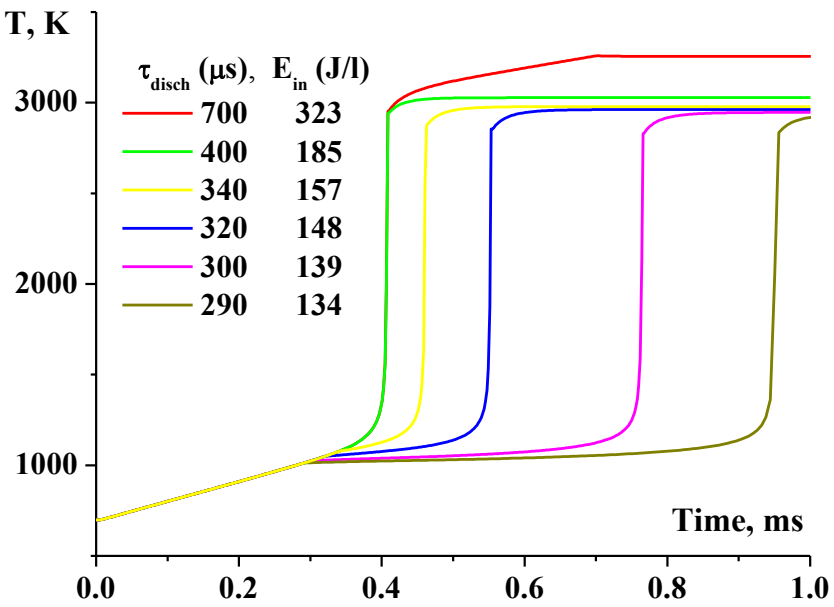

Fig.5.2.1.3. Gas temperature evolution for variable energy input. C_2H_4:O_2:N_2=1:3:12. P=1atm, T=700K.

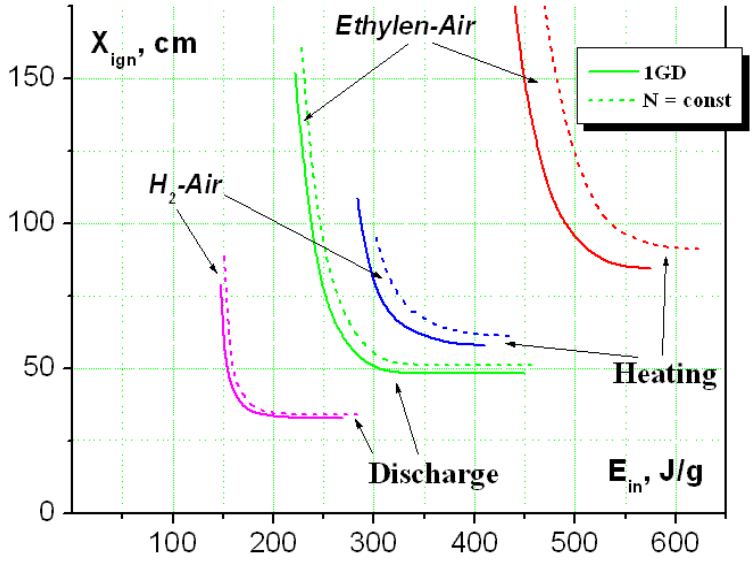

Fig.5.2.1.4. Ignition times at thermal and discharge initiation for H_2 and C_2H_4 fuels. P=1atm, T=700K. Comparison of 1-D gasdynamic model and constant density approach.

Table 5.2.1. Power benefit predicted for the fast ignition (Tg=700K, P=1Bar, Air, C2H4).

Mode, Tign=600µs	Heating	DC	Pulse 5µs	Pulse 10ns
W/G, J/g	520	265	230	210

References to section 5.2.1.

1. Akishev Yu. S., Kochetov I. V., Leonov S. B., Napartovich A. P. Production of chemical radicals by self-sustained discharge in air gas flow. // Proceedings of 5th International Workshop on Magneto-Plasma Aerodynamics for Aerospace Applications, Moscow, IVTAN, April 2003.A. Napartovich, I. Kochetov, S. Leonov, —Study of dynamics of air-hydrogen mixture ignition by non-equilibrium discharge in high-speed flow", J. of High Temperature (rus), No. 5, 2005, p.667.

3. Yu. S. Akishev, A. A. Deryugin, I. V. Kochetov, A. P. Napartovich, and N. I. Trushkin, J. Phys. D.: Appl. Phys., **26**, 1630, 1993.

4. Yu. S. Akishev, I. V. Kochetov, A. P. Napartovich et al, Plasma Physics Rep., **26**, 157-163, 2000.

5. Yu. S. Akishev, A. A. Deryugin, N. N. Elkin, I. V. Kochetov, A. P. Napartovich, and N.I.Trushkin, Plasma Physics Rep., 20, 437, 1994.

6. KINTECH, Kinetic technologies, *Chemical Workbench, www.kintech.ru.*

5.2.2. Two-stage scheme of plasma-based flameholding.

Two-stage mechanism of Plasma-Assisted Combustion was announced recently by G. Mungal, M. Cappelli with coauthors for convective flame [1-2], and by S. Leonov, V. Sabelnikov with coauthors for supersonic non-premixed flame [3-4]. The idea may be briefly described as follows: in case of hydrocarbon fueling and low temperature, flame stabilization by non-equilibrium plasma occurs by means of a two-step process. During the first step the plasma induces active radicals production and so-called "preflame" (or fuel reforming in terms of Stanford's team), which may be simplified as production of H_2, CH_2O, and CO. In spite of bright luminescence, this zone does not experience significant temperature and pressure increase. This "preflame" or "cool flame" [5-7] appears as a source of active chemical species that initiates (under favorable conditions) the second step of normal "hot" combustion, characterized by high temperature and pressure rise. Now this idea is promoted as one of the most important features of plasma method for the combustion enhancement.

It should be noted, that the two-zone mechanism of fuel ignition at low and moderate initial gas temperatures is not a specific feature of the plasma-assisted chemical processes. The overview of Sokolik [6] contains an excellent discussion of cold ignition and its role in the ignition process of heavy hydrocarbon fuels for internal combustion engines. In our case, generation of a notable amount of active chemical species by nonequilibrium plasma in air-fuel mixtures is the main cause for the two-zone mechanism. To illustrate this statement, we performed numerical simulations of the problem with following simplifications (in comparison with experiment): 1) isochoric ignition of premixed ethylene-air mixture 2) filamentary gas discharge was replaced by a uniform glow discharge. Gas residence time within experimental discharge zone is about 0.1 ms. The time interval in the numerical model was about 0.1 ms, which corresponds to the residence time within experimental discharge zone.

Our physical-chemical model is a consistent combination of two approaches [8]: classical thermal combustion theory (GRI Mech3 combustion mechanism) and glow discharge plasma kinetics. The equations of thermal and plasma chemistry are solved in isochoric approximation in parallel with the Boltzmann equation for the electron energy distribution function. It was shown in [9] that isochoric model is in a satisfactory agreement with results computed in frame of a system of 1D gas-dynamic equations in a plug flow model. GRI Mech3 combustion mechanism is widely used, its applicability is proven at temperatures higher than about 1100 K. Plasma kinetic model was validated for low temperature 300 K atmospheric pressure glow discharge in air [10]. This model includes evolution equations for charged particles' densities,

excited atom and molecules‘ densities, and electric circuit equation. Additional cross sections for electron scattering from C_2H_4 molecules were taken from [11].

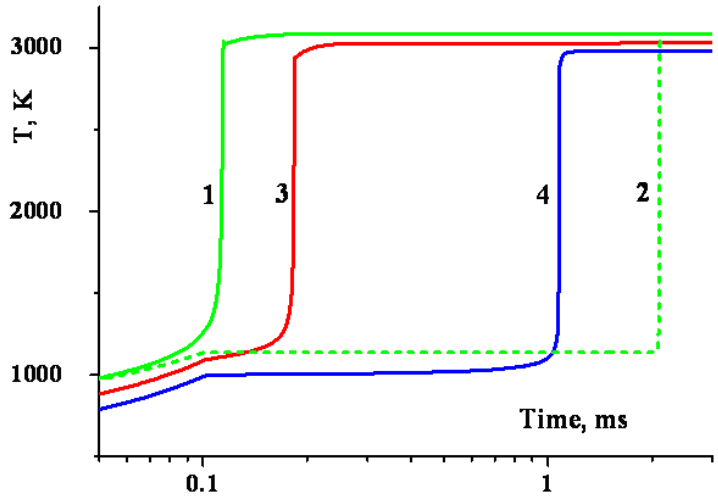

Fig.5.2.2.1. Calculated evolution of gas temperature at three different initial temperatures: 1, 2 – 800 K, 3 – 700 K, 4 – 600 K; 1, 3, 4 –plasma induced ignition, 2 – heating induced ignition. Input energy is 300 J/g. Discharge or heating time is 0.1 ms.

In this section we present the result of simulations, which clearly illustrates the two-zone mechanism of plasma-assisted ignition. Fig.5.2.2.1 shows the gas temperature evolution during ignition process of ethylene for three different initial mixture temperatures: 600K, 700K and 800K. For comparison, the gas temperature evolution induced by thermal heating equivalent to total discharge energy input (300 J/g) at the initial gas temperature 800 K is shown. At initial temperatures 600 and 700 K (curves 3 and 4) there exists post discharge zone (>0.1 ms) with slow growth of the gas temperature finishing with explosion-like growth corresponding to thermal combustion. Duration of this zone diminishes strongly at initial temperature increase. The decisive role of the discharge in ignition is clearly seen when comparing data for initial gas temperature 800 K for plasma-assisted and thermal initiation of combustion (curves 1 and 2).

It is expected that for homogeneous distribution non-equilibrium plasma discharge diminishes the energy needed to initiate the combustion [9-11]. The threshold energy was calculated in [11 see also section 5.2.1] for initiating homogeneous plasma combustion of the premixed ethylene-air mixture in conditions typical for scramjet. The threshold energy was about 210 J/g. This large value requires a powerful electricity source. One of the ways to reduce the threshold energy is to use the non-homogeneous discharge allowing you to utilize the chemical energy released in the large energy input. If the non-uniform plasma discharges is used to initiate the ethylene-air mixtures combustion, the specific energy for ignition was shown in [4] to be several times less than in the case of homogeneous discharge.

Characteristic feature of plasma ignition is the oxygen atoms production during the discharge and after its termination. Main mechanisms of the atomic oxygen production are the molecular oxygen dissociation in collisions with electronically excited nitrogen molecules and dissociation of oxygen molecules by the electrons of the plasma. After generation the oxygen atoms quickly react with the ethylene molecules. Intermediate compounds CO, CH_2O, CH_2CO, etc are produced in the process of chemical reaction. At low energy input, this stage lasts a long time. After a certain period of time the rapid process of ignition (second stage) starts, which results in complete combustion.

The process of ignition is usually described in the various mechanisms of combustion, for example, GRI 3.0, Konnov, UBC 2.0. These mechanisms are verified for burning at high temperatures. Generation of radicals at low temperatures, even in the presence of chain reactions, results in so large values of the induction time that the process of inflammation becomes random with a huge spread of the induction time. Therefore, the question of their fitness at lower temperatures is still open. Excitation of a mixture by the discharge produces high concentration of radicals, which diminishes strongly fluctuation values, so that the time of induction is a well-defined quantity. The correctness of the description of this stage depends on the values of constants used in chemical reactions involving radicals, generated by the discharge.

The growth of the gas temperature for the conditions of scramjet has been studied in [11] for different deposited energy inputs in the discharge. The increase in temperature was found to have a two-stage character. The aim of this work is to study the stages of plasma initiation by varying the initial composition of the gas mixture and the parameter E/N (E is electric field, N is the density of neutral particles), which can be varied in the given range by using different types of discharge. We study the predicted induction time variation due to different combustion models usage.

Calculations were performed using the Chemical WorkBench (CWB) [13], which implements the solution of chemical and ion-molecular kinetics equations together with the Boltzmann equation for electron energy distribution function and the equation for the translational gas temperature. Ignition of ethylene-air mixture in the channel scramjet was described in the plug flow approximation at the constant volume. Such an approximation gives similar results for the induction time in comparison with the solution of the full system of equations of the stationary one-dimensional gas dynamics [14]. Calculations were performed using various mechanisms of combustion.

Calculations were carried out for the expected conditions of scramjet combustion chamber: the initial temperature of 700 K and static pressure of 1 atm. The dependence of the induction time on the value of E/N in the discharge is shown at variable gas composition (ER) in Fig.5.2.2.2a. Optimum for E/N is due to the presence of a maximum in the part of the electron energy, which is used for the radicals production. The induction time dependencies on the mixture composition are compared in Fig.5.2.2.2b for discharge and thermal initiation (ER = 1 corresponds to the stoichiometric mixture). Note, that the thermal energy input is greater than the discharge energy about 2.5 times. Such a choice is made to ensure that the induction times were of the same order.

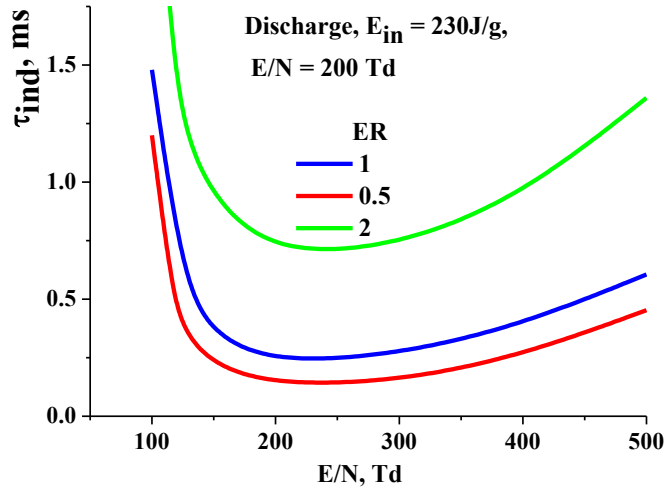

a.

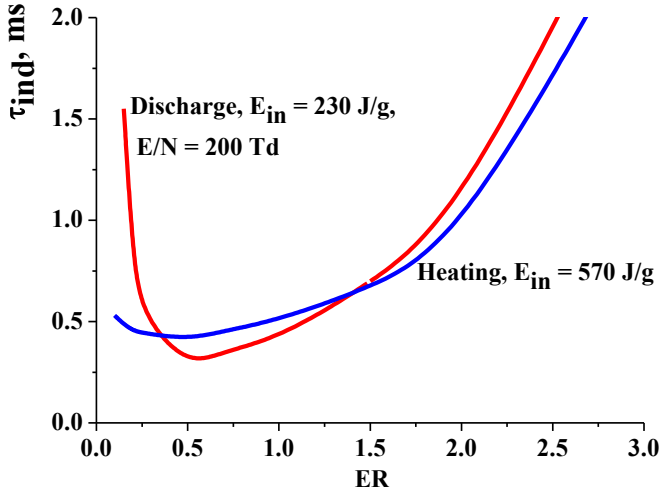

b.

Fig.5.2.2.2. Dependence of the induction time on the E/N for different mixtures C_2H_4 – air (a); for discharge and thermal initiation (b).

In addition, calculation with different mechanisms of combustion was found to results in a spread in several times of the intermediate products concentrations in the first stage. It is shown that the difference in the calculated values of the threshold energies for various

mechanisms of combustion significantly is greater in plasma initiation than in the heat initiation.

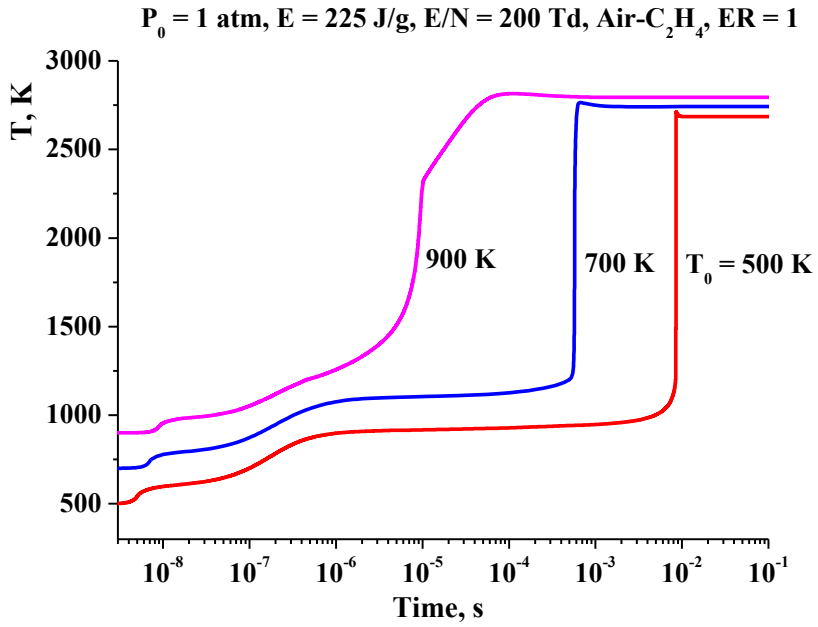

Fig.5.2.2.3. Dynamics of gas temperature. P_0 = 1 atm, E = 225 J/g, E/N = 200 Td, Air-C_2H_4, ER = 1.

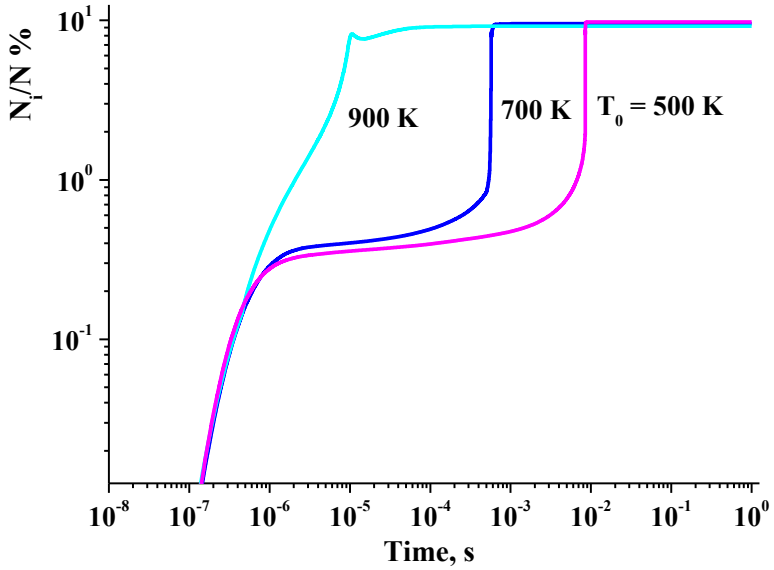

Fig.5.2.2.4. Dynamics of water vapors concentration. P_0 = 1 atm, E = 225 J/g, E/N = 200 Td, Air-C_2H_4, ER = 1.

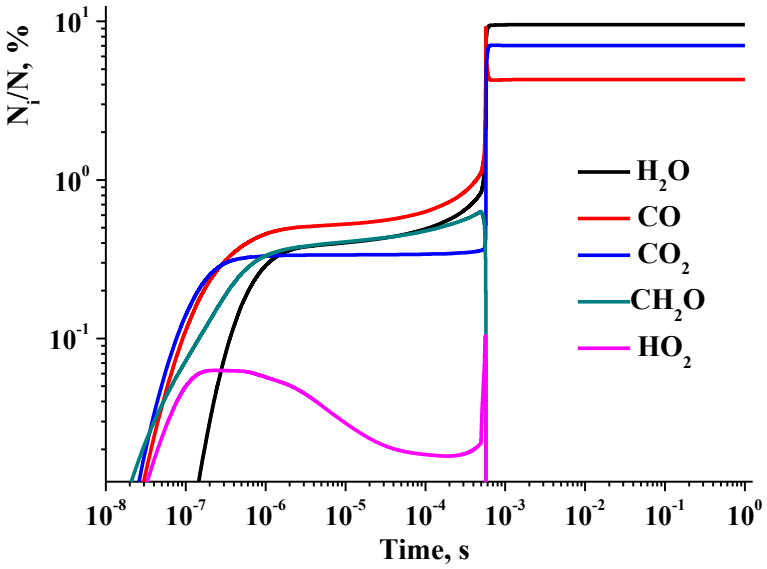

Fig.5.2.2.5. Species concentration at "cold" stage. P_0 = 1 atm, E = 225 J/g, E/N = 200 Td, Air-C_2H_4, ER = 1, T = 700 K.

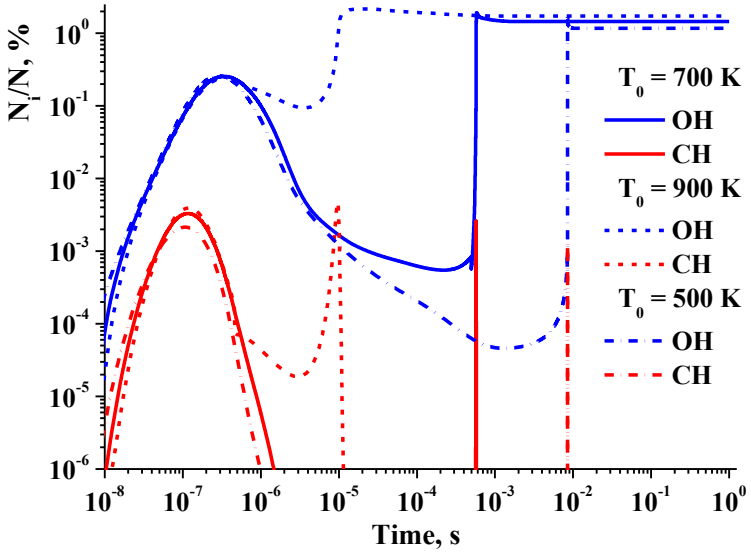

Fig.5.2.2.6. Concentration of main diagnostable species. P_0 = 1 atm, E = 225 J/g, E/N = 200 Td, Air-C_2H_4, ER = 1.

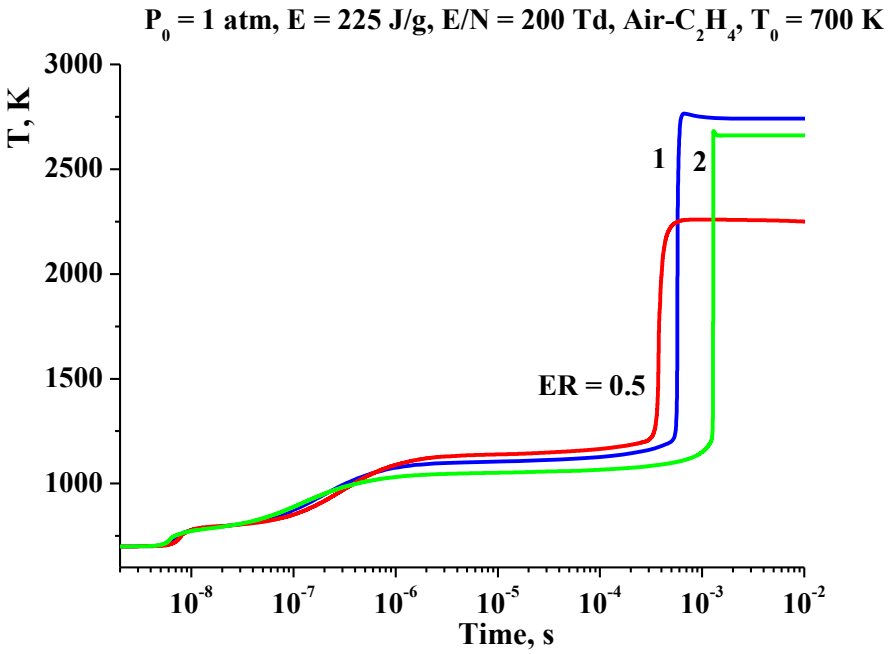

Fig.5.2.2.7. Gas temperature at ER variation. P_0 = 1 atm, E = 225 J/g, E/N = 200 Td, Air-C_2H_4, T_0 = 700K.

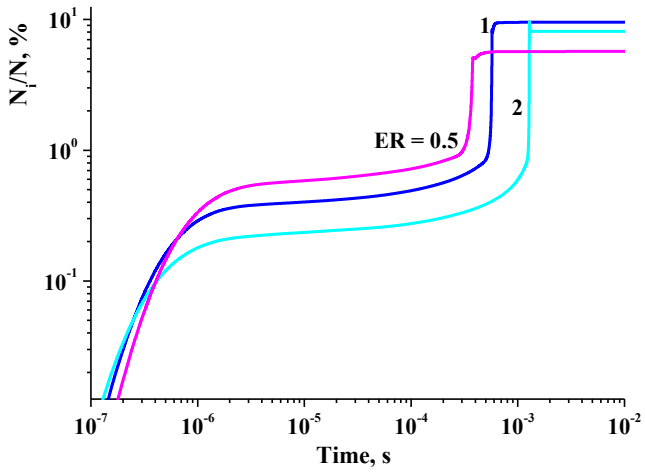

Fig.5.2.2.8. Dynamics of water vapors concentration. P_0 = 1 atm, E = 225 J/g, E/N = 200 Td, Air-C_2H_4, T_0 = 700 K.

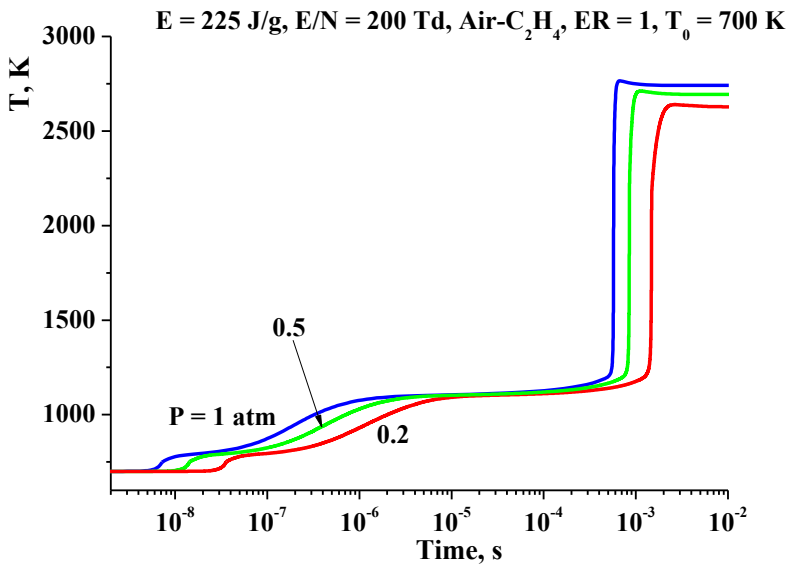

Fig.5.2.2.9. Gas temperature at pressure variation. T_0 = 700 K, E = 225 J/g, E/N = 200 Td, Air-C_2H_4, ER = 1.

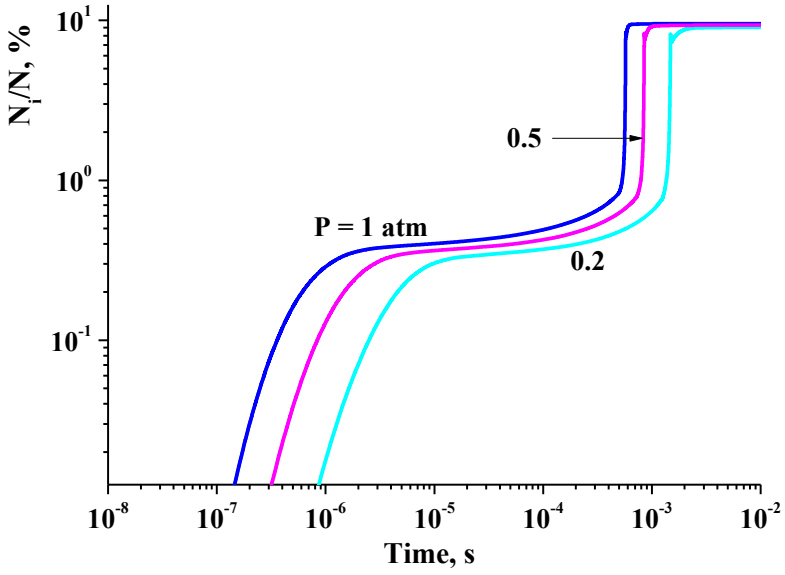

Fig.5.2.2.10. Dynamics of water vapors concentration, pressure effect. ER = 1, E = 225 J/g, E/N = 200 Td, Air-C_2H_4, T_0 = 700 K.

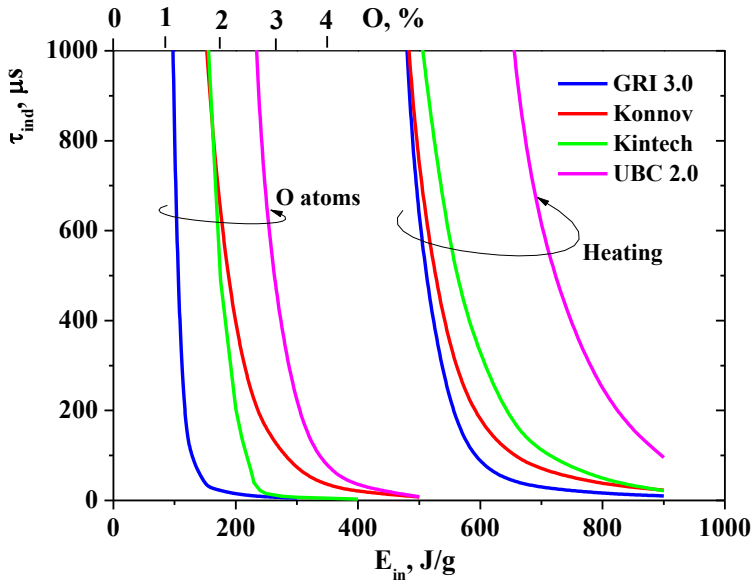

Fig.5.2.2.10. Comparison of heat-based ignition and ignition by O atoms due to different combustion models. P = 1 atm, Air-C_2H_4, ER = 1, T_0 = 700 K.

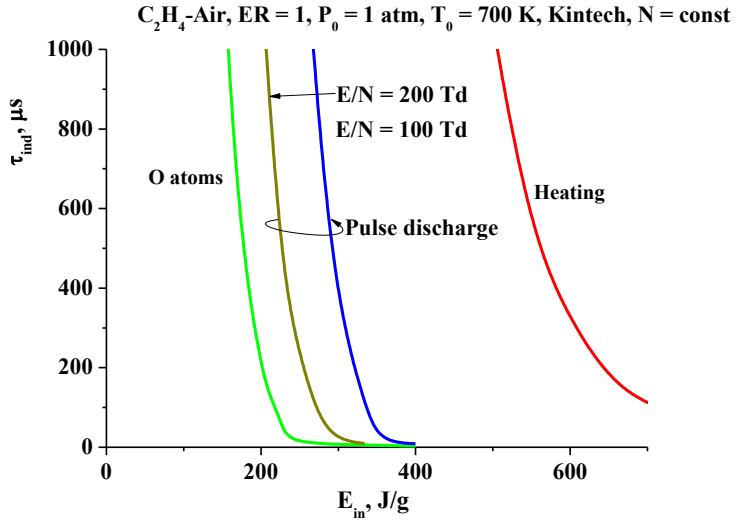

Fig.5.2.2.11. Comparison of heat-based ignition, glow discharge ignition, and ignition by O atoms. P = 1 atm, Air-C_2H_4, ER = 1, T_0 = 700 K.

Main idea pushed forward by the last efforts is that the plasma assistance for combustion enhancement occurs on sophisticated multistage manner. Under some conditions the multistage combustion is observed without plasma of electrical discharge; see [5-6] for example. But at the plasma assisted combustion the kinetic mechanism of ignition looks to be principally multistage (at least, two stages) process, as it is pointed in some last publications. To prove such a mechanism of combustion the diode laser absorption spectroscopy (DLAS) is applied

for the remote measurement of temperature, total pressure and concentration of water vapor (see section 5.1).

References to section 5.2.2.

1. Hyungrok Do, M. Godfrey Mungal, and Mark A. Cappelli "Jet Flame Ignition in a Supersonic Crossflow Using a Pulsed Nonequilibrium Plasma Discharge", *IEEE Transactions on Plasma Science*, Vol. 36, No 6, Dec 2008, pp. 2918-2923
2. Wookyung Kim, M. Godfrey Mungal, Mark A. Cappelli, "The role of in situ reforming in plasma enhanced ultra lean premixed methane/air flames", *Combustion and Flame*, 157 (2010), 374–383
3. Leonov S.B., Carter C., Yarantsev D.A. "Experiments on Electrically Controlled Flameholding on a Plane Wall in Supersonic Airflow", Journal of Propulsion and Power, 2009, vol.25, no.2, pp.289-298
4. Sergey Leonov, Dmitry Yarantsev, Vladimir Sabelnikov, Electrically Driven Combustion near Plane Wall in M>1 Duct, 3rd EUCASS Proceedings, July 2009, Versailles, France
5. Basevich, V. Ya. Chemical kinetics in the combustion processes. In: "Handbook of heat and mass transfer". V. 4 (Ed. N.Cheremisinoff), Houston: Gulf. 1990, p. 769
6. Sokolik A. S., "Self-ignition and combustion in gases", *UFN (rus)*, XXIII, issue 3, 1940, pp.209-250
7. Kim W., Mungal M. G., and Cappelli M. A., "Formation and Role of Cool Flames in Plasma-assisted Premixed Combustion," *Appl. Phys. Lett.*, vol. 92, 051503, Feb. 2008.
8. I. Kochetov, A. Napartovich, and S. Leonov, "Plasma ignition of combustion in a supersonic flow of fuel–air mixtures: Simulation problems," *J. High Energy Chem*., vol. 40, no. 2, pp. 98–104, 2006.
9. 1. Leonov S., Bityurin V., Bocharov A. et al. Hydrocarbon fuel ignition in separation zone of high speed duct by discharge plasma. *Proc. 4th Workshop "PA and MHD in Aerospace Applications"*. M: IVTAN. 2002.
10. Starikovskaia S. M., Plasma Assisted Ignition and Combustion, 2006, *J. Phys. D: Appl. Phys.*. V. 39. R 265.
11. Kochetov I. V., Leonov S. B., Napartovich A. P., 2006, Plasma ignition of combustion in a supersonic flow of fuel–air mixtures: Simulation problems, *J. High Energy Chem*., **40**, 98.,
12. Napartovich A. P., Kochetov I. V., Leonov S. B., 2010, Numerical modeling of ignition premixed ethylene-air mixture by system of micro-discharges, *Teplophizika Visokikh Temperatur,* **48**, 60.
13. KINTECH. *Kinetic technologies. Chemical Workbench* (http//www.kintech.ru).
14. Leonov S. B., Yarantsev D. A., Napartovich A. P., Kochetov I. V., 2006, Plasma-Assisted Combustion of Gaseous Fuel in Supersonic Duct, *IEEE Transactions on Plasma Science*, **34**, 2514.

5.2.3. Numerical analysis of fuel ignition by filamentary plasma. Mixing effect.

Such parameters of a discharge as E/N (E is the electric field strength, N is the gas number density) and electric current density or electron number density are strictly correlated by discharge nature. In order to find rates of processes involving electrons it is necessary to address the electron Boltzmann equation where from the electron energy distribution function (EEDF) could be calculated. To account properly excitation and dissociation of molecules in the discharge one has to guarantee acceptable accuracy of electron scattering cross sections used in the model. The key criterion for evaluation of their accuracy is a good agreement between calculated and available measured transport and kinetic coefficients for each component of the gas mixture. Traditionally, a set of cross sections for a given species, which satisfies this criterion, is called the ‗self-consistent' set.

Actually, development of a non-thermal discharge with required characteristics in high-speed, high-pressure supersonic gas flow is questionable. As was noted by authors [1-2], there are experimental data indicating that plasma chemical conversion of methane is more effective when discharges have filamentary form. We anticipate that usage of non-uniform (filamentary) plasma may accelerate essentially ignition of premixed fuel – air flows.

One of the most attractive schemes of the ignition of combustible mixture is figured as a system of filamentary discharge located periodically in front direction, as it is shown in Fig.5.2.3.1. Such type of discharge can be formed by special multi-electrodes system. In this section the result of numerical experiment in a model gasdynamic situation is presented.

Typical duration of the discharge's electrical pulse is much shorter than the characteristic gasdynamic time. That is why the power release can be described as in a fixed volume V_0. The excited gas zone is expanded and mixed with non-excited gas. Two physical processes are appeared at this moment: a cooling due to the mixing and the thermal power deposition as the result of combustion. A comprehensive model of mixing and combustion is rather complex, especially in a real kinetic approach.

To examine this approach the model was developed for burning initiation by a series of periodically positioned transverse filamentary-like discharges in approximation of distributed mixing of excited and non-excited gas streams. The model includes self-consistent simulations of the discharge of a small radius in supersonic flow of ethylene-dry air mixture [1] with followed gradual mixing of excited gas with main flow, see Fig.5.2.3.1. Mixing process was characterized by time interval between beginning of mixing and its termination by exhaust of main stream, Δt_{mix}, and the ratio of the final volume to the initial plasma volume, V/V_0. The

calculations were performed for the ethylene-air premixed composition at initial pressure 1Bar and initial temperature 700K.

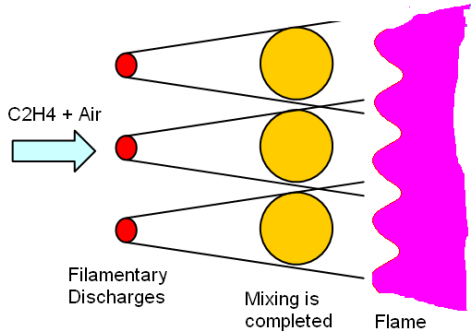

Fig.5.2.3.1. Scheme of analysis of ignition by filamentary discharge.

In the model the expansion from the volume V_0 to the volume V and mixing are supposed to be started right after the electrical pulse (1μs) and completed in predefined time t_{mix}. The temperature is being found based on energy balance equation. Components' concentration is reduced due to redistribution in a current volume as follows:

$$\frac{dN_i}{dt} = \left(\frac{dN_i}{dt}\right)_{UNIFORM} - \frac{N_i}{t_{mix}}\left(1 - \frac{V}{V_0}\right).$$

An initial diameter of the discharge's filament is small comparing with a location's space period. At the same time the mixed zone covers whole exposed area during a short time. Concentration of radicals and molecules formed by the discharge is reduced in accordance with the volumetric law (mixing + expansion). Extra molecules N_2, O_2, and C_2H_4 are come from the fresh mixture:

$$\frac{dN_i}{dt} = \left(\frac{dN_i}{dt}\right)_{UNIFORM} - \frac{N_i - N_i^0 \frac{T_0}{T}}{t_{mix}}\left(1 - \frac{V}{V_0}\right),$$

where N_i^0, T_0 – concentration and temperature of initial gases; T – current temperature in mixed volume. Under these conditions the most correct approach is the approximation of the constant gas pressure.

The physical-chemical model is a consistent combination of two approaches [2]: classical thermal combustion theory (close to GRI Mech3 combustion mechanism) and glow discharge plasma kinetics. The equations of thermal and plasma chemistry are solved in isochoric approximation in parallel with the Boltzmann equation for the electron energy distribution function. It was shown previously that isochoric model is in a satisfactory agreement with results computed in frame of a system of 1D gas-dynamic equations in a plug flow model. GRI Mech3 combustion mechanism is widely used, its applicability is proven at temperatures

higher than about 1100 K. Plasma kinetic model was validated for low temperature 300 K atmospheric pressure glow discharge in air. This model includes evolution equations for charged particles‘ densities, excited atom and molecules‘ densities, and electric circuit equation.

The discharge and external electrical circuit were modeled by a capacitance and the discharge channel resistivity (self-consistent model). The discharge filament radius was predefined as 0.5mm, energy deposition in this case was 480 J/g. Typical waveforms of the reduced electrical field and the current density are shown in Fig.5.2.3.2. The electrical field at the current maximum was E/N=150Td. A main mechanism of the plasma effect on chemical reactions rate is the atomic oxygen generation. The part of discharge energy, which is spent for the oxygen generation, is shown in Fig.5.2.3.3 depending on the electric field. The calculations are fulfilled for the initial gas parameters and composition. The direct molecular dissociation by electron impact takes about 14% at E/N = 160Td. A total effective dissociation includes collisions with electronically excited nitrogen. The maximal part of energy taken for the O2 dissociation is about 58% at E/N = 205Td, when the direct heating is taken into account as well.

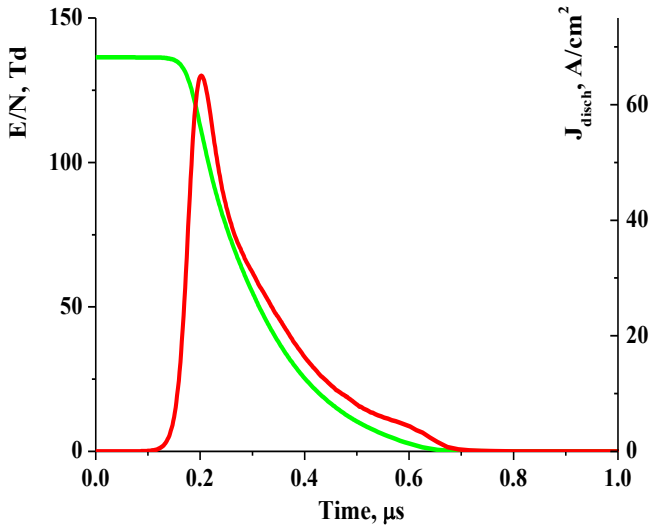

Fig.5.2.3.2. Dynamics of reduced electric field and current density. Specific power deposition 480 J/g. T=700K, P =1Bar, N_2:O_2:C_2H_4= 12:3:1, R = 0.5mm.

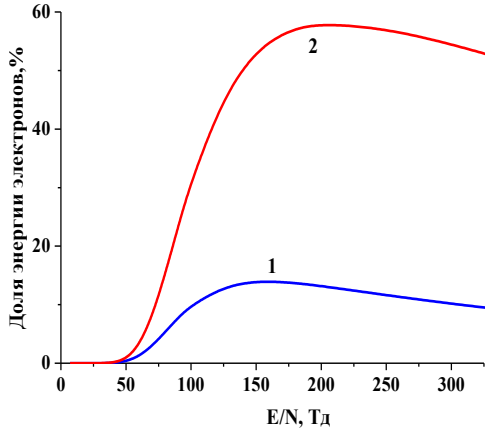

Fig.5.2.3.3. Part of discharge energy (%) spent for O2 dissociation in mixture N_2:O_2:C_2H_4= 12:3:1. 1 – direct dissociation by electron impact; 2 – total effect including electronically excited N2.

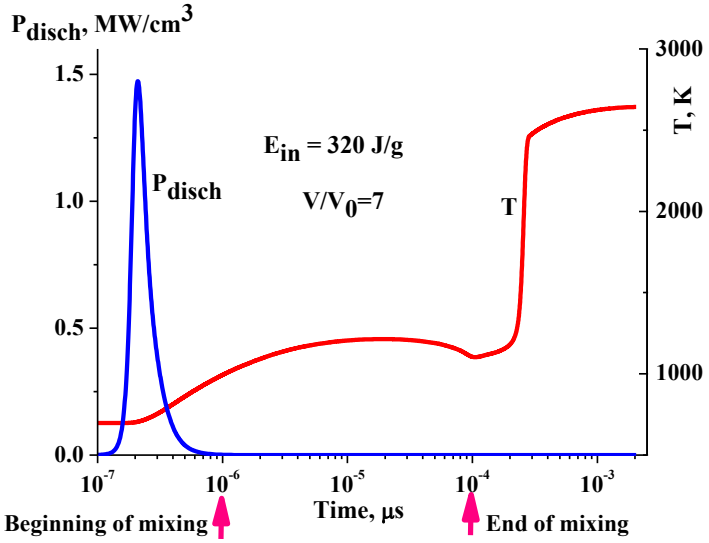

Fig.5.2.3.4. Dynamics of plasma power and the gas temperature at distributive mixing. V/V_0=7, t_{mix}=100μs.

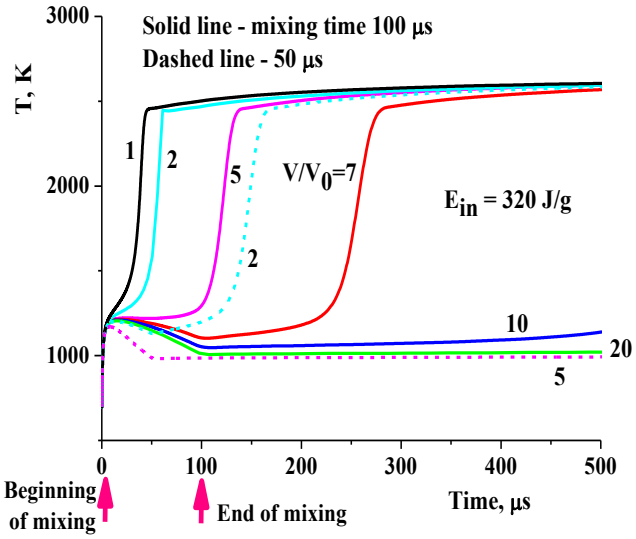

Fig.5.2.3.5. Dynamics of gas temperature depending on mixing degree V/V0 and the mixing duration t_{mix}. Solid lines are for t=100μs, dashed lines are for t=50μs.

Figure 5.2.4 presents dynamics of the discharge power and the gas temperature. One of important features is non-monotonous behavior of the gas temperature. One can see some temperature decrease at the end of the mixing. The effect may be explained by a competition of mixing with relatively cold gas and heating due to chemical reactions. At the parameters of interaction chosen in this particular case a local temperature maximum is observed at the beginning of the mixing. Figure 5 shows the temperature evolution at variation of V/V0. For the time scale t<500μs the mixing degree V/V0=10 is a critical value. At reduced time of mixing the time of ignition is increased dramatically. In this case the cooling is prevailed over heat release.

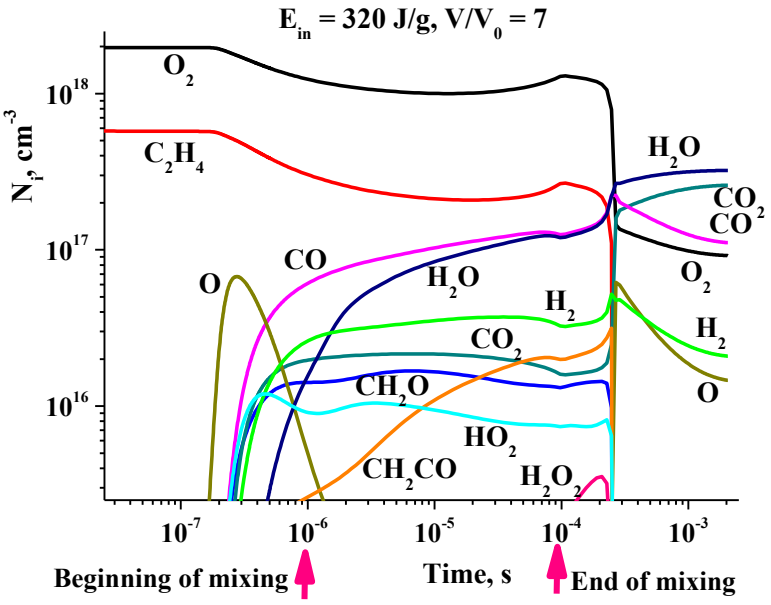

Fig.5.2.3.6. Dynamics of molecules and radicals concentration at discharge initiation and distributive mixing. The conditions are the same as in Fig.5.2.3.4.

The dynamics of molecules and radicals concentration is presented in Fig.5.2.3.6. At the beginning one can see a significant increase of the atomic oxygen concentration. Then so-called «cool flame» takes place, when the molecules CO, CH_2O, H_2, HO_2, CH_2CO, and others are generated. At t>10μs but before the end of mixing, some rise of the O_2 and C_2H_4 concentration is observed due to coming of fresh gas. Depending on conditions the full combustion may or may not follow these preliminary stages.

The ignition time is one of the most important characteristic of the combustion processes. At the analysis of results this time was defined as the point of maximal derivative of the temperature dynamics curve. Usually this time is equal to the maximal concentration of the CH radicals, and can be useful for optical diagnostics of the ignition process. Figure 5.2.7 illustrates the ignition time depending on mixing degree and the mixing time. At mixing time

100μs and mixing degree V/V0=12 the ignition time is more than 600μs. The faster mixing leads to faster cooling and bigger ignition time.

In practical problem of plasma-based ignition and flameholding in ducts there is more convenient to present data in terms of length of ignition than of ignition time. The curves in Fig.5.2.3.8 presents the results of simulation of the ignition length of ethylene-air mixture depending on mixing time at initial flow velocity M=2.0. Well seen that the ignition can be realized on the length X=0.6m at plasma energy release W/G=45J/g for mixing time t=100μs, and W/G=175J/g for mixing duration 50μs. Figure 5.2.8 also shows how the predicted induction time for combustion of ethylene-air mixture depends on the energy input per mass of gas flow in the case of filamentary discharge for two values of mixing time. At Δt_{mix} =100 and Δt_{ind} =50 μs the required reduced energy input is about 40 J/g, that is remarkably lower than for uniform discharge.

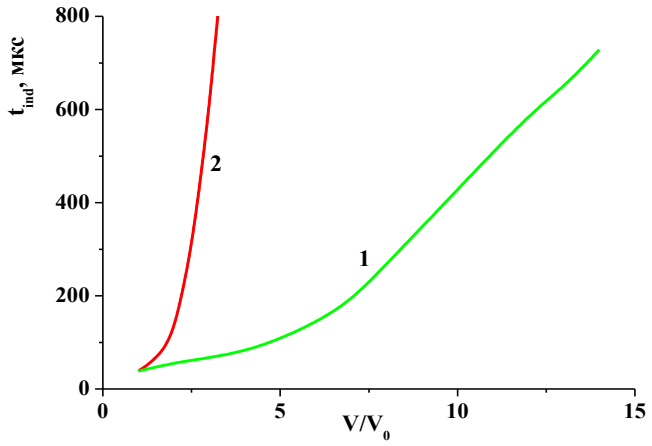

Fig.5.2.3.7. Ignition time vs mixing degree. 1 – mixing time t=100μs; 2 – t=50μs. The conditions are the same as for Fig.5.2.3.2.

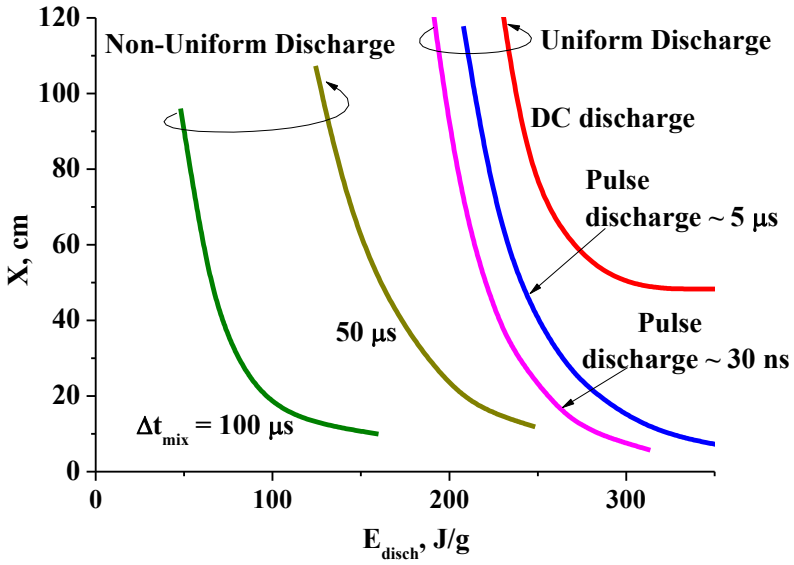

Fig.5.2.3.8. Length of ignition depending on energy release and the discharge mode. M = 2. Other conditions are the same as in Fig.5.2.3.2.

Herewith one can find the data for homogeneous DC discharge and pulse discharges of different pulse duration [3]. Non-homogeneous discharge possesses an obvious benefit in this regard. Comparison of the specific energies needed to ignite the mixture by non-homogeneous discharge, variety of homogeneous discharges, and by the heating is presented in Table.5.2.1. The use of non-homogeneous short-pulse discharge allows one to reduce the required power in 5times comparing with a homogeneous discharge, and in order of magnitude in comparison with the heating of the gas.

Table 5.2.1. Comparison of the energy levels required for the ethylene-air mixture ignition in M=2 flow. Combustor length 0.6m.

	Non-homogeneous	Homogeneous discharge			Heat
Mode	Pulse, mixing 100μs	Pulse ns discharge	Pulse μs discharge	DC discharge	
W/G, J/g	45	210	230	265	520

Figure 5.2.9 shows the ignition time vs specific energy deposition at different initial fuel concentrations: lean mixture, stoichiometric mixture, and rich mixture. It should be considered the less benefit of this method for a lean mixture due to less temperature elevation at the fuel oxidation.

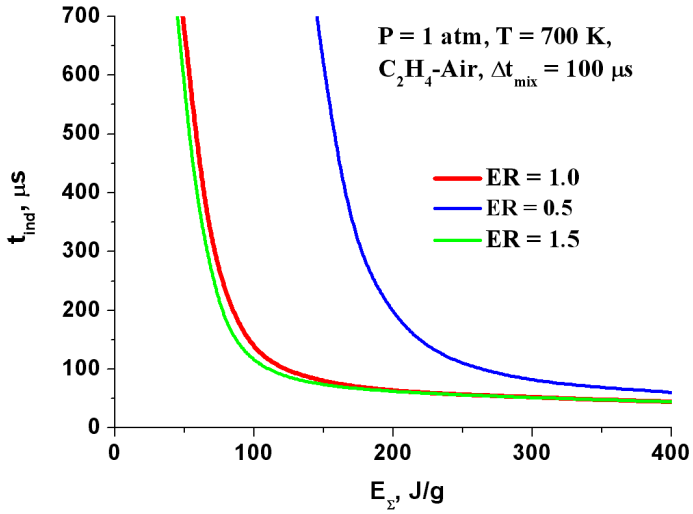

Fig.5.2.3.9. The ignition time vs specific energy deposition at different initial fuel concentrations. Mixing time t=100us, T=700K, P=1Bar.

Reference to section 5.2.3.

1. *I. Kochetov, A. Napartovich, and S. Leonov,* ―Plasma ignition of combustion in a supersonic flow of fuel–air mixtures: Simulation problems," *J. High Energy Chem*., vol. 40, no. 2, pp. 98–104, 2006.

2. *Pushkarev A., Zhu Ai-Min, Li Xio-Song, Sazonov R.,* V International Symposium on Theoretical and applied Plasma Chemistry, l.1, 23, 2008

3. *Sergey B. Leonov, Yury I. Isaenkov, Dmitry A. Yarantsev, Igor V. Kochetov, Anatoly P. Napartovich, Michail N. Shneider* ―Unstable Pulse Discharge in Mixing Layer of Gaseous Reactants", 47th AIAA Aerospace Sciences Meeting and Exhibit (Orlando, FL, USA, 5-8 January 2009), AIAA-2009-0820.

4. *Sergey B. Leonov, Yury I. Isaenkov, Alexander A. Firsov, Dmitry A. Yarantsev, Michail N. Shneider*, ―High-Power Filamentary Pulse Discharge in Supersonic Flow", 48th AIAA Aerospace Sciences Meeting and Exhibit (Orlando, FL, USA, 4-7 January 2010), AIAA-2010-0259.

5. *I. Kochetov, A. Napartovich, and S. Leonov,* ―Numerical simulation of plasma ignition in supersonic flow", 5-th International Symposium ―Thermochemical and Plasma Processes in Aerodynamics". St-Petersburg. ―Raduavionica". 2006. p.25.

5.2.4 How it might work in future?

The effective operation of scramjet in wide range of flow Mach numbers looks as one of the most technically difficult challenges in design of hypersonic vehicles powered by air-breathing engines. The most promising way is a scramjet possessed with a flexible gasdynamic configuration (including inlet, injection system, combustor, and nozzle) depending on Mach number and altitude of the flight. Unfortunately, this approach is not supported properly by technical issues: materials, gears, etc. Commonly discussed tradeoff assessment consists of a fixed geometrical configuration based on some "characteristic" Mach number of operation. It definitely demonstrates worse performance for lower and higher values of Mach numbers both.

To improve an overall capability of scramjet with fixed geometry of the duct some extra methods could be applied, for instance: (a) staged fuel injection; (b) additional flameholding at low temperature (plasma as well); and a few others. The penalty of such a philosophy is a rise of total pressure loses and, as a consequence, a decrease of specific impulse and thrust coefficient.

This work proposes an advanced approach how to expand an operational field of scramjet to off-design values of Mach number at fixed geometry of gasdynamic duct. It is based on experimental results in so-called "Plasma-Assisted Combustion" domain obtained during last years in JIHT RAS. Some results are presented in this Report. Particularly, there were found out the following:

- The result of the plasma generation in flow is not only in heating and active media production, but in modification of supersonic flow structure, including artificial separation, vorticity, etc. At proper modes the plasma localization and parameters in reacting flow are self-adjusted with zones of chemical reaction. These feedbacks are important feature of active flame control by electrical discharges.
- In case of hydrocarbon fuel and low temperature conditions flame stabilization by non-equilibrium plasma occurs by means of two-phase process. In the first phase the plasma induces the fuel reforming, which may be simplified by H2 and CO production. In spite of bright luminescence this zone doesn't concomitant with a significant temperature elevation and the pressure increase. This so-called "cold flame" appears as a source of active chemical species to initiate (under favorable conditions) the second phase of "normal" flame characterized by temperature and pressure rise.

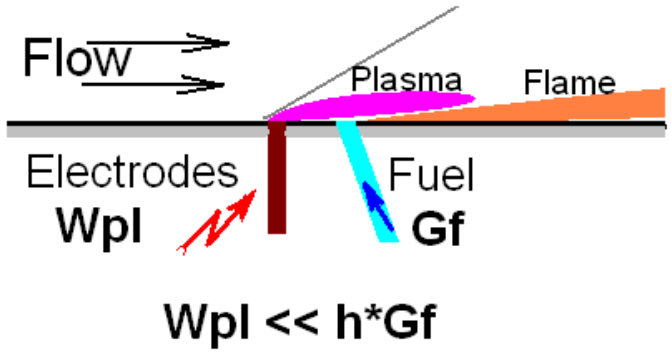

Fig.5.2.4.1. Plasma-based unit: injector + flameholder.

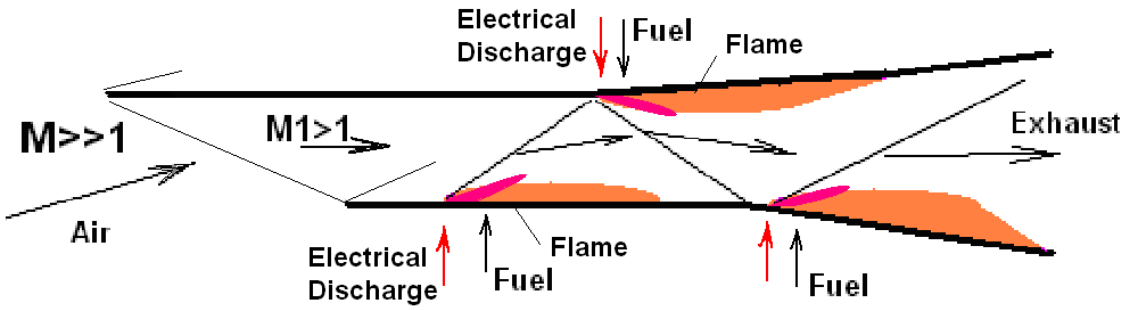

Fig.5.2.4.2. Staged-fuelled plasma-based high-speed combustor.

The idea of the method of supersonic flameholding and combustion control by plasma of electrical discharge is based on mentioned above and is composed with several issues, namely: (1) instead of fixed separation zones based on mechanical elements (wallstep, cavity, pylon, strut, etc.) the area of local separation is being created by near-surface electrical discharge plus jets of fuel based on flush-mounted electrodes and orifices (see Fig.5.2.4.1); (2) the plasma generator and fuel injector are composed together as an single unit utilized for fuel ignition, flameholding, and combustion control; (3) those units location along the duct, theirs activation and switching off, the magnitude of impact are chosen based on maximal efficiency of engine and steered by active feedbacks (see Fig.5.2.4.2).

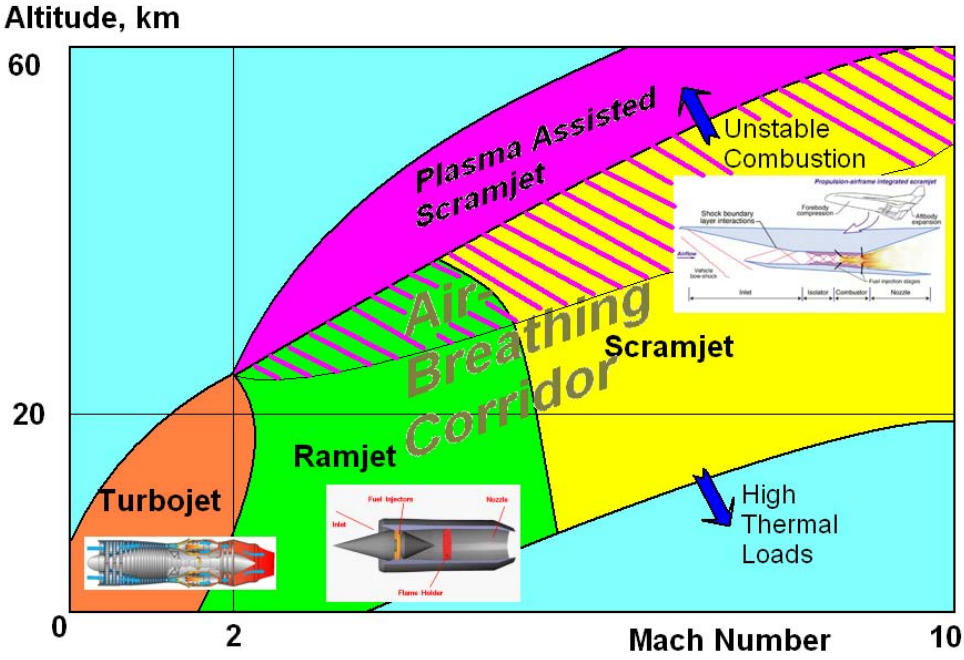

Fig.5.2.4.3. Expanding of air-breathing corridor due to plasma application. Qualitative scheme.

Prospectively the utilizing of this method might lead to reduce total pressure losses under non-optimal conditions, to enhance of operation stability, and, consequently, to spread of air-breathing corridor of scramjet operability as it shown schematically in Fig.5.2.4.3.

Reference to section 5.2.4.

Sergey Leonov, Vladimir Sabelnikov –ELECTRICALLY DRIVEN SUPERSONIC COMBUSTOR", Proceedings of 6th European Symposium on Aerothermodynamics for Space Vehicles, 2-7 November 2008, Versailles, France

6. Conclusions.

Some key problems related to supersonic combustion and flame stabilization are difficult to solve for the practical implementation of such a technology, especially in the case of non-optimal conditions and the use of hydrocarbon fuel. Among of them are global ignition at low temperature and flame stabilization in a predefined combustor location (which may not be the optimum location for combustion). Plasma-based methods of combustion management are now considered promising tools in this field.

Several reviews and important works have been published recently [see section 3.1]. Based in part on these publications, we believe the efforts, with few exceptions, can be divided into the following categories: 1) simulations of non-equilibrium kinetics of combustion; 2) basic experiments on plasma-chemical kinetics; 3) low-speed flame stabilization experiments employing a nonequilibrium discharge; 4) application of ~~"p~~lasma torches"; 5) high-speed ignition and flameholding experiments; and, 6) mixing experiments. Obviously the list of references does not cover the entire field. The approach of this work is to devise an experiment of practical interest for supersonic combustion. The main issues here are the use of supersonic flow, air mass flow-rate up to G_{air}=1 kg/s, a non-premixed fuel-air composition, and no physical flameholding devices within the flowpath.

Several mechanisms of the effect of plasma on flow structure, ignition, and combustion processes might be listed: 1) fast local ohmic heating of the medium; 2) nonequilibrium excitation and dissociation of air and fuel molecules due to electron collisions and UV radiation; 3) momentum transfer in electric and magnetic fields; and, 4) shock/instability generation. In different situations the significance of each of these topics can be varied. In some cases an amplification of the effect due to mutual impact and interference is critically important, as is observed in this work, where the flow-structure control by electrical discharge and gas excitation work together for ignition and stabilization of a high-speed flame.

Of course, heating of the medium by the discharge leads to an increase in the rate of the chemical reactions, not only in the vicinity of the discharge but also downstream. Furthermore, the discharge can induce a strong shock waves and flow separation areas at sufficiently high levels of power deposition. In this way one can create a zone with favorable conditions for combustion with increased residence time, improved rates of mixing, and increased temperature. Also, fuel-air reaction rates are increased due to the formation of radicals and atomic species through excitation by electrons in the electric field and by more complex processes. Deposition of active particles may also reduce the level of required external power.

Another benefit of this scheme is that local shock waves—generated by the obstruction imposed by the discharges—can improve the mixing process and can initiate chemical reactions due to gas heating at the shock front.

Based on both theoretical and experimental studies, it appears that nonequilibrium and nonuniform discharge's operation modes provide more flexibility in implementation and, very possibly, higher performance per unit power or energy. Nonequilibrium power deposition into the gas leads to the creation of species possessing higher reactivity in comparison with those found at equilibrium conditions. It is important also that the plasma is generated ~~"in~~-situ", just in the place of fuel-oxidizer interaction, to diminish the effect of fast relaxation and/or mixing with the surrounding air. A possible method to reduce the power consumption is to treat only a part of gas volume with nonuniform plasma. A preferable structure may look like a geometrically adjusted *grate*; here, a flamefront propagates the distance between separate plasma filaments faster than it can be blown out. An additional requirement is that a reasonable technical solution be a practical one. The experimental approach described herein is to design and configure nonequilibrium, spatially nonuniform discharge that can be practically implemented.

The plasma method to improve supersonic combustor performance has proposed and tested by authors, which is based on the generation of plasma-induced local unsteady separation. The artificial plasma-induced zones of the flow separation can be applied instead of mechanical devices such as a ramp or a cavity, especially under non-optimal or unsteady operational modes of the combustor. The flame stabilization regimes could occur at a relatively low level of extra energy deposition. The authors have studied the effects of a transversal discharge on flameholding in M=2 flow in cavity, behind backwise wallstep, and along a plane wall. The air temperature was varied in range 300-750K. The main physical effects observed of the plasma on the flowfield are that it heats the gas, generating high concentrations of radicals in the process, and that it modifies the flowfield, potentially inducing separation. The maximum effect at minimal power deposition can be realized with ~~"in~~-situ" plasma generation, nonequilibrium composition, and a nonuniform discharge structure.

Ignition and flameholding were realized for H_2 and C_2H_4 fueling on a plane wall by using a transversal electrical discharge at relatively low power deposition (2-3% of flow enthalpy). The power threshold for a hydrogen flameholding was measured to be W_{pl}<3 kW. The combustion completeness was estimated to be reasonably high, >90% in optimal experimental configurations, with both hydrogen and ethylene fuels. The thermal choking of the duct was observed at G_{H2}>1g/s, in spite of the fact that the duct design included an inclined wall for area

relief. The power threshold for flameholding with ethylene fueling was measured to be W_{pl}≥4 kW. In comparison with hydrogen fueling, a main difference with ethylene fueling was that thermal choking was not observed, even at the maximum discharge power of W_{pl}>10 kW. Furthermore, the completeness of the ethylene combustion decreased with increased fuel mass flow rate.

Energetic Threshold	H2 (T0=300K)	C2H4 (T0=300K)	C2H4 (T0=500K)	C2H4 (T0=650K)
Threshold of ignition in cavity and behind wallstep	1kW	2.5kW	4kW	≈5kW
Threshold of flameholding in shear layer over wallstep	<3kW	3.5kW	≈5kW	≈10kW
Threshold of flameholding over plane wall	<3kW	>4.5kW	>5kW	>8kW

The table presents statistically averaged data on power threshold. The energetic threshold measured for ignition and flameholding by the discharge in this case can be compared with that when employing a cavity and a backward-facing wallstep. In the latter cases, the discharge was configured such that the anode-cathode pairs are located with one electrode just upstream and the other just downstream of the step, and this configuration forces the discharge into the cavity (and otherwise it would remain in the shear layer). It can be seen that comparable power levels are required for flameholding with the wallstep or on the plane wall. We consider this as a positive result for a practical implementation. Note that the threshold for flameholding with this configuration does not decrease (improve) as the static temperature increases from 300 to 500-670K, contrary to expectation. A working hypothesis is that an increase of the temperature leads to intensification of the gas circulation in separation zone and gas exchange between separated zone and main flow.

The experiments were carried out on the plasma-assisted combustion of liquid hydrocarbon in cold air and under the heater operation. It was demonstrated a low intensity of the combustion under the experimental conditions. At the same time the possibility to promote the liquid hydrocarbon combustion by addition of hydrogen or ethylene was demonstrated as well.

The position of the flamefront was visualized by schlieren-streak technique. At constant fuel flow rate, the flamefront can be controlled by the discharge power in accordance with a qualitative law: higher power = shorter distance between the point of the fuel injection and the flamefront. Another important feature is that ~~"n~~o discharge = no combustion" at all

conditions/fuels tested. Moreover, switching off the discharge promptly leads to flame extinction.

Several diagnostic methods were significantly modified to be properly applied under conditions of high-speed flow, discharge, and combustion. At the first time for the facility PWT-50 the results were obtained based on laser-based absorption spectroscopy, namely: gas temperature distribution in zone located below the combustion area and H2O concentration in the same points. Those measurements were performed for the hydrogen and ethylene combustion both. The gas temperature occurs in a range T_{st}=*900-1100K* for hydrogen and T_{st}=*400-750K* for ethylene. The water vapors partial pressure was measured as high as P_{H2O}=*1-35Torr* depending on operation mode. These measurements prove of previously estimated level of combustion completeness and verify the two-stage model of PAC.

The effectiveness criterion of the plasma-based technique was proposed at the first time. This criterion compares the discharge power with calculated value of power required for selfignition of composition being mixture on air and gaseous fuel. The effectiveness of described technique faced a very high level, as it shown in the table for three geometrical configurations and two values of air temperature.

Table of effectiveness. Ethylene feeding: G_{air}=0.8 kg/s; G_{C2H4}=1÷2 g/s	T_0=293K	T_0=500K
Effectiveness for cavity	>100	
Effectiveness for wallstep	>270	>130
Effectiveness over plane wall	>75	>50

The air heater was adjusted and tested in typical operation modes. The method of heating consists of electrical and chemical power release both. The kinetic analysis of pollutions impact due to the heater operation was performed. As it was noted, the H2O and CO2 effects are small. At the same time the effect of NO addition by the air heater can be substantial. The experiments were carried out on the plasma-assisted combustion of ethylene in cold air and under the heater operation at temperatures T0=300-750K and in pulse mode at T0<1100K. It was demonstrated the reducing of intensity of the fuel combustion at increase of the gas temperature under the experimental conditions.

Usually it is mentioned that non-equilibrium plasma (characterized by higher level of E/N) occurs more effective in terms of fast fuel ignition. In our particular case it should be considered two main factors of successful fuel ignition and flameholding: (1) the discharge

power; and (2) length of the discharge filaments (reflects a time of interaction). All other factors appeared as much less important. Special experimental series shown a generation of sequence of active zones of reacting gas moved downstream from the place of immediate plasma-fuel interaction. These zones appear as hotbeds of consequent flamefront.

Based on experimental observations and data of numerical simulations authors have formulated two-stage model of plasma-assisted combustion. Main idea pushed forward is that the plasma assistance for combustion enhancement occurs on sophisticated multistage (two-stage, at least) manner. During the first step the plasma induces fuel reforming, which may be simplified as production of H_2, CH_2O, and CO. In spite of bright luminescence, this zone does not experience significant temperature and pressure increase. This so-called –cold flame" appears as a source of active chemical species that initiates (under favorable conditions) the second step of normal –hot" combustion, characterized by high temperature and pressure rise. Under some conditions the multistage combustion is observed without plasma of electrical discharge. But at the plasma assisted combustion the kinetic mechanism of ignition looks to be principally multistage process, as it is pointed in some last publications, see Attachment 1.

2D and 3D Navier-Stokes CFD simulation was performed to provide both a greater physical insight and a prediction of the critical parameters for the corresponding plasma-ignition experiment. The model includes the supersonic duct, the discharge (contoured heat source), fuel injection, and chemical kinetics. The results show a good agreement with the experimental data for cavity and wallstep configurations. The simulations were a very helpful at establishment of optimal fuel injectors‘ location and number of fuel orifices. The next important result was in verifying of the idea, why the discharge effect on flameholding weakens at the gas temperature increase. At the same time the model has demonstrated a strict deficiency in geometrical configuration close to the plane wall.

It might be concluded that the formal objectives of the project were reached; expected results were obtained and considered in this Technical Report and Final Technical Report as of March 2009. Several scientifically new results were obtained, reported, and published due to the project‘s efforts and being, initially, outside of the project‘s tasks. Among of those we may highlight the following:

- Plasma-based supersonic flameholding on the plane wall at inflow generated electrical discharge was demonstrated at the first time;
- Two-stage mechanism of plasma-assisted combustion was formulated, at the first time for M>1 flow;

- The DLAS method was successfully applied for detail measurements of the gas temperature and the combustion efficiency;
- New scheme of plasma-improved combustor is proposed for further consideration.

At the same time this work opens some new questions and problems...

Authors express their deep acknowledgements to the funding Party and ISTC

Attachment 1: List of published papers with abstracts

1. S. Leonov, V. Gromov, A. Kuriachy, D. Yarantsev –Mechanisms of Flow Control by Near-Surface Electrical Discharge Generation", 43th AIAA Aerospace Sciences Meeting and Exhibit, Reno, NV, 10-13 January 2005, AIAA-05-0780.

The paper is devoted mainly to problem of flow management by the discharge plasma excited inflow. It could be related to the newly-developed field of Magneto Plasma Aerodynamics. Discharge plasma technology promises the advantages in a field of the boundary layer control, including stabilization of line of laminar-turbulent transition, guiding of separation processes, and control of the local shocks position. The paper presents and discusses results of recent experimental and analytic study of the problem in this field of interest. Specific prospective for plasma applications in the area of effective control of the duct-driven flows are discussed.

2. A. Napartovich, I. Kochetov, S. Leonov, –Study of dynamics of air-hydrogen mixture ignition by non-equilibrium discharge in high-speed flow", J. of High Temperature (rus), No. 5, 2005, p.667.

For the first time, a numerical model was developed combining traditional approach of thermal combustion chemistry with advanced description of the plasma kinetics based on solution of electron Boltzmann equation. This approach allows us to describe self-consistently strongly non-equilibrium electric discharge in chemically unstable (ignited) gas. Our model includes an electron Boltzmann equation solver calculated in parallel with kinetic equations for charged particles, excited molecular states, ion-molecule reactions and chemical reactions. Calculations were performed for the initial gas temperature 700 K and static gas pressure 1 bar for the hydrogen and ethylene mixed with air at varied energy input into the gas flow for stoichiometric compositions. Effect of chemically active species produced in the discharge on ignition delay time was studied for conditions of steady state glow discharge for both mixtures, while effectiveness of pulse-periodic discharge in shortening ignition time was explored for hydrogen-air stoichiometric mixture only. A remarkable reduction of ignition delay time relative to thermal initiation was predicted for both fuels at a modest energy cost. Energy efficiency turned out to be comparable for continuous and pulsed modes of the discharge operation.

3. Yarantsev D.A., Leonov S.B., Biturin V.A., Savelkin K.V. –Spectroscopic Diagnostics of Plasma-Assisted Combustion in High-Speed Flow", AIAA/CIRA 13th International Space Planes and Hypersonic Systems and Technologies Conference, 16-20 May 2005, Capua, Italy, AIAA-2005-3396.

Spectroscopic investigation of hydrocarbons (ethylene) combustion in airflow at the presence of filamentary surface discharge is presented in this paper. Survey spectrum under the discharge-assisted combustion in the wavelength range 200-800nm have been measured. Molecular bands that are typical both for the combustion – OH, CH, CN, C2 and for the discharge – N2, H2 are typically observed in the spectrum. It has to be noted here, that presence of OH, CH, CN and C2 radicals doesn't indicate the combustion reactions themselves. These molecules can be generated and exited by the electrical discharge. Rotational and vibrational temperatures for different molecules have been measured by fitting calculating spectra and experimental ones. A simulation of spectrums were performed by original software. Examples of the measurement are presented.

4. S.B. Leonov, K.V. Savelkin, D.A. Yarantsev, V.G. Gromov –Aerodynamic Effects due to Electrical Discharges Generated Inflow" Proceedings of –European Conference for Aerospace Sciences" (EUCASS), Moscow, July, 2005

The plasma of electrical discharges in airflow is considered as the quite promising method for flow/flight control and combustion enhancement. The plasma application in field on aerospace science defined the conditions of discharges generation: pressure P=0.1-1Bar, velocity of the flow V=100-1000m/s. Characteristic temperature of gas can be from T=200K (ambient conditions) to T≤2kK for combustion chamber. Under such a condition the plasma of electrical discharges appears in filamentary form due to specific instability, like a superheating one. This

plasma can effect on flow structure and parameters not locally only. From the other side the properties of the filamentary plasma under so specific conditions are known not perfectly. This experimental work was aimed in study of pulse filamentary plasma behavior at high-speed flow, in magnetic field and at expanded range of gas temperature.

5. S. B. Leonov, V. A. Bityurin, D. A. Yarantsev , A. P. Napartovich, I. V. Kochetov, –Plasma-Assisted Ignition and Mixing in High-Speed Flow", Proceedings of the 8th International Symposium on Fluid Control, Measurement and Visualization, Chengdu, China, 19-23 August 2005.

The model experiments on duct-driven supersonic flow control have been executed last time on the base of short-time wind tunnel. Plasma deposition has been provided by surface plasma generator with specific power input W=100-500W/cm^2. Plasma parameters have been measured by optic spectroscopy. Flow structure was observed by fast Schlieren system. Pressure distribution was measured by multi-channel fast-response transducer. The strong effect of electric discharge on the flow-field structure and shocks position was detected, as well as the effects of local and global separation. An appropriate physical model of the phenomena is described here. The energetic threshold of the ignition has been measured. The ignition effect was compared for different level of E/N parameter. The inflow mixing intensification is one of the key problems of high-speed combustion. Possible mechanisms of plasma/MHD-induced mixing are discussed. The experimental results on filamentary pulse discharge effect on flow in magnetic field and without it are demonstrated in different aerodynamic situations. The test on pulse discharge influence on flow structure and parameters under supersonic condition has been carried out in special dielectric test section of PWT-10 facility. The discharge can be characterized by the following parameters: pulse duration more than 50us (actually it has been limited by discharge channel breakage due to blowout of plasma filament by flow), maximal discharge current 100-150A, steady-stage gap voltage U=500-800V, inter-gap distance 50mm, mean E/n parameter value 30Td, averaged input power up to W=50kW, spectroscopically defined rotational temperature Tg≈3kK. Structure of the discharge was registered by the high-speed line-scan camera AVIVA (line-rate of 50kHz; exposure time of 6mcs). We have obtained temporal behavior of the thin crossing slice of the discharge.

6. Sergey B. Leonov, Dmitry A. Yarantsev, Valery G. Gromov, Yuri I. Isaenkov, Victor R. Soloviev, –The Gas-Dynamic Phenomena Associated with Surface Discharge in High-Speed Flow", Proceedings of 15th International Conference on MHD and MPA, 24-27 May 2005, Moscow, IVTAN.

The results of experimental, computational, and analytical study for a problem of flow control by electrical discharge application are presented in the paper**.** Two main topics are considered: the characteristics of different types of discharge in the flow and the discharge plasma effects on high-speed flow structure and properties. Three discharge types were explored: quasi-DC surface discharge, transversal pulse discharge, and dielectric barrier discharge (DBD). The mechanisms of flow modification are revealed to be quite different for these discharge types. There was shown that the surface plasma generation near an inlet rupture shifts the appropriate SW upstream. The angle of a new SW depends on power release and sort of gas applied. In a case of air a huge post-plasma extrusive layer is observed that is in accordance with an idea of the mechanism of slowed V-T relaxation. The thickness and the length of this layer depend on static pressure in test section (higher pressure – shorter extrusive layer). In a case of argon and CO2 such a layer was much weaker. The attendant oblique SW has the angle close to Mach characteristic and is conjugated with the "old" shock. The stagnation pressure in the test section downstream plasma accompanied SW is changed negligibly in the last case. A preliminary conclusion is that the mechanism of V-T relaxation can play important role in airflow with non-equilibrium plasma generation. It allows significant elongation of surface discharge effect on flow structure in inlet's configuration.

7. Leonov S.B., Biturin V.A., Yarantsev D.A. –Plasma-Induced Ignition and Plasma-Assisted Combustion in High Speed Flow." In –Non-Equilibrium Processes", v.2, pp.104-115: –Plasma, Aerosols, and Atmospheric Phenomena", TORUS-PRESS, 2005, 392p.

Two main domains were considered in this experimental work: an enhancement of the ignition of non-premixed air-fuel composition by plasma, and the mixing intensification by the discharge generation inflow. The effects of gas movement; external magnetic field and high temperature were explored. It was done separately and under combined influence. The filamentary plasma behavior inflow and in magnetic field is described. The results are useful at design of practical devices for ignition, mixing and flow structure modification.

8. S. Leonov, I. Kochetov, A. Napartovich, D. Yarantsev. Plasma-Assisted Ignition and Flameholding in High-Speed Flow // Paper AIAA-2006-0563, 44th AIAA Aerospace Sciences Meeting & Exhibit, 9-12 January 2006, Reno, NV.

   Properties of different electrical discharges are reviewed for applications in the Plasma-Induced Ignition and Plasma-Assisted Combustion in high-speed flow. Nonequilibrium, unsteady, and nonuniform modes are under analyses. Numerical simulations of uniform non-equilibrium discharge effect on the premixed hydrogen and ethylene-air mixture in supersonic flow demonstrate an advantage of such a technique over a heating. At the same time, the energetic price occurs rather large to be the scheme practical. A reduction of required power deposition and mixing intensification in non-premixed flow could be achieved by nonuniform electrical discharges. Experimental results on multi-electrode discharge maintenance behind wallstep and in cavity of supersonic flow are presented. The model test on hydrogen and ethylene ignition is demonstrated at direct fuel injection.

9. I. Kochetov, A. Napartovich, S. Leonov –Plasma ignition of combustion in a supersonic flow of fuel-air mixtures: Simulation problems", J. High Energy Chemistry, **40**, 98–104, 2006.

   Numerical simulations of ignition of H_2 and C_2H_4 mixtures with dry air by continuous glow discharge in a supersonic flow demonstrated a remarkable shortening of ignition times at reasonably low energy input. Ignition of H_2 fuel is much easier (faster and at lower energy inputs) than of C_2H_4. Numerical simulations of H_2 ignition by continuous glow discharge predict low sensitivity of burning acceleration effect to the ratio fuel/oxidizer while gradually diminishing with fuel dilution. A remarkable reduction of ignition delay time relative to thermal initiation was predicted for both fuels at a modest energy cost. Energy efficiency turned out to be comparable for continuous and pulsed modes of the discharge operation. Initiation of H_2/air mixture combustion by pulse discharges of a few microsecond duration is about 20% more energetically economical than the continuous discharge.S. B. Leonov, D. A. Yarantsev , A. P. Napartovich, I. V. Kochetov –Plasma-Assisted Chemistry in High-Speed Flow", Proceedings of the International Conference on Gas Discharges and their Applications, Xi'an, China, 11-14 September 2006, paper L18.

   Fundamental problems related to the high-speed combustion are analyzed. The result of plasma-chemical modeling is presented as a motivation of experimental activity. Numerical simulations of uniform non-equilibrium discharge effect on the premixed hydrogen and ethylene-air mixture in supersonic flow demonstrate an advantage of such a technique over a heating. Experimental results on multi-electrode discharge maintenance behind wallstep and in cavity of supersonic flow are presented. The model test on hydrogen and ethylene ignition is demonstrated at direct fuel injection.

11. S. Leonov, C. Carter, M. Starodubtsev, D. Yarantsev Mechanisms of Fuel Ignition by Electrical Discharge in High-Speed Flow // Paper AIAA-2006-7908, 14th AIAA/AHI Space Planes and Hypersonic Systems and Technologies Conference, Canberra, Australia, Nov. 6-9, 2006

    The field of Plasma-Induced Ignition and Plasma-Assisted Combustion in high-speed flow is under consideration. A short review of efforts in this field is presented. The main mechanisms of electrical discharges effect on high-speed combustion are analyzed. The result of plasma-chemical modeling is shown as a motivation of experimental activity. A reduction of required power deposition and mixing intensification in non-premixed flow could be achieved by nonuniform and nonequilibrium modes of electrical discharge. Experimental results on multi-electrode discharge maintenance behind a wallstep and in a cavity of supersonic flow are presented. 3D Navier-Stokes (NS) simulations of the discharge effect on flow structure were

made to define the optimal experimental configurations. They were a basis for a model test of hydrogen ignition in supersonic flow with direct fuel injection. 2D NS simulations of hydrogen combustion with a nonequilibrium chemical model were performed and compared with experimental data. For the first time the results is published on plasma-assisted combustion of non-premixed composition near the plane wall in M=2, T=300K flow.

12. Sergey B. Leonov, and Dmitry A. Yarantsev –Plasma-induced ignition and plasma-assisted combustion in high-speed flow" // **IOP**, Plasma Sources Science and Technology, **16** (2007), p.132-138, stacks.iop.org/PSST/16/132

    The paper presents the results of lab-scale experiment on ignition of non-premixed fuel-air composition in high-speed flow by electrical discharge. The concept of Plasma-Induced Ignition and Plasma-Assisted Combustion is considered on the basis of three main ideas: the medium heating/excitation by discharge, fuel-air mixing intensification, and flow structure control in the vicinity of reaction zone. The experiments were fulfilled under conditions of model supersonic combustor in standard aerodynamic configurations with backwise wallstep and cavity on the wall. The electrical discharge was organized in specific electrodes arrangement where the plasma filaments crossed an area of gas circulation. The ignition of hydrogen and intensification of ethylene-air chemical reactions were demonstrated for direct fuel injection into the fixed separation zone at low gas mean temperature. The experiments were supported by 3-D Navier-Stokes numerical simulations. An energetic threshold of fuel ignition under separation and in a shear layer of supersonic flow has been measured.

13. Leonov, S. B., Yarantsev, D. A., Napartovich, A. P., Kochetov, I. V. –Plasma-Assisted Combustion of Gaseous Fuel in Supersonic Duct", **Plasma Science, IEEE Transactions on**, Dec. 2006, Volume: 34, Issue: 6, pp.2514-2525

    The field of Plasma-Induced Ignition and Plasma-Assisted Combustion in high-speed flow is under consideration. Nonequilibrium, unsteady, and nonuniform modes are analyzed as the most promising to reduce a required extra power. Numerical simulations of uniform non-equilibrium continuous and pulse discharge effect on the premixed hydrogen and ethylene-air mixtures in supersonic flow demonstrate an advantage of such a technique over a heating. At the same time, the energetic price occurs rather large to be the scheme practical. A reduction of required power deposition and mixing intensification in non-premixed flow could be achieved by nonuniform electrical discharges. Experimental results on multi-electrode discharge maintenance behind wallstep and in cavity of supersonic flow are presented. The model test on hydrogen and ethylene ignition is demonstrated at direct fuel injection.

14. S. Leonov, –Gasdynamic Phenomena Concomitant with Plasma-Assisted Combustion Experiments", Proceedings of the 7th International Workshop on Magneto-Plasma Aerodynamics, 17 - 19 April 2007, JIHT RAS, Moscow, Russia

    The paper presents a short review of world-wide efforts in a field of plasma-assisted combustion and flameholding, as well as the results of experimental work on plasma assisted combustion in supersonic airflow obtained in JIHT RAS during the last 3 years. Experimental results on multi-electrode nonuniform discharge maintenance behind wallstep and in cavity of supersonic flow are presented. The model test on hydrogen and ethylene ignition is demonstrated at direct fuel injection to low-temperature high-speed airflow.

15. Sergey B. Leonov and Dmitry A. Yarantsev. –Hydrogen and Ethylene Combustion Assisted with Filamentary Discharge in Supersonic Flow", NEPCAP Proceedings, Dagomis, June 2007.

    Experimental results on the multi-electrode DC discharge maintenance near the plane wall and its impact on the model high-speed combustor performance are presented. Distinctive peculiarities of the spectroscopic diagnostics at such conditions are discussed. For the first time the results are presented on plasma-assisted combustion of non-premixed composition near the plane wall in M=2, T=300K flow. This scheme demonstrates an effective flameholding in supersonic flow under non-optimal conditions.

16. Sergey B. Leonov, Campbell Carter –Plasma-Assisted Combustion and Flameholding in High-Speed Flow", Invited Lecture, Proceedings of IWEPAC-3, September 17-20, 2007, Falls Church, VA, U.S.A

Several fundamental problems related to high-speed combustion are under consideration, including fuel ignition under low temperature, induction time reduction, air-fuel mixing intensification, flame-front stabilization, completeness of combustion enhancement, etc. At least four mechanisms of the effect of plasma on ignition and combustion processes might be listed: ohmic heating (1), active radicals and particles deposition (2), plasma/MHD mixing (3), and plasma-induced flow structure steering (4). In some important situations, the active radicals‘ generation by plasma has a synergetic effect on the ignition, i.e. the required power occurs much less than for a thermal initiation of the reactions. The result of plasma-chemical modeling is presented as a motivation of experimental activity.

17. S. B. Leonov, V. N. Sermanov, V. R. Soloviev, D. A. Yarantsev –Supersonic Rupture‘s Shock Control by Electrical Discharge” Proceeding of the Fifth International Conference on Fluid Mechanics, Aug.15-19, 2007, PaperF27; Shanghai, China; Tsinghua University Press & Springer

    The objective of this work is to study the phenomena associated with interaction of near-surface electrical discharge and high-speed flow; specifically, to demonstrate a steering effect of plasma in model supersonic inlet. It is clear that the power release to the flow is able to modify some part of the flowfield. But in the most cases the magnitude of influence is not high enough, the impact is quite local, and its efficiency is rather low. The idea of this work is to analyze the conditions when the local plasma generation leads to notable modification of flow structure in relatively distant zone downstream of the discharge location. The experimental data presented show significant and effective impact of electrical discharge on shocks‘ configuration in supersonic flow.

18. Yu. I. Isaenkov, S. B. Leonov, M. N. Shneider –Mixing Intensification by Electrical Discharge in High-Speed Flow” Proceeding of the Fifth International Conference on Fluid Mechanics, Aug.15-19, 2007, PaperF28; Shanghai, China; Tsinghua University Press & Springer

    The paper considers the results of experimental and analytic efforts on the filamentary transversal pulse discharge application for mixing intensification in high-speed gas flow. Two methods are demonstrated experimentally: active mixing by filamentary discharge in transversal magnetic field, and mixing due to development of huge instability with consequent fast turbulent expansion in after-discharge channel. The mechanism of the phenomena was described theoretically for quiescent ambient conditions. It is supposed that effect of fast turbulent expansion is effective for an acceleration of mixing in the non-premixed reactant multi-component flow.

19. Sergey B. Leonov –Plasma-Assisted Aerodynamics: Approach and Problem of Measurements”, Keynote Lecture, Proceedings of FLUCOME2007, September 17-19,2007, Tallahassee, FL, USA

    The paper considers several distinctive ideas of the —Plasma Aerodynamics”. A general approach is based on the reveal of main physical mechanisms of electrical discharges interaction with a gas flow: heating, electro-dynamic, magneto-dynamic, and chemical activation. The results of model experiments are discussed: drag reduction by in-front-of-body plasma generation; supersonic flow structure control by near-surface discharge; boundary layer actuation by dielectric barrier discharge (DBD); high-speed combustion intensification. In each specific case the problem is arisen of suitable diagnostics application.

20. S. B. Leonov, C. Carter, K. V. Savelkin, V. N. Sermanov, and D. A. Yarantsev, “Experiments on Plasma-Assisted Combustion in M=2 Hot Test-Bed PWT-50H,” 46th AIAA Aerospace Sciences Meeting and Exhibit (Reno, Nevada, USA, 7-10 January 2008), AIAA-2008-1359.

    The paper considers the results of several years‘ efforts in field of Plasma-Assisted Combustion in high-speed airflow. Electrical discharge generated straight in M=2 flow is applied for different geometric configurations: cavity, backwise wallstep, and on a plane wall. Hydrogen and ethylene ignition and flameholding are demonstrated experimentally at air temperature T0=300-670K. Parametric dependences of the flameholding effect on fuel feeding, gas temperature, geometry, discharge power, etc. are described. The effect of —cold” combustion is

shown under lean and rich mixture. The physical mechanism of combustion breakdown is discussed. The experiments are supported by 3D Navier-Stokes simulations.

21. Sergey B. Leonov, "High-Speed Flow Control by Electro-Discharge Plasma Technique", Invited paper, Proceedings of 2nd International Conference "Recent Advances in Experimental Fluid Mechanics", 3-6 March 2008, K.L.College of Engineering, Vijayawada, India.

    The paper presents a short review of world-wide efforts in a field of plasma-assisted aerodynamics and plasma-induced combustion, as well as the results of experimental work in this field obtained in the Laboratory of Experimental Plasma Aerodynamics JIHT RAS last years. The inflow mixing intensification is one of the key problems of high-speed combustion. Possible mechanisms of plasma/MHD-induced mixing are discussed. The experimental results on filamentary pulse discharge effect on flow in magnetic field and without it are demonstrated in different aerodynamic situations. The peculiarities of the filamentary discharge appearance in high temperature and high-speed flow explored experimentally are discussed in details.

22. Sergey B. Leonov, Dmitry A. Yarantsev, Campbell Carter, Transversal Electrical Discharge as a New Type of Flameholder, 15th AIAA International Spaceplanes and Hypersonic Systems and Technology Conference, Dayton, OH, Apr-May 2008, AIAA-2008-2675.

    The paper describes experimental results on gaseous fuel ignition and flameholding controlled by an electrical discharge in high-speed airflow. The geometrical configuration does not include any mechanical or physical flameholder. The fuel is non-premixed and injected directly into the air crossflow from the combustor wall. A multi-electrode, nonuniform transversal electrical discharge is excited on the same wall, between flush-mounted electrodes, upward the fuel injector. Initial gas temperature is much lower than the value for autoignition of hydrogen and ethylene. Results are presented for wide range of fuel mass flow-rate and discharge power deposited into the flow. This coupling between the discharge and the flow presents a new type of flameholder over a plane wall for high-speed combustor.

23. Sergey Leonov, Vladimir Sabelnikov "ELECTRICALLY DRIVEN SUPERSONIC COMBUSTOR", Proceedings of 6th European Symposium on Aerothermodynamics for Space Vehicles, 2-7 November 2008, Versailles, France

    The paper considers a new method of supersonic combustor steering under non-optimal conditions, specifically, at low gas temperature. The method is based on near-surface electrical discharge application for flow management and flameholding. The experimental results on flameholding at gas temperature T0=300-760K are presented. The hydrogen and ethylene were injected directly into the M=2 flow from the wall at overall ER<0.2. The electrical discharge of filamentary type between flush mounted electrodes on the wall is used for a flame promotion. The power deposited is W_{pl}/H_{tot}<2-5% of flow total enthalpy. The fuel ignition, and flameholding are demonstrated experimentally at combustion completeness η>0.9. The pressure elevation due to combustion is measured in accordance with operation mode. The fact is specially pointed that the discharge switching off leads to immediate extinction of the hydrogen/ethylene flame. The power threshold of fuels ignition over the plane wall was measured by variation of power deposition and the fuel mass flow rate. Based on the experimental data a new scheme of supersonic combustor is proposed. Local zones of combustion in multiple directly wall-fueled sections are supported by electrical discharges. Cross-section's expansions are adjusted with those zones of intensive reactions. This scheme is supposed to be quite prospective for practical apparatuses.

24. Sergey Leonov, Campbell Carter, Dmitry Yarantsev "DISCHARGE-BASED FLAMEHOLDING in HIGH-SPEED AIRFLOW", Proceedings of the XVII International Conference on Gas Discharges and Their Applications, Cardiff University, UK, 7-12 September 2008

    The paper considers the results of experimental and computational study of basic properties of the transversal filamentary near-surface electrical discharge in supersonic flow and a possible application of such a discharge as a new type of flameholder.

25. С. Б. ЛЕОНОВ, Д. А. ЯРАНЦЕВ –УПРАВЛЕНИЕ ОТРЫВНЫМИ ЯВЛЕНИЯМИ В ВЫСОКОСКОРОСТНОМ ПОТОКЕ С ПОМОЩЬЮ ПРИПОВЕРХНОСТНОГО ЭЛЕКТРИЧЕСКОГО РАЗРЯДА", МЖГ, №6, 2008

Приведены результаты экспериментального и расчетного исследования взаимодействия пристеночного электрического разряда со сверхзвуковым воздушным потоком в канале постоянного сечения. Описаны особенности генерации приповерхностного разряда в потоке. Продемонстрированы режимы с возникновением отрыва потока за областью разряда. Предложена модель взаимодействия. Исследован режим газодинамического экранирования механического препятствия на стенке канала. Приведены данные по изменению параметров основного потока вследствие генерации пристеночного разряда. Проведено сравнение с результатами расчета на основе упрощенной модели взаимодействия.

26. Sergey B. Leonov, Dmitry A. Yarantsev, "Near_Surface Electrical Discharge in Supersonic Airflow: Properties and Flow Control", Journal of Propulsion and Power, 2008, vol.24, no.6, pp.1168-1181, DOI: 10.2514/1.24585

The results of experimental and numerical investigations of the interaction between the near-wall electrical discharge and supersonic airflow in an aerodynamic channel with constant and variable cross-sections are presented. Peculiar properties of the surface quasi-DC discharge generation in the flow are described. The mode with flow separation developing outside the discharge region is revealed as specific feature of such a configuration. An interaction model is proposed on the basis of measurements and observations. A regime of gasdynamic screening of a mechanical obstacle installed on the channel wall is studied. Variation of the main flow parameters caused by the surface discharge is quantified. The ability of the discharge to shift an oblique shock in an inlet is demonstrated experimentally. Influence of relaxation processes in non-equilibrium excited gas on flow structure is analyzed. Comparison of the experimental data with the results of calculations based on the analytical model and on numerical simulations is presented.

27. Sergey B. Leonov, Yury I. Isaenkov, Dmitry A. Yarantsev, Igor V. Kochetov, Anatoly P. Napartovich, Michail N. Shneider –Unstable Pulse Discharge in Mixing Layer of Gaseous Reactants", 47th AIAA Aerospace Sciences Meeting and Exhibit (Orlando, FL, USA, 5-8 January 2009), AIAA-2009-0820.

The paper considers the results of experimental and computational efforts on study of the filamentary transversal pulse discharge dynamics in high-speed airflow close to contact zone of two co-flown gases. Recently the effect of fast development of the post-discharge channel instability at stagnant conditions and in high-speed flow was observed experimentally. This instability possesses form of lateral jets escaping. The mechanism of acceleration of post-discharge channel turbulent expansion was described earlier for ambient conditions. But the experiment has shown a wider zone of disturbance and a higher speed of spreading out. The second discussed idea is the filamentary discharge movement in medium at gradient concentration of different components. The discharge position and dynamics of mixing layer depend on the discharge parameters and physical properties of gases involved. It is considered that the result of interaction can be controlled by means of small additives in the gas. The effects found are supposed to be applied for high-speed combustion enhancement due to non-equilibrium excitation of air/fuel composition and mixing acceleration of non-premixed multi-components flow. The problem of plasma-assisted mixing was discussed earlier, particularly in frames of MHD approach.

28. *M. A. Deminsky, I. V. Kochetov, A. P.Napartovich, S. B. Leonov* "Numerical Study of Stages of Ignition of Ethylene-Air Mixture by Plasma Initiation", The 9th International Workshop on Magneto-Plasma Aerodynamics, Moscow, Russia, April 13-15, 2010

Calculations were performed using the Chemical WorkBench (CWB), which implements the solution of chemical and ion-molecular kinetics equations together with the Boltzmann equation for electron energy distribution function and the equation for the translational gas temperature. Ignition of ethylene-air mixture in the channel scramjet was described in the plug flow approximation at the constant volume. Such an approximation gives similar results for the

induction time in comparison with the solution of the full system of equations of the stationary one-dimensional gas dynamics. Calculations were performed using various mechanisms of combustion.

29. *A.A. Firsov, S.B. Leonov, A.B. Miller* "Numerical simulation of supersonic flow in convergent-divergent duct with discharge supply", The 9th International Workshop on Magneto-Plasma Aerodynamics, Moscow, Russia, April 13-15, 2010

    В работе представлены результаты численного моделирования сверхзвукового потока M=2 (V=500 м/с) в канале переменного сечения при взаимодействии с электрическим разрядом. Было рассмотрено влияние мощности разряда и положения электродов на структуру потока. Проведено сравнение двух пакетов численного моделирования гидро-аэродинамики (CFD). Основная цель работы – получение дополнительных данных о взаимодействии потока, разряда, и модели канала переменного сечения, которые затруднительно получить в реальном эксперименте.

30. *D. Yarantsev, Yu. Isaenkov, S. Leonov, M. Shurupov*, "Localization of the Pulse Discharge in Two-Gases Flow" The 9th International Workshop on Magneto-Plasma Aerodynamics, Moscow, Russia, April 13-15, 2010

    Одной из актуальных задач плазменно-индуцированного горения в высокоскоростном потоке является быстрое смешение газов при инжекции топлива в окислитель. Способом реализации этого процесса может быть инициирование в среде газодинамических возмущений при помощи импульсного субмикросекундного филаментарного разряда. В связи с этим становится актуальным исследование особенностей геометрической формы и локализации импульсного разряда при его распространении вблизи границы двух газов. Эксперименты проводились в закрытой камере, в которой была организована ламинарная низкоскоростная струя CO2. Конструкция электродов позволяет инициировать разряд как внутри струи, так и вблизи ее границы. Для визуализации газодинамических процессов использовалась теневая съемка. Помимо визуализации производились измерения электрических параметров разряда (пояс Роговского и высокоскоростной делитель). Запуск теневой съемки синхронизирован с запуском разряда посредством оптического генератора.

31. *Sergey Leonov, Campbell Carter, Dmitry Yarantsev* "Experiments on Electrically Controlled Flameholding on a Plane Wall in Supersonic Airflow", *Journal of Propulsion and Power*, 2009, vol.25, no.2, pp.289-298

    We described experiments on gaseous fuel ignition and flameholding controlled by an electrical discharge in high speed airflow. The geometrical configuration does not include any mechanical or physical flameholder. The fuel is nonpremixed and injected directly into the air crossflow from the combustor bottom wall. A multi-electrode, nonuniform transversal electrical discharge is excited, also on the bottom wall, between flush-mounted electrodes. The initial gas temperature is lower than the value for autoignition of hydrogen and ethylene. Results are presented for a wide range of fuel mass flow rate and discharge power deposited into the flow. This coupling between the discharge and the flow presents a new type of flameholder over a plane wall for a high-speed combustor.

32. *M A Bolshov, Yu A Kuritsyn, V V Liger, V R Mironenko, S B Leonov, D A Yarantsev*, "Measurements of gas parameters in plasma-assisted supersonic combustion processes using diode laser spectroscopy", *QUANTUM ELECTRON*, 2009, **39** (9), 869–878. DOI: 10.1070/QE2009v039n09ABEH014044

    The paper describes results of temperature and water vapors concentration in supersonic combustion zone.

33. *М. А. Большов, Ю. А. Курицын, С. Б. Леонов, В. В. Лигер, В.Р.Мироненко, Д. А. Яранцев* «Измерение температуры и концентрации паров воды в сверхзвуковой камере сгорания методом абсорбционной спектроскопии». The 8th International Workshop on Magneto-Plasma Aerodynamics, Moscow, Russia, March 31 — April 2, 2009 – ТВТ, №7, 2009

    В статье рассматривается задача измерения параметров зоны высокоскоростного нестационарного горения при стабилизации фронта пламени электрическим разрядом. В

работе применен приповерхностный разряд на плоской стенке между электродами, установленными в плоскости стенки. Представлены базовые экспериментальные результаты при температуре торможения воздушного потока T0=300-760K. В качестве топлива используются водород и этилен, непосредственно инжектируемые со стенки в поток M=2 при ER<0.1. Приведены результаты измерения температуры газа и концентрации водяных паров в зоне реакции, полученные методом ДЛАС. Показано, что использование электрического разряда позволяет достичь полноты сгорания топлива η>0.9.

34. *A. P. Napartovich, I. V. Kochetov, S. B. Leonov* Modeling of premixed ethylene-air flow ignition by non-uniform non-thermal plasma, The 8th International Workshop on Magneto-Plasma Aerodynamics, Moscow, Russia, March 31 — April 2, 2009 – ТВТ, №7, 2009

    Развита теоретическая модель воспламенения предварительно перемешанной смеси воздуха с этиленом, инициированного стримерным разрядом в сверхзвуковом потоке. Анализируется система, включающая в себя микро-стримерный разряд с последующим смешением возбужденных и невозбужденных областей. Численно продемонстрировано, что использование неоднородного разряда с последующим смешением возбужденной и невозбужденной областей потока смеси этилена с воздухом может резко уменьшить вкладываемую в разряде энергию в расчѐте на полный поток, минимально необходимую для инициирования горения.

35. *Sergey B. Leonov, Yury I. Isaenkov, Alexander Firsov,* –Mixing Intensification in High-Speed Flow by Unstable Pulse Discharge, 40th AIAA PDL Conference, San-Antonio, June 22-25, 2009, Paper AIAA-2009-4074

    The paper describes results of experimental efforts on the filamentary transversal pulse discharge dynamics in high-speed airflow. The effect of fast turbulent expansion of the post-discharge channel is studied experimentally in order to enhance mixing processes of fuel and oxidizer and reduce the time of ignition. It is shown experimentally that the pulse-repetitive discharge disturbs the flown gas significantly if the time period between individual pulses is about *d/V*, where d = inter-electrode gap, V= flow velocity.

36. *Sergey Leonov, Dmitry Yarantsev, Vladimir Sabelnikov*, Electrically Driven Combustion near Plane Wall in M>1 Duct, 3rd EUCASS Proceedings, July 2009, Versailles, France

    An ultimate objective of this work is to enhance the performance of air-breathing engines in transient modes. The paper presents the result of laboratory-scale experiments on ignition of non-premixed fuel-air composition in high-speed flow by near-surface electrical discharge. The experiments were fulfilled under conditions of model supersonic combustor on the plane wall without any mechanical flameholder. The ignition and flameholding of hydrogen-air and ethylene-air compositions were demonstrated for direct fuel injection into the flow at low (T_0=300-750K) gas temperature. The power deposited was W_{pl}/H_{tot}<2-5% of flow total enthalpy. The power threshold of fuels ignition over the plane wall was measured by variation of power deposition and the fuel mass flow rate. The combustion completeness was estimated to be reasonably high, η>0.9, with both hydrogen and ethylene fuels under optimal conditions.

37. *M.A. Bolshov, Y.A. Kuritsyn, V.V. Liger, V.R. Mironenko, S.B. Leonov, D.A. Yarantsev,* –Measurements of the temperature and water vapor concentration in a hot zone by tunable diode laser absorption spectrometry", *Appl. Phys. B*, vol. 100, 2010, p. 397.

    A tunable diode laser absorption spectroscopy (TDLAS) technique and appropriate instrumentation was developed for the measurement of temperature and water vapor concentrations in heated gases. The technique is based on the detection of the spectra of H2O absorption lines with different energies of low levels. The following absorption lines of H2O were used: 7189.344 cm−1, 7189.541 cm−1, 7189.715 cm−1. Spectra were recorded using fast frequency scanning of a single distributed feedback (DFB) laser. A unique differential scheme for the recording of the absorption spectra was developed. An optimal technique for fitting the experimental spectra was developed. The validated TDLAS technique was applied for detection of temperature and H2O concentration in the post-combustion zone of a supersonic (M = 2) air-fuel flow. Hydrogen and ethylene were used as the fuel. The combustion process was ignited

and sustained by a pulsed electric discharge. Presentation of the transient absorption spectra as 2D images was used as the first step of data processing. The estimated precision of the temperature measurement was ±40 K. The high signal-to-noise ratio enabled the reconstruction of the temporal behavior of temperature with a resolution of ~1ms.

Attachment 2: List of presentations at conferences and meetings with abstracts

1. I.V. Kochetov, S.B. Leonov, A.P. Napartovich, E.A. Filimonova, D.A. Yarantsev "Plasma-chemical reforming of the hydrocarbon fuel in the air flow", International Workshop on "Thermochemical and plasma processes in aerodynamics" Saint-Petersburg, 19-21 June, 2006.

   The paper and presentation are dedicated to theoretical and experimental investigation of the process of hydrocarbon fuel plasma-chemical reforming in the airflow for the purpose of reduction of the combustion induction time.

2. Sergey B. Leonov, Igor B. Matveev "First Test Results of the Transient Arc Plasma Igniter in a Supersonic Flow", Paper, Proceedings of IWEPAC-3, September 17-20, 2007, Falls Church, VA, U.S.A

   This paper and presentation considers the idea and the first test results of the combined cycle plasma torch (CCPT) application for flame holding in high-speed combustors. The CCPT was developed by Applied Plasma Technologies (APT) and is based on a low-power transient discharge plasma pilot with fuel or air-fuel mixture feeding into the arc chamber, so that the main thermal effect is provided by chemical reactions in a plasma-activated medium.

3. Sergey B. Leonov, Dmitry A. Yarantsev, "Flameholding due to electrical discharge generation on plane wall of supersonic duct.", Proceedings of ICPCD 2008, Moscow, Russia, 10-12 November 2008

   The presentation dedicates the last achievements in a field of active flameholding in high-speed flow under non-optimal conditions by means of near-surface electrical discharge. В докладе представлены последние достижения в области стабилизации фронта высокоскоростного горения в неоптимальных условиях при помощи приповерхностного электрического разряда.

4. S. Leonov, Yu. Isaenkov, D. Yarantsev "Pulse Discharge in Mixing Layer of Reacting Gases", Book of Abstracts, 61th Annual Gaseous Electronics Conference 14- 17 October, 2008, Dallas-Addison Marriott Quorum, Dallas, TX, USA

   A subject of consideration is the dynamic of filamentary pulse discharge generated along contact zone of two co-flown gases. Experimental facility consists of blow-down wind tunnel PWT-50, system of the high-voltage pulse-repetitive feeding, and diagnostic equipment (schlieren device; pressure, voltage, current, radiation sensors; spectroscopic system; etc.) Typical parameters: p=0.2-1Bar, velocity M=0-2, pulse duration τ=0.1-1μs, power release W=20-100MW. Recently the effect of enormously fast turbulent expansion of the post-discharge channel was observed experimentally [S. Leonov, oth., AIAA Paper 2005-0159 and S. Leonov, oth. "Physics of Plasmas", v.15, 2007]. In this paper a result of parametrical study of the mixing efficiency due to instability development are discussed. The next announced item is that the discharge position and dynamics depend on the test parameters and physical properties of gases involved. The result of interaction can be controlled by the discharge's duration and current as well as by small additives to the gas. The effects found can be applied for high-speed combustion enhancement due to mixing acceleration in multi-components flow.

5. *М. А. Деминский, И. В. Кочетов, С. Б. Леонов, А. П. Напартович, Б. В. Потапкин,* Удельные энергии плазменного инициирования для обеспечения горения в сверхзвуковом потоке топливно-воздушной смеси, Труды 6го Международного симпозиума "Термохимические и плазменные процессы в аэродинамике", Санкт-Петербург, 12-14 мая, 2008, Холдинговая компания "Ленинец"

   Определены удельные энергии, необходимые для плазменного инициирования горения предварительно перемешанной водородно-воздушных и этилен-воздушных смесей в сверхзвуковом потоке в условиях типичных для ГПВРД. Исследовано влияние вида разряда на эффективность плазменного инициирования. Показано, что основными механизмами плазменного инициирования в рассматриваемых условиях являются диссоциация молекул кислорода при столкновениях с электронно-возбужденными молекулами азота и диссоциация электронами плазмы. Исследовано влияние молекул кислорода в нижнем синглетном электронно-возбужденном состоянии (СК) на порог

плазменного инициирования в водородно-воздушных смесях. Из-за больших сечений возбуждения различных внутренних степеней свободы молекул азота на возбуждения СК идет незначительная доля мощности разряда, и его влияние на плазменное инициирование незначительно.

6. С.Б. Леонов, Стабилизация фронта пламени электрическим разрядом за уступом и на плоской стенке сверхзвукового канала. Труды 3й Школы-семинара по Магнито-плазменной Аэродинамике, Москва, ОИВТ РАН, апрель 2008.

   Подробно представлены экспериментальные результаты по зажиганию топлива в сверхзвуковом потоке и стабилизации фронта пламени при T0=300-760K. В качестве топлива используются водород и этилен, непосредственно инжектируемые со стенки в поток M=2 при ER<0.1. В работе использовался приповерхностный разряд на плоской стенке между электродами, установленными «заподлицо». Величина вложенной в разряд электрической мощности составляла W_{pl}/H_{tot}<2% от полной энтальпии потока, тогда как тепловая мощность вследствие горения превышала W_{com}/H_{tot}>100% при низкой начальной температуре газа. Стабилизация фронта горения получена при полноте сгорания топлива η>0.9. Приведены данные по положению фронта и росту давления и зависимости от начальной температуры. Специально отмечается, что разряд несет как функцию инициатора пламени, так и регулятора структуры потока. Выключение разряда приводит к немедленному срыву горения. Приведены данные по порогу горения в зависимости от мощности разряда и расхода топлива.

7. Sergey Leonov –Ignition and Flameholding in M>1 Airflow by Electrical Discharge: 10years‘ Experience”, Invited Lecture, 47th AIAA Aerospace Sciences Meeting and Exhibit (Orlando, FL, USA, 5-8 January 2009), AIAA-2009-0000.

   A main objective of this work as a whole is to enhance the performance of air-breathing engines in transient modes. The concept of Plasma-Induced Ignition and Plasma-Assisted Combustion is considered on the basis of three main ideas: the medium heating/excitation by discharge, fuel-air mixing intensification, and flow structure control in the vicinity of reaction zone. A short review of recent works is done based on available publications. The paper presents also the result of lab-scale experiments on ignition of non-premixed fuel-air composition in high-speed flow by electrical discharge made during the last 10 years. The experiments were fulfilled under conditions of model supersonic combustor in standard aerodynamic configurations with backwise wallstep, in cavity, and on the plane wall. The electrical discharge was organized in specific electrodes arrangement where the plasma filaments crossed an area of gas circulation. The ignition and flameholding of hydrogen-air, ethylene-air, and kerosene-air compositions were demonstrated for direct fuel injection into the fixed separation zone at low gas temperature. An energetic threshold of fuel ignition under separation and in a shear layer of supersonic flow has been measured. Some ideas for the mixing intensification are discussed as well. They are proved by model experimental demonstrations.

8. *Leonov S. B.,* –Ignition and Flameholding of Gaseous Fuels by Electrical Discharge in M>1 Airflow”, Invited lecture, 2nd EUCASS ATW, Les Houches, France, October 11-16, 2009

   The presentation dedicates the last achievements in a field of active flameholding in high-speed flow under non-optimal conditions by means of near-surface electrical discharge.

9. *Sergey B. Leonov* –Visualization of unsteady electrical discharges in high-speed flow”, Keynote Lecture, Proceedings of 10th ASV International Conference, Publication by SRM University, Nagar, Tamil Nadu, India, 2010, pp.1-11

   Specific experimental technique in Plasma-Assisted Aerodynamics is discussed in the presentation. The results of several experiments are presented to demonstrate abilities of non-standard methods of visualization as well. Among of them the high-power pulse discharge instability; the unsteady near-surface discharge in supersonic flow; the DBD over a contoured airfoil; and others.

10. *Sergey B. Leonov* –Plasma-Based Supersonic Flameholding at low ER”, 3th International scientific and Technical Conference –Aeroengines of XXI century”, 30Nov-3Dec 2010.

The presentation dedicates the last achievements in a field of active flameholding in high-speed flow under non-optimal conditions by means of near-surface electrical discharge.

Attachment 3: Information on patents and copy rights

No